DESIGN, SYNTHESIS, AND APPLICATIONS OF NOVEL POLYESTERS BASED ON NATURAL METABOLITES

Devin G. Barrett

A dissertation submitted to the faculty of the University of North Carolina at Chapel Hill in partial fulfillment of the requirements for the degree of Doctor of Philosophy in the Department of Chemistry.

Chapel Hill
2010

Approved by

Advisor: Dr. Muhammad Yousaf

Chair: Dr. Matthew Redinbo

Dr. Kevin Weeks

Dr. Valerie Ashby

Dr. Joseph DeSimone

ABSTRACT

DEVIN G. BARRETT: DESIGN, SYNTHESIS, AND APPLICATIONS OF NOVEL POLYESTERS BASED ON NATURAL METABOLITES

(Under the direction of Dr. Muhammad N. Yousaf)

As the biomedical and biotechnological fields expand, the design of novel materials will be essential in order to meet new requirements. Specifically, the field of tissue engineering continuously evolves as new materials and medical information are gathered. Scaffolds for tissue engineering need to be strong and flexible so that they can accommodate the body's natural movements. A class of potential soft tissue scaffolds – biodegradable polyester elastomers – has become a very popular option for these applications. Although useful, the ability to chemically tailor these materials for application-specific needs is challenging. Being able to easily append biologically relevant molecules onto tissue scaffolds would add a new and critical level of control over the interactions of cells and tissues with the materials. We have focused on the design of polyketoesters based on natural monomers, many of which are FDA approved for use in humans. The presence of ketones allows for facile and efficient chemical modifications that enable one polyester backbone to accommodate multiple functions. Because thermal polycondensation was used to synthesize these polyesters, the macromolecular properties of the final polymers can be tailored to fit the needs of a particular application by varying the starting materials and the curing conditions.

This work is dedicated to my father, who defined himself in large part through "the University of the people," and to my wife and family for their encouragement. Many thanks to my colleagues for their support and advice: Dr. Eugene Chan, Debjit Dutta, Dr. Diana Hoover, Brian Lamb, Dr. Eun-Ju Lee, Wei Luo, Wyetta Palmby, Sungjin Park, Abigail Pulsipher, Tina Searcy, and Nathan Westcott.

TABLE OF CONTENTS

LIST OF TABLES

TABLE

LIST OF FIGURES

FIGURE

LIST OF ABBREVIATIONS

αKG	α-ketoglutaric acid
AA	Adipic acid
CHDM	1,4-Cyclohexanedimethanol
DCM	Dichloromethane
DMF	*N,N*-Dimethylformamide
DMI	Dimethyl itaconate
DMSO	Dimethyl sulfoxide
DSC	Differential scanning calorimetry
EtOH	Ethanol
FDA	Food and Drug Administration
GPC	Gel permeation chromatography
HD	1,6-Hexanediol
IA	Itaconic acid
MeOH	Methanol
NMR	Nuclear Magnetic Resonance
PBS	Phosphate buffered saline
PDI	Polydispersity index
PDKDC	Poly(diol 4-ketopimelate -*co*- diol citrate)
PDMS	Poly(dimethylsiloxane)
PEG	Poly(ethylene glycol)
PErD	Poly(erythritol dicarboxylate)
PFPE	Perfluoropolyether

PRINT	Particle/Pattern Replication in Non-wetting Templates
PTK	Poly(triol α-ketoglutarate)
RS	Rupture strain
SEM	Scanning electron microscopy
TGA	Thermogravimetric analysis
THF	Tetrahydrofuran
UTS	Ultimate tensile stress
YM	Young's modulus

LIST OF SYMBOLS

T_g	Glass transition temperature
T_m	Melting temperature
$\langle M_n \rangle$	Number-average molecular weight
Q_s	Percent soluble fraction

Chapter I

LITERATURE REVIEW OF CURRENT BIODEGRADABLE POLYESTER THERMOSETS

1.1 Introduction

The field of tissue engineering has emerged in order to offer a method to repair and/or replace injured tissue.[1-3] Synthetic polymer/tissue systems have the potential to offer an alternative to organ transplantation when the tissues are damaged and cannot be healed.[1-3] Recent research has suggested that tissue scaffolds should closely mimic the mechanical profiles of the corresponding natural tissues. Throughout the human body, many diverse biological materials exist, all demonstrating unique sets of mechanical characteristics.[4-8] Not only do heart valves, bladder, smooth muscle, collagen fibers, and elastin all exhibit different mechanical properties, but their strengths and flexibilities vary over several orders of magnitude. Therefore, significant research has been aimed at designing biocompatible scaffolds that offer mechanical versatility. Polyester elastomers are one such class of materials that has demonstrated this mechanical diversity. These polymers are hydrolytically degradable, and have thus gained popularity for use in the field of tissue engineering.[9, 10] Additionally, polyester elastomers frequently exhibit degradation rates that can be tuned for a particular application.[11-13]

In the last decade, as synthetic polyester elastomers have become popular options for soft tissue engineering, research has investigated a wide range of biomaterials with mechanical properties that recreate those of the natural tissue.[5,6,14-17] The flexibility and strength of a tissue scaffold have been shown to enhance cellular behavior and/or tissue proliferation.[18-21] Of the previously synthesized polyester scaffolds, examples of both thermosets and thermoplastics have been described.[9,10,13,22] When compared to thermoplastic materials, thermosets offer several advantages that are critical for biomedical applications. For example, thermoset polyester elastomers can be designed to be completely amorphous,

Table 1.1 Mechanical Properties of Some Polyester Biomaterials

Material	Young's Modulus (MPa)	UTS (MPa)	Rupture Strain (%)	Biological Testing	Reference
PGS[a]	0.282	> 0.5	> 267	yes	23,27,28
PPS[b]	0.37 – 378.0	0.57 – 17.64	11 – 205	yes	29,30
PAPS[c]	2.45 – 4.24	1.33 – 1.69	64 – 92	yes	31-33
PDC[d]	1.60 – 13.98	2.93 – 11.15	117 – 502	yes	35,36
POCDA[e]	5.91 – 32.64	1.47 – 10.71	200 – 260	yes	52
PEC[f]	0.25 – 1.91	0.51 – 1.51	140 – 1506	no	53
PGD[g]	136.55[p] (1.08)[q]	7[p] (0.45)[q]	225[p] (123)[q]	yes	54
PDM[h]	0.98 – 4.04	0.21 – 4.16	25 – 737	yes	59
PGSC[i]	0.61 – 3.26	0.63 – 1.46	51 – 170	no	60,61
PGSC-CNT[j]	6.6 – 9.2	2.8 – 4.4	40 – 44	yes	65
PPSC[k]	0.60 – 1.23	0.87 – 2.12	225 – 431	no	66
PPSC-nHAp[l]	0.29 – 3.60	0.89 – 8.21	256 – 320	yes	67
POCOS[m]	0.19 – 1.10	0.24 – 0.63	127 – 231	no	68
PGSA[n]	0.048 – 1.375	0.054 – 0.498	47.4 - 170	yes	71-73
PBM[o]	12 – 930	4.5 – 37	12 – 47	no	85

[a] poly(glycerol sebacate); [b] poly(polyol sebacate); [c] poly(1,3-diamino-2-hydroxypropane–*co*–polyol sebacate); [d] poly(diol citrate); [e] diamine-containing poly(1,8-octanediol citrate); [f] poly(PEG citrate); [g] poly(glycerol dodecanedioate); [h] poly(1,12-dodecanediol malate); [i] poly[(glycerol sebacate) citrate]; [j] composites of poly[(glycerol sebacate) citrate] and carbon nanotubes; [k] poly[(1,2-propanediol sebacate) citrate]; [l] composites of poly[(1,2-propanediol sebacate) citrate] and nanocrystalline hydroxyapatite; [m] poly(1,8-octanediol citrate -*co*- 1,8-octanediol sebacate); [n] poly(glycerol sebacate acrylate); [o] poly(but-2-ene-1,4-diyl malonate); [p] tested at room temperature; [q] tested at 37 °C.

allowing for consistent degradation rates and a linear loss of mechanical properties.[9,23] Additionally, polyester thermosets often degrade in a manner that allows for the retention of the three-dimensional (3D) structure throughout hydrolysis.[23] On the contrary, thermoplastic elastomers often contain crystalline regions, which can cause heterogeneous hydrolytic degradation and a non-linear loss of mechanical strength.[24,25] As a result, thermoplastic materials often suffer a loss of their 3D geometry.[23,26]

1.2 Thermal Polycondensation of Biodegradable Polyesters

Recently, thermal polycondensation has evolved into a popular strategy for designing versatile polyester biomaterials.[10,13,22] By starting with monomers of average functionality greater than 2, polymer chains cross-link and create thermosets. This technique has experienced an increase in use due to several factors: its ease, its flexibility, and the resulting materials. The ease of this polymerization strategy is difficult to match; monomers are heated in a partial vacuum in order to form esters. Due to variations in monomer choice, the length of the curing period will vary. However, the final product is always a cross-linked polyester. No organic chemistry training is necessary to perform these reactions as no complex synthetic transformations are required. Due to the simplicity of this method, a wide range of scientists can develop biomaterials. Additionally, thermal polyesterification is a very flexible synthetic strategy. Application-specific properties can be imparted on the final material through the choice of polyol or polyacid.[10,13,22] The main limitations of this strategy are the melting and boiling points of the monomers. The monomers should remain in the liquid state during the synthetic procedure (often between 100 °C and 150 °C and under partial vacuum). However, an incredibly large number of polyols and polyacids satisfy this single criterion. Finally, the polyesters elastomers that have been designed with thermal polycondensation are simple and effective. These polyester biomaterials are excellent candidates for future biomedical and biotechnological applications.

Synthetic and elastomeric polyesters have been designed with thermal polycondensation to incorporate a wide variety of monomers. Some polymers have been based on starting materials that are endogenous to the human metabolism.[22] The choice of molecules that are naturally present in the human metabolism offers a route to minimize

toxicity. Some materials have also been thermally polymerized so as to comprise starting materials from other successful biomaterials.[13,22]

1.2.1 Poly(Glycerol Sebacate)

Current interest in thermally cross-linked polyester networks is largely due to the pioneering work of Dr. Robert Langer. In 2002, poly(glycerol sebacate) (PGS), a polyester that is analogous to vulcanized rubber, was introduced (Figure 1.1).[27] By heating glycerol and sebacic acid for several days, esterification led to the formation of a pre-polymer, which can be melted or dissolved for further fabrication processes. The design of PGS was motivated by the need for biodegradable materials that are robust in terms of their mechanical properties. A strong and biocompatible polyester elastomer was hypothesized to be potentially useful in a wide range of biomedical applications. Glycerol and sebacic acid are endogenous to the human metabolism, minimizing potential cytotoxic effects after degradation.[22] PGS achieved a Young's modulus (YM), an ultimate tensile stress (UTS), and a rupture strain (RS) of 0.282 MPa, > 0.5 MPa, and > 267 %, respectively. *In vitro* biocompatibility was also explored by seeding fibroblasts onto PGS-coated glass petri dishes. When compared to a positive control of poly(lactide–co–glycolide) (PLGA), cells displayed normal morphologies and proliferated well. *In vivo* testing was then performed by subcutaneously implanting PGS films in rats. Based on the formation of fibrous capsules and the general inflammatory response, PGS implants exhibit less negative physiological consequences than similar PLGA implants. Also, subcutaneous PGS implants were undetectable after 60 days, indicating that they were completely resorbed by the rats with no scarring or permanent deformation to the histological structure.

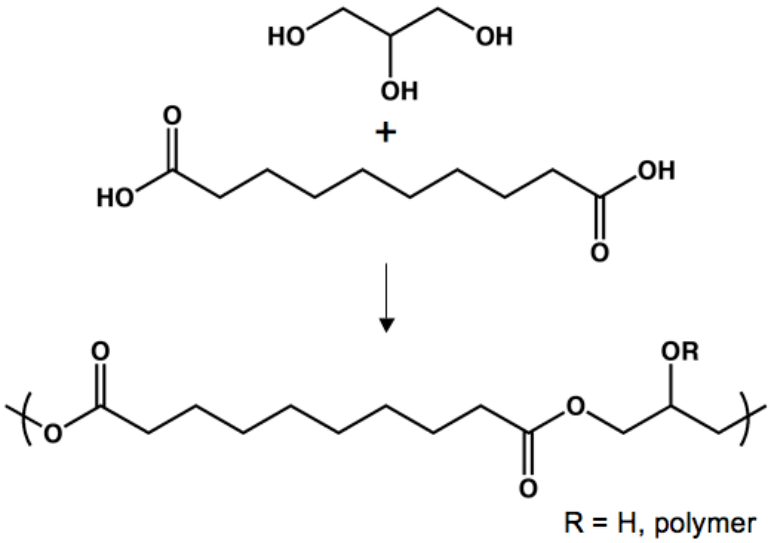

Figure 1.1. Synthesis of poly(glycerol sebacate).

The ways in which the mechanical properties and geometry of the material change during hydrolysis are important characteristics of implanted biodegradable materials. PGS was studied throughout the course of *in vivo* degradation in order to determine the timescale during which its mechanical and geometrical characteristics were maintained.[23] Throughout the 35-day study, PGS samples maintained their overall geometry. Conversely, PLGA implants were distorted significantly within 14 days. This observation was further characterized with scanning electron microscopy in order to visualize the surfaces of PGS and PLGA after implantation. PGS films had similar surface topologies during the course of the study, while holes and cracks were often observed in PLGA elastomers. The rate of mass loss is also important because it is intimately linked to mechanical integrity. PGS demonstrated a linear rate of mass loss and mechanical strength loss with respect to time. PLGA samples experienced a dramatic loss in mechanical strength by day 7 and in mass by day 21. These findings are most likely explained by different mechanisms of degradation for

PGS (surface erosion) and PLGA (bulk degradation). The preliminary results indicate that PGS should be a successful biomaterial with many *in vivo* applications.

Recently, PGS was used to create myocardial tissue scaffolds.[28] Designing grafts for myocardial repair has been difficult due to the need to recreate cardiac anisotropy. The majority of previous candidates have been incompatible with the fabrication of a truly biomimetic system. Taking inspiration from natural collagen fibers that form a honeycomb-like scaffold for cardiac muscle fibers, Engelmayr *et al.* fabricated similar structures composed of PGS. Upon mechanical testing, the relationship between stress and strain in the preferred and the cross-preferred directions demonstrated anisotropic behavior. Further studies were conducted by comparing the rigidity and flexibility of PGS to those of an adult rat's right ventricular myocardium to explore whether PGS honeycomb scaffolds could be used *in vivo*. Both the microfabricated PGS and the natural rat tissue showed anisotropic behavior with similar stress-strain relationships. After simulating physiological loading in a fatigue bath and determining the effect of *in vitro* cell culturing on the anisotropy, PGS honeycomb-like scaffolds were found to be promising, but not yet ideal, materials for myocardial repair. Additionally, after seeding, neonatal rat heart cells oriented in the preferred direction without any external stimuli; this phenomenon is not often observed in isotropic scaffolds. Finally, heart cell contractility could be induced by electrical stimulation with directionally dependent electrical excitation. After these preliminary studies, the Langer research group believes that PGS honeycomb-like scaffolds offer a potential route to functional myocardium repair through tissue engineering.

1.2.2 Poly(Polyol Sebacate)

Sebacic acid has also been combined with several sugar alcohols, generating a wider range of sebacate-based biomaterials with distinct properties.[29,30] All of the sugar alcohols – xylitol, sorbitol, mannitol, and maltitol – are non-toxic and mostly used as sugar substitutes in foods. Sugar alcohols are ideal monomers for thermal polymerization because they do not discolor and degrade upon melting the way that sugars can. By combining these sugar alcohols with sebacic acid, seven different poly(polyol sebacate) (PPS) materials were synthesized (Figure 1.2). By altering the equivalents of the diacid, the mechanical and physical properties of the resulting polyesters could be tuned. The PSS series of biomaterials were able to achieve a wide range of YM (0.37 – 378.0 MPa), UTS (0.57 – 17.64 MPa), and RS values (205.16 – 10.90 %). Additionally, despite the large number of hydroxyl groups in the monomers, the water swelling of these polymers could be controlled, with values ranging from 1.40 % to 6.28 %. Interestingly, the different PPS materials were able to elicit very different cellular morphologies upon adhesion. When cells were seeded to two of the materials synthesized from sorbitol or mannitol, few were able to attach; of those that did, the morphologies were limited to round, spherical geometries. In order to assess the potential of PPS in biomedical applications, polymer samples were subcutaneously implanted in rats. After 10 days *in vivo*, the observed inflammatory response was mild for all of the polyester samples, which were surrounded by thin fibrous capsules. After 12 weeks *in vivo*, a thicker fibrous capsule was observed around all of the samples. However, the capsule formation was determined to be comparable to or less than that of PLGA, the commonly used FDA-approved polyester. In general, these materials appear to offer incredible potential for use in the biomedical fields. The ability to tune the mechanical strength, flexibility,

hydrophobicity, and non-fouling behavior of PPS will allow access to large spectrum of future applications.

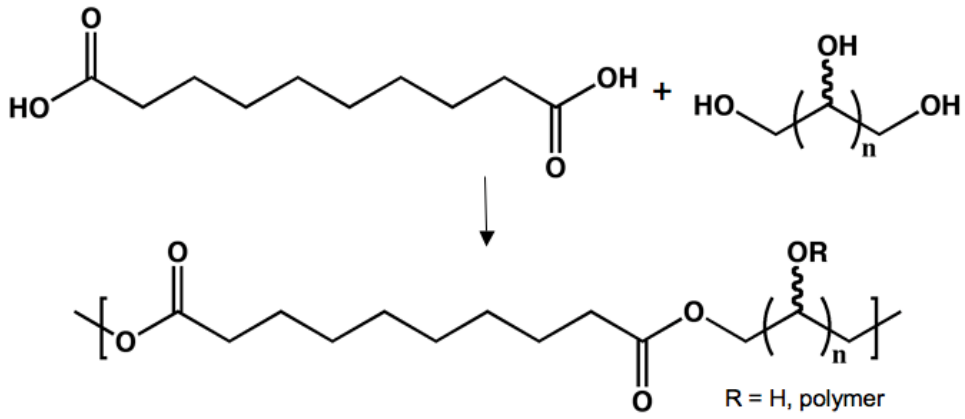

Figure 1.2. Synthesis of poly(polyol sebacate).

1.2.3 Poly(Amino Alcohol Sebacate)

After designing PGS, the Langer research group focused on synthesizing a similar material that exhibited longer *in vivo* degradation rates. This goal was accomplished by including amines in the starting materials to install hydrolytically stable amide bonds throughout the polyester matrix.[31-33] The thermal polymerization of sebacic acid, 1,3-diamino-2-hydroxypropane, and either glycerol or D,L-threitol led to the synthesis of poly(1,3-diamino-2-hydroxypropane–co–polyol sebacate) (PAPS) composed of non-toxic monomers (Figure 1.3).[34] The YM, UTS, and RS range from 1.45 – 4.34 MPa, 0.24 – 1.69 MPa, and 21 – 92 %, respectively. Additionally, *in vitro* degradation studies were conducted in a sodium acetate buffer with a pH of 5.2 for 6 weeks. PAPS materials experienced 42.8 % - 97.0 % hydrolytic degradation. Post-polymerization modifications are also possible through conjugation reactions aimed at the unreacted, free amines. Overall, PAPS materials were non-toxic in *in vitro* and *in vivo* settings, with projected *in vivo* degradation half-lives of

up to 20 months. In terms of inflammatory response, macrophage concentration, and fibrous capsule formation observed in subcutaneous implants, PAPS demonstrated milder foreign body response than FDA-approved PLGA implants.

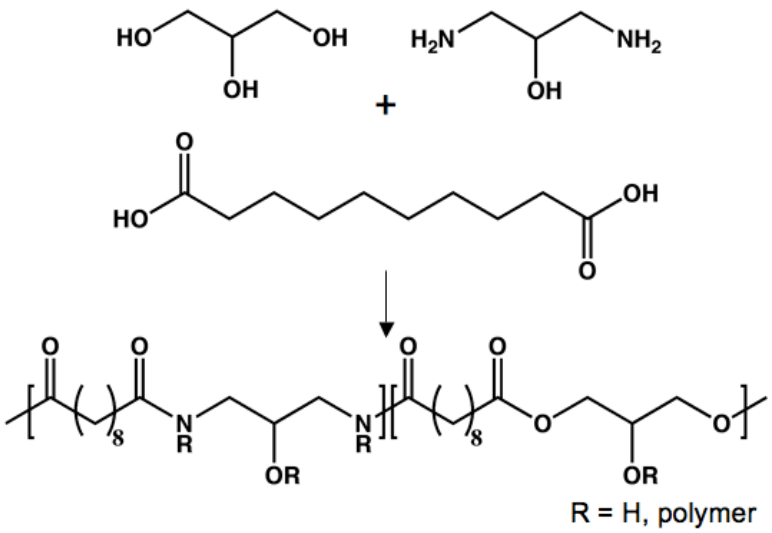

Figure 1.3. Synthesis of poly(1,3-diamino-2-hydroxypropane–co–polyol sebacate).

1.2.4 Poly(Diol Citrate)

In order to create elastomeric polyester thermosets, the research group of Dr. Guillermo Ameer found an ideal tri-functional monomer in the Citric Acid Cycle (CAC). The cardinal publications from Dr. Ameer's group described polyester elastomers based on citric acid, which includes three acid groups and one alcohol.[35,36] These biomaterials were synthesized by polycondensation with aliphatic diols: 1,6-hexanediol, 1,8-octanediol, 1,10-decanediol, and 1,12-dodecanediol (Figure 1.4). While several polyols were tested, the majority of the research focused on poly(1,8-octanediol citrate) (POC). Using a simple fabrication process, non-toxic monomers, and curing conditions that allow for facile tuning of physical and mechanical properties, inexpensive polyesters that have exceptional potential in soft tissue engineering were produced. Similar to PGS, the curing process involves

heating the pre-polymer solution. However, POC was able to form elastomeric thermosets at significantly milder temperatures (37 °C). By adjusting the curing temperature and duration, POC obtained YM of 0.92 MPa to 16.4 MPa, UTS up to 6.1 MPa, and a maximum strain of 502 % at rupture. The YM and UTS compare well to those of elastin from bovine ligaments (1.1 MPa and 2 MPa, respectively).

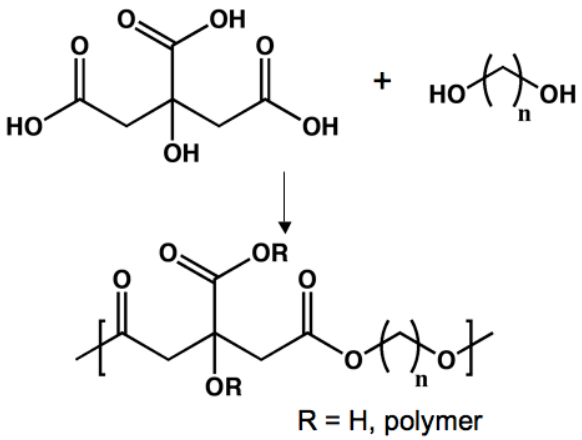

Figure 1.4. Synthesis of poly(diol citrate).

The applications of POC have primarily been directed towards the design of cardiovascular tissue scaffolds.[37,38] Accordingly, the toxicity of these materials was explored with human aortic smooth muscle cells (HASMCs) and human aortic endothelial cells (HAECs). When compared to a positive control of poly(L-lactide) (PLL), POC films are biocompatible with both HASMCs and HAECs. Finally, the *in vivo* response of Sprague-Dawley rats to implanted POC films was monitored, with no chronic inflammatory response observed. Additionally, several different types of scaffolds were designed to explore the fabrication potential of POC. These constructs were soft and able to fully recover from deformation. One example of these scaffolds, a biphasic and tubular device with a non-porous, skin-like interior and a porous exterior, has been used in blood vessel engineering.

In order to determine if biphasic tubular POC scaffolds would be acceptable for *in vivo* applications, several characteristics were studied, including biocompatibility and mechanical properties.[39] After observing implanted poly(diol citrate) (PDC) scaffolds *in vitro* and *in vivo*, potential surgical problems (compliance mismatch and thrombosis) could be identified and avoided. Because the mechanical properties of PDC could easily be tuned over a wide range, the mechanical characteristics of the PDC scaffolds could be well matched to those of native blood vessels.[40] These tubular devices achieved YM of ~ 1.5 MPa, UTS of ~ 3 MPa, and rupture elongation of ~ 350 %. Testing also determined the biphasic scaffolds to have a compressive modulus of 0.152 MPa, indicating that the materials are soft and able to fully recover from deformation. Compliance values and burst pressure (12.7 % and > 120 mmHg, respectively) also imply that PDC hybrid scaffolds could excel as potential synthetic blood vessels.

In vitro biocompatibility testing determined that these materials do not affect cells negatively when compared to a positive control of PLL. Additionally, various cell types could be seeded on different segments of the scaffold. HASMCs were seeded to the porous exterior phase, while HAECs were cultured on the skin-like, non-porous interior of the artificial blood vessel. This compartmentalization of cells may further the efforts to design blood vessel scaffolds that closely mimic the local environment of natural vessels.[41] *In vivo* biocompatibility was also studied to fully comprehend the biomedical potential of biphasic PDC constructs. Subcutaneous implantation of these devices demonstrated a foreign body response similar to that of PLL and allowed for significant tissue ingrowth.

The Ameer group continued their research in vascular tissue engineering by fabricating hybrid materials of POC and expanded polytetrafluoroethylene (ePTFE).[37] The

standard-of-care for current vascular grafts involves either ePTFE or surface-modified ePTFE tubes. While these options have been effective for large-diameter blood vessel applications (> 6 mm diameter), ePTFE small-diameter blood vessels have been less successful due to complications, including graft occlusion due to blood clots.[42,43] The ePTFE surface is inherently thrombogenic and its hydrophobicity can reduce the efficiency with which a layer of endothelial cells can form.[43-45] Efforts to minimize graft failure by enhancing endothelialization currently focus on the immobilization of non-degradable polymers, graft coatings, and the conjugation of biomolecules. However, this process can introduce potential coating-based problems due to cost, long-term efficacy, compliance, and biological response.

Based on the previous success of biphasic tubular POC scaffolds, the Ameer group explored their polyesters as a suitable coating for ePTFE vascular grafts. Without negatively affecting compliance, the biocompatibility was improved in hybrid polyester-ePTFE devices. Additionally, the presence of POC coating reduced platelet adhesion, aggregation, and activation, when compared to control ePTFE grafts. *In vivo* testing was performed so that surgically relevant, live-animal data could be gathered. When compared to ePTFE controls, the amount of macrophages present and the thickness of the fibrin coagulum were both significantly reduced for the hybrid grafts.

In order to observe the full potential of POC in vascular surgery, biodegradable vascular scaffolds were prepared.[46] Unlike the POC-ePTFE hybrid grafts, completely degradable devices were designed by replacing ePTFE with a non-porous POC tube. In order to compare POC to other biomaterials, platelet adhesion and activation was first studied on glass, ePFTE, PLGA, and POC. While fewer platelets attach to POC than any of the other

materials, the platelets also display very spherical morphologies. Extended and spread platelet morphologies are associated with aggregation and activation, which leads to clotting.[47,48] The anti-thrombogenic properties of the biodegradable POC graft make it a good candidate for blood vessel engineering. Additionally, plasma recalcification kinetics are significantly lower for POC, relative to PLGA, glass, and ePTFE. POC also displays coagulative properties that are much more suitable for contact with blood than PLGA and tissue culture plastic. The inflammatory response was monitored *in vitro* by assessing the activation of human THP-1 cells based on changes in the level of IL-1β and TNF-α.[49,50] When compared to a positive control, lipopolysaccharide, these materials, including POC, all caused THP-1 cells to produce low levels of activation markers. POC also achieved satisfactory protein adsorption and hemolysis values, comparable to PLGA, ePTFE, and tissue culture plastic. Finally, HAECs were seeded while flowing onto POC scaffolds. Although nearly 100 % of cells attached to glass surfaces, only 69 % were remained on POC constructs. While cell adhesion values were non-ideal, over half of HAECs were able to remain on POC surfaces under physiological shear stress conditions, a result that indicates excellent promise for future vascular engineering.

The extreme versatility of PDC polyesters has recently been demonstrated in two unique manuscripts. First, the ability of POC to successfully deliver DNA to cells was described.[51] Porous POC films were prepared using NaCl as a porogen in order to create scaffolds that aided nutrient transport and cell infiltration. The polyester thermosets were then incubated with DNA by the addition of naked plasmid DNA (pDNA) or polyplexes of polyethyleneimine (PEI) and DNA. Scaffolds were able to incorporate 0.70 μg of naked

pDNA (35.1 % efficiency) or 1.56 μg of PEI/DNA polyplexes (77.8 % efficiency). Additionally, surface-immobilized pDNA was susceptible to subsequent washing procedures.

The *in vitro* release of both forms of DNA from POC scaffolds was also studied. Naked pDNA displayed a burst release, with over 70 % release observed after 8 h. After 2 d, over 90 % of the pDNA had dissociated from the polyester scaffolds. Contrastingly, PEI/DNA polyplexes demonstrated sustained release that occurred gradually over the course of the 5-week study. Approximately 50 % of the polyplexes released by day 6; from day 6 to day 36, ~ 25 % of the PEI/DNA polyplexes dissociated in a liner manner. Although pDNA released with higher efficiency than the polyplexes, the absolute amount of DNA that released was larger for the PEI/DNA particles due to the difference in loading capacities.

In vitro transfection was also demonstrated with HEK293 and porcine aortic smooth muscle (PASM) cells. PEI/DNA polyplexes dramatically outperformed pDNA. Sustained transgene expression was observed for surface-associated polyplexes in PASM and HEK293 cells until day 9 and day 12, respectively. In order to fully validate POC as a gene delivery vehicle, *in vivo* tests were conducted in live mice. All scaffolds seemed to integrate well with the surrounding tissue. However, unexpectedly, PEI/DNA polyplexes, which demonstrated sustained *in vitro* transfection, did not induce transgene expression. Scaffolds that were functionalized with naked pDNA were able to cause cells to express EGFP, which was visualized by immunohistochemical staining. Further research is needed in order to better understand the complicated relationship between *in vitro* and *in vivo* transgene expression.

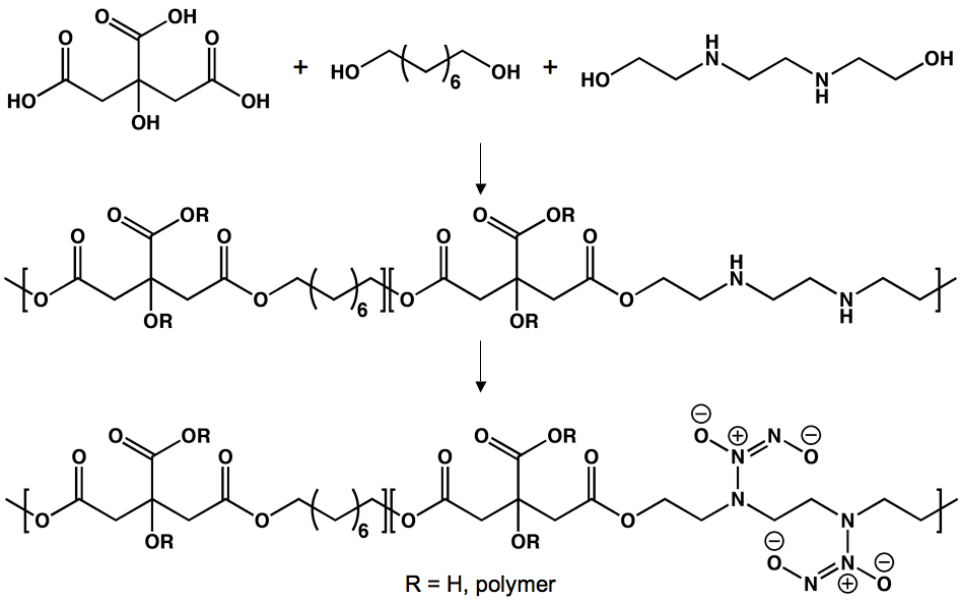

Figure 1.5. Synthesis of poly(1,3-diamino-2-hydroxypropane–co–polyol sebacate).

The second unique demonstration of the versatility of PDC describes the design of scaffolds capable of releasing nitric oxide (NO).[52] NO has been shown to play a critical role in neural transmission, vasodilatation, and cardiovascular homeostasis. Biomedical implants that are able to release NO are attractive due to their ability to reduce the risk of thrombosis. In order to create PDC-based NO donors, N,N'-bis(2-hydroxyethyl)ethylenediamine (BHED) was used as a diol, in addition to 1,8-octanediol. The resulting polymers contained secondary amines, which are able to react with NO to form diazeniumdiolates. Under physiological conditions (pH = 7.4, 37 °C), diazeniumdiolates release two equivalents of NO.

Diamine-containing POC (POCDA) was synthesized by the standard thermal polycondensation route, with the addition of 5, 10, or 15 % BHED (Figure 1.5). Initially, these thermosets were characterized without the formation of diazeniumdiolates. The mechanical properties of these poly(ester amine)s indicated that POCDA was stronger than the original POC. The YM, UTS, and RS were 5.91 – 32.64 MPa, 1.47 – 10.71 MPa, and 200 – 260 %, respectively. The non-functionalized polymers demonstrated mass loss of 5 –

7 % after 2 weeks, 7 – 12 % after 4 weeks, and ~ 20 % after 6 weeks. Additionally, PASM cells were able to attach to POCDA films, spreading and proliferating well.

NO-release was observed indirectly by monitoring the nitrite concentration in the polymer-containing supernatants. Although all of the materials contained secondary amines capable of forming diazeniumdiolates, the POCDA that contained 5 % BHED was unable to produce any NO. The 10 % and 15 % formulations, however, were able to release NO. ePTFE vascular grafts were also coated with POCDA containing 10 % BHED. The polymeric coatings minimally altered the compliance of the grafts, when using 6.3 wt % coated grafts; a lesser amount of 4.5 wt % did not affect the grafts' compliance at all. While these grafts were able to release NO for 2 or 3 days, the total NO that was released was significantly less than expected, based on the results of the bulk films. Further research is continuing to determine ways to improve the efficiency of NO-release and to improve the mechanical properties of the final grafts.

Similar to materials described by the Ameer lab, Ding *et al.* focused on polymerizing citric acid with a short oligomer of ethylene glycol (Mn = 200 g/mol).[53] Curing the resulting pre-polymer at several different conditions led to poly(PEG citrate) (PEC), a series of rapidly degrading polyesters (Figure 1.6). PEC was cured at 120 °C for a period of time ranging from 15 – 36 h. Compared to other materials described in this chapter, the final elastomers were soft and flexible due to relatively short curing durations. YM, UTS, and RS varied between 0.25 – 1.91 MPa, 0.51 – 1.51 MPa, and 139.5 – 1505.5 %, respectively. The unique quality of the PEC polyesters that differentiates it from other materials is its rapid degradation rate. All PEC polymers exhibited more than 60 % mass loss after 96 h. As a comparison, most of the other materials described herein experience hydrolysis on the course

of weeks, if not months. Future applications will concentrate on soft tissue engineering due to the mechanical properties of these materials.

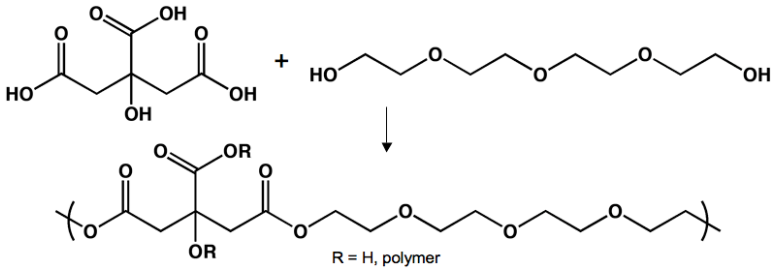

Figure 1.6. Synthesis of poly(PEG citrate).

1.2.5 Poly(Glycerol Dodecanedioate)

Similar to the previously mentioned PGS, another polyester thermoset was developed by combining glycerol and dodecanedioic acid (Figure 1.7).[54] The resulting poly(glycerol dodecanedioate) (PGD) has one main characteristic that makes it unique, relative to PGS. The glass transition temperature of PGD is ~ 32 °C – above room temperature but below physiological temperature. If deformation was induced above the T_g, the material immediately recovered to its original dimensions. However, if PGD was elongated at temperatures that are less than the T_g, the material was able to hold the new shape resulting from the strain. After this cold deformation, the original shape could be recovered by heating the sample above 32.0 °C. Accordingly, the mechanical properties varied greatly based on the temperature. At room temperature, PGD achieved a YM, UTS, and RS of 136.55 MPa, 7 MPa, and 225 %, respectively. However, above the T_g (37 °C), PGD displays a vastly different mechanical profile: a YM of 1.08 MPa, an UTS of 0.45 MPa, and a RS of 123 %. In addition to shape memory properties, PGD displays many beneficial characteristics of potential biomaterials for future *in vivo* applications. As previously mentioned, glycerol is naturally occurring, with roles in lipid biosynthesis, gluconeogenesis, and glycolysis.

Dodecanedioic acid is also endogenous to human metabolism, resulting from the ω-oxidation of lauric acid.[55-58] Cytotoxic properties were therefore expected to be minimal, as these monomers are compatible with biological systems. In order to explore this hypothesis, human aortic fibroblasts (HAFs) were seeded on PGS-coated glass slides and polystyrene plates. The cell density on polystyrene plates was higher than that of cells on PGS-coated slides for approximately 2.5 weeks. However, at that time point, the cell density on PGS surpassed the density of HAFs on polystyrene. Cell viability and growth were monitored with the WST-1 assay. HAFs were viable throughout the course of the study, with similar trends on PGD and polystyrene. In order to further understand the applications that would be suitable for PGD, the *in vitro* degradation rates were explored. By immersing polyester samples in phosphate buffered saline (PBS) at 37 °C for 20, 40, and 90 day, the mass loss due to hydrolysis was calculated. A negligible change in mass was observed after 20 days; only 6 % mass loss occurred after 40 days. Over the course of the entire study (90 days), a total of 13 % mass loss was noted. This result was considered ideal, as the longer hydrolytic lifetime would allow more time for natural tissue to populate a PGD device.

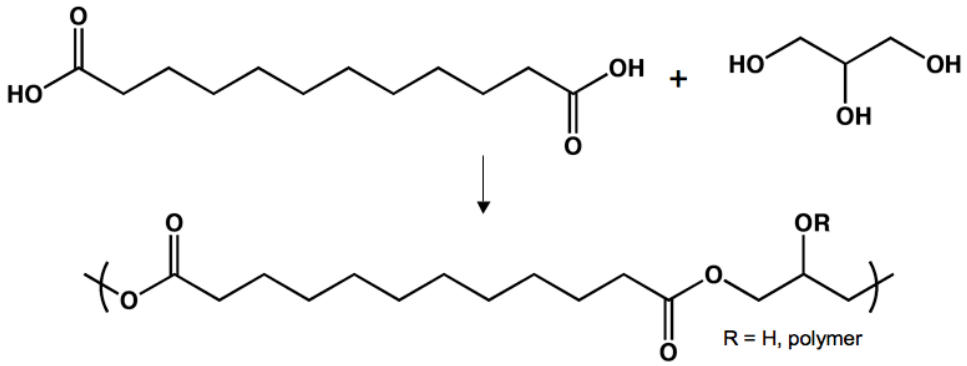

Figure 1.7. Synthesis of poly(glycerol dodecanedioate).

1.2.6 Poly(1,12-Dodecanediol Malate)

In 2009, a novel polyester was described in literature that introduced a new monomer to thermal polycondensation – malic acid (Figure 1.8).[59] An intermediate in the CAC, malic acid is naturally present in the human metabolism. With ideal melting properties for thermal polycondensation, malic acid is a diacid that can act as a cross-linking agent due to the presence of a secondary alcohol. By combining this monomer with 1,12-dodecanediol at several different curing conditions, a series of poly(1,12-dodecanediol malate) (PDM) polyester thermosets were designed. Similar to other materials described in this chapter, a viscous pre-polymer was obtained that could be added to molds in order to create 3-dimensional scaffolds. Focusing on future applications of soft tissue engineering, PDM was designed to be flexible and elastic. These expectations were realized when mechanical evaluation revealed a range of YM (0.98 – 4.04 MPa), UTS (0.21 – 4.16 MPa), and RS (25.27 – 737.48 %).

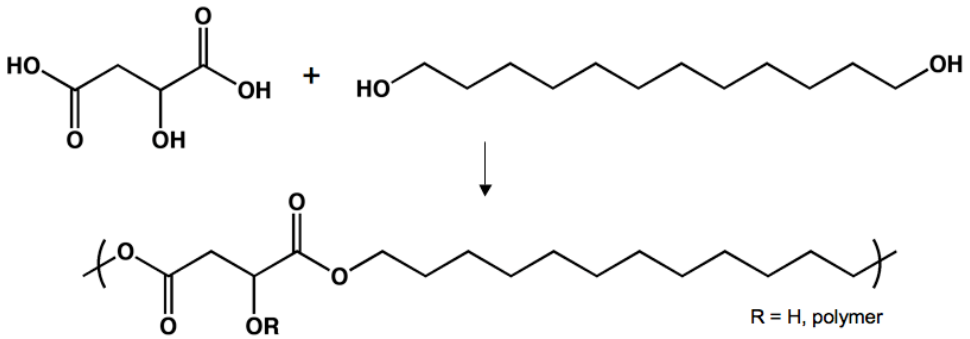

Figure 1.8. Synthesis of poly(1,12-dodecanediol malate).

The fact that malic acid naturally occurs in mammalian cells was thought to minimize the potential for cytotoxic effects of the PDM series of biomaterials. In order to test this hypothesis, L929 mouse fibroblasts were seeded onto PDM films that were cured at different temperatures and for different lengths of time. Cell proliferation was observed to be similar

on all materials, including an unspecified positive control. Also, over the course of a 4-week study in PBS, the PDM polyesters lost between 1 % and 9% of their mass due to degradation. In consideration of future applications in the biomedical fields, scaffolds were designed that have relevance to tissue engineering. Using a supercritical CO_2 foaming method, a porous PDM scaffold was fabricated. The resulting films were able to achieve up to 65 % porosity. To date, the *in vitro* characterization of the PDM series of polyester thermosets indicates that they have potential as soft tissue scaffolds. Further *in vivo* studies will be required in order to determine future success of these materials.

1.2.7 Poly[(Glycerol Sebacate) Citrate]

In an effort to improve upon their thermoplastic poly(glycerol sebacate) (TMPGS), the research group of Dr. Li Liu looked to incorporate citric acid.[60,61] In order to improve mechanical strength and geometric stability during degradation, PGS pre-polymers were combined with citric acid, which acted as a cross-linker (Figure 1.9). The resulting poly[(glycerol sebacate) citrate] (PGSC) demonstrated macromolecular properties that made it more suitable as a tissue scaffolding material, relative to TMPGS.[62-64] PGSC differs from the majority of the other materials created by thermal polycondensation because it requires two synthetic steps. However, the ease of this polymerization methodology is not lost on PGSC; the process is still efficient and catalyst-free.

The transition from a thermoplastic material to a thermoset was accompanied by several changes in polymer characteristics of PGSC. Compared to the earlier TMPGS, both the sol fraction and the degree of swelling decreased due to cross-linking between polyester chains.[62-64] Also, the TMPGS series of polyesters were able to achieve YM and UTS of 0.05 – 0.70 MPa and 0.10 – 0.70 MPa, respectively. Novel PGSC thermosets displayed a YM

range of 0.61 – 3.26 MPA and exhibited 0.63 – 1.46 MPa UTS; RS for these elastomers varied between 51 – 170 %. As all materials were completely amorphous at room temperature, all deformations in the PGSC materials were completely reversible. Because these materials were designed with biomedical applications in mind, hydrolytic degradation was also monitored. By adjusting the duration of the curing period, the degradation rates could be controlled. However, by incorporating sebacic acid, hydrolysis would proceed slower than other materials discussed in the chapter due to the hydrophobic nature of that monomer. During a 4-week study, PGSC materials displayed 12 – 23 % mass loss. A notable difference when compared to TMPGS, the 3-dimensional geometry of the PGSC samples was maintained throughout degradation.

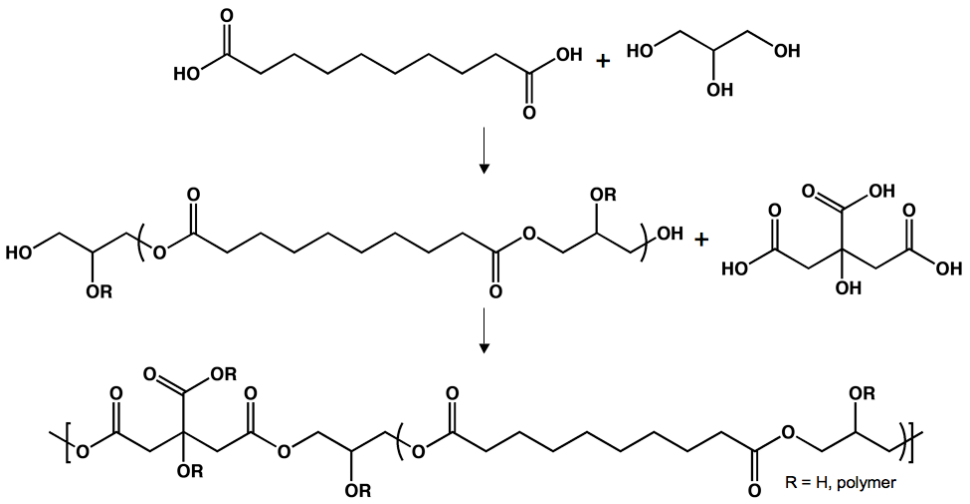

Figure 1.9. Synthesis of poly[(glycerol sebacate) citrate].

PGSC was also utilized in a series of composites containing carbon nanotubes (CNTs).[65] After synthesizing pre-polymers, CNTs were added to the polyester reaction and stirred to evenly distribute them. Four different composites were designed: 0.5, 1, 2, and 3 wt % CNTs, with a control of pure PGSC. Mechanically, these composites outperformed the

polyester control (YM = 6.9 MPa; UTS = 2.7 MPa). The addition of CNTs resulted in significant increases in the YM (6.6 – 9.2 MPa) and the UTS (2.8 – 4.4 MPa). In addition, the composites displayed similar RS (40 – 44 %), compared to PGSC (40 %). Also, the presence of the CNTs had dramatic effects on the degradation profiles of the hybrid materials. All four composites (0.5, 1, 2, 3 wt % CNTs) experienced hydrolysis at approximately the same rate, which was slower than that of PGSC. After 46 d of degradation the PGSC-CNT materials had lost ~ 40 – 50 % of their initial masses; pure PGSC lost ~ 90 % of it mass in the same amount of time.

In vitro cytotoxicity was also studied in order to determine the practicality of utilizing PGSC composites as a biomaterial in future applications. Cells were cultured in composite extracts. Interestingly, the pure polyester (no CNTs) was the most cytotoxic material, by far, at the 7 d time point. The addition of the CNTs into the polymeric matrix dramatically increased the biocompatibilities of the resulting composites. One hypothesis regarding this trend is that the CNTs are able to absorb the acidic sol fraction. However, this explanation may not be entirely accurate, as the presence of the CNTs did not significantly affect the sol fraction of the composites, relative to pure PGSC.

1.2.8 Poly[(1,2-Propanediol Sebacate) Citrate]

A series of manuscripts have recently been prepared that describe the synthesis of another two-step polyester elastomer simlar to PGSC. Sebacic acid and 1,2-propanediol were combined in the initial step, resulting in oligomers (Figure 1.10).[66] To form pre-polymers, citric acid was again used as the cross-linking agent due to its prevalence in biology and its propensity to impart mechanical strength to resulting materials. The final materials were named poly[(1,2-propanediol sebacate) citrate] (PPSC). The curing step was

consistently short (12 – 36 h), leading to soft and flexible polyester elastomers. In addition to the duration of the post-polymerization period, the ratio of monomers was also altered in order to gain further control of the macromolecular properties of PPSC. Considering all versions of these materials based on the different cross-linking conditions, the YM ranged between 0.60 – 1.23 MPa, the UTS spanned between 0.87 – 2.12 MPa, and the RS varied between 225 – 431 %. Although the different curing conditions imparted large effects on the mechanical properties, the hydrophobicity did not change significantly between the different polymers. The many versions of PPSC only achieved a range of contact angle measurements of approximately 5 ° (64 – 69 °). Despite the fact that hydrophobicity is one factor in determining the rate of degradation, the PPSC thermosets were still able to achieve a broad distribution of hydrolysis rates. By varying the curing conditions, mass loss of ~ 85 % can be tuned to occur after 2, 2.5, or 3 weeks. Further control over hydrolytic degradation should be possible by creating new temperatures and lengths of time for post-polymerization.

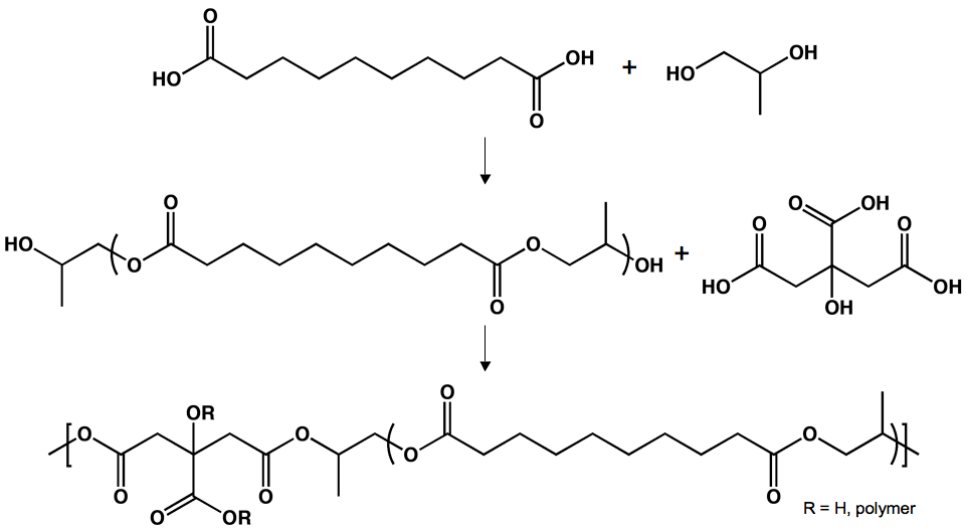

Figure 1.10. Synthesis of poly[(1,2-propanediol sebacate) citrate].

In addition to characterizing the bulk PPSC materials, a series of composites were also studied.[67] By incorporating nanocrystals of hydroxyapatite (nHAp) into the polyester matrix, the mechanical characteristics of the thermosets were dramatically altered. By controlling the amount of nHAp in the polymers (5 – 20 wt %), PPSC achieved YM, UTS, and RS of 0.29 – 3.60 MPa, 0.89 – 8.21 MPa, and 256 – 320 %, respectively. The hydrophobicity of these materials was also affected by the composition, with contact angles varying between 96 ° and 112 °. Additionally, the *in vitro* degradation rates of these materials were shown to decrease when incorporating larger amounts of nHAp into the polyester matrix; the mass loss varied between 60 % in 11 days (5 wt % nHAp) and 40 % in 26 days (20 wt % nHAp).

These materials were expected to be biologically benign as all of the monomers have been successfully incorporated into other biomaterials.[22] In order to determine whether PPSC-nHAp would follow the same pattern, L929 mouse fibroblasts were cultured with medium that contained extracts from the different composites. Comparing cell proliferation and morphology, composites with 10, 15, and 10 wt % nHAp were determined to be non-cytotoxic. Results also indicated that inclusion of larger amounts of nHAp in the polyesters seemed to increase the biocompatibility of these PPSC hybrid materials.

1.2.9 Poly(1,8-Octanediol Citrate -co- 1,8-Octanediol Sebacate)

In another tangent to the work of Dr. Langer and Dr. Ameer, a unique combination of their monomers led to the design of a new polyester elastomer.[68] Sebacic acid, citric acid, and 1,8-octanediol were co-polymerized, resulting in poly(1,8-octanediol citrate -co- 1,8-octanediol sebacate) (POCOS) (Figure 1.11). However, while PGSC was synthesized in a two-step process, POCOS only requires a single step; all of the monomers are combined and

randomly polymerized together. These polyesters were also shown to be compatible with fabrication strategies, such as compression molding and particulate leaching, which have shown promise in the design of cell scaffolds. Additionally, while only 3 materials were synthesized, their mechanical properties show a good variety between soft and moderate materials. The range of YM, UTS, and RS for POCOS are 0.19 – 1.10 MPa, 0.24 – 0.63 MPa, and 127 – 231 %, respectively. Uniquely, the material resulting from 2 parts 1,8-octanediol, 1 part citric acid, and 1 part sebacic acid was both the strongest and most flexible material. This ratio allows for the material to be flexible without sacrificing mechanical strength. In addition, the inclusion of sebacic acid in the starting materials increases the *in vitro* hydrolytic degradation due to the hydrophobic characteristics of this monomer. While a host of POCOS thermosets can be prepared by altering monomer feed ratios and curing conditions, to date, no subsequent manuscripts have described the design of other POCOS materials or their biocompatibilities.

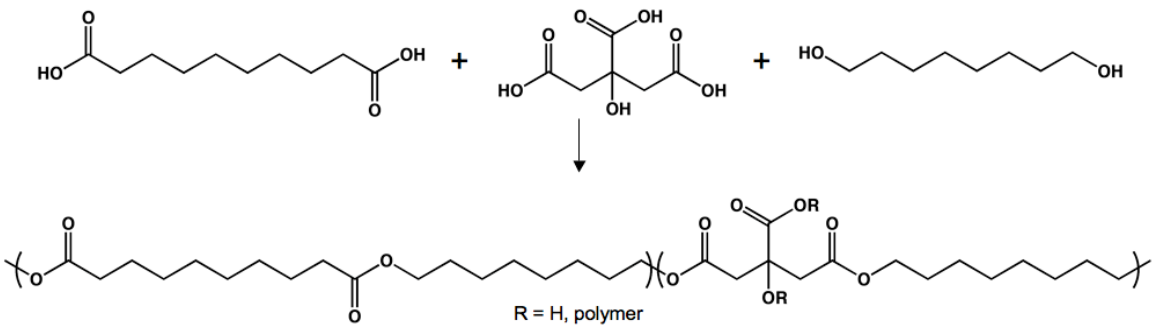

Figure 1.11. Synthesis of poly[(1,2-propanediol sebacate) citrate].

1.3 Photocurable Biodegradable Polyesters

Although both photocurable and thermally cured thermosets continue to be the focus of a significant portion of biomaterial research, the ability to cross-link biodegradable

materials with light offers many benefits over thermal gelation. Significantly faster curing periods (minutes vs. days) and lower curing temperatures (room temperature vs. 80 – 150 °C) are easily accessible through photocuring. As such, photo-initiated cross-linking provides a route to a curing process that is less harsh when compared to thermal cross-linking procedures. As such, fragile cargos, including therapeuticss and proteins, can be encapsulated in thermosets that are cured with light; this characteristic enables the design of drug releasing particles, stents, and sutures.[69,70]

1.3.1 Poly(Glycerol Sebacate Acrylate)

One limitation to the PGS system is that long-term thermal curing could limit encapsulation or application. In an attempt to overcome this challenge, Nijst *et al.* described the design of a photocurable PGS with tunable mechanical properties and degradation rates.[71,72] By deprotonating free hydroxyl groups and appending acrylate groups, irradiation with UV light yielded elastomeric networks (Figure 1.12). Additionally, by varying the degree of acrylation relative to the molar equivalents of free alcohols in the PGS pre-polymer, the mechanical characteristics and degradation rates of the resulting materials could be finely tuned. The YM, UTS, and RS ranged from 0.05 to 1.38 MPa, 0.05 to 0.50 MPa, and 47 to 170 %, respectively. Interestingly, the PGSA pre-polymer could be combined with other acrylated molecules, offering extended control of macromolecular properties. The co-polymerization of PEG-diacrylate with PGSA enabled further control of characteristics such as mechanical strength, water swelling, hydrophobicity, and degradation rates. *In vitro* biocompatibility was determined by observing adhesion and proliferation of primary human foreskin fibroblasts on different PGSA films.

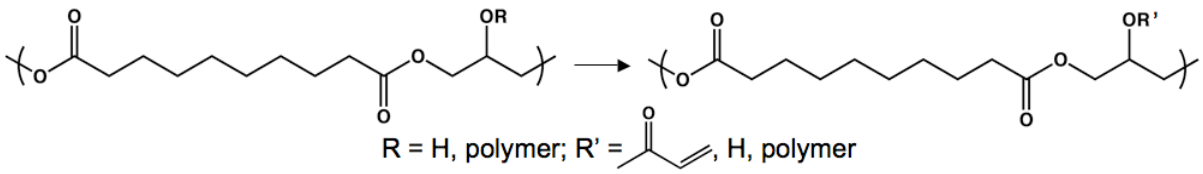

Figure 1.12. Synthesis of poly(glycerol sebacate acrylate).

The Langer research group very quickly found a practical and inventive application for the photocurable PGSA. There is a need for strong biodegradable adhesives that can remain attached to tissue while not undergoing permanent deformation when faced with stress. Such a material could be used to replace sutures and staples or to aid in the treatment of ulcers and burns. There seemed to be great potential for PGSA in this regard due to its biocompatibility and the ability to tune its macromolecular properties. In order to design a biodegradable adhesive, Mahdavi *et al.* drew inspiration from the gecko's ability to adhere to vertical and inverted surfaces.[73] Research has observed that this phenomenon is based on the micro- and nano-textured feet of geckos, and many examples of gecko-based adhesives have been previously described for material purposes.[74,75] However, by transferring micro- and nano-scale features to PGSA from etched silicon wafers, gecko-like adhesive tapes aimed at biomedical applications were fabricated. In order to allow the embossed PGSA films to irreversibly bond to tissues in wet conditions (as would be needed *in vivo*), the PGSA surface was functionalized with a carbohydrate-based coating. Oxidized dextran was chosen due to the presence of aldehydes, which serve two purposes: (1) free alcohols can react with oxidized dextran to form hemiacetals, creating a covalent anchor between the carbohydrate chains and PGSA and (2) aldehydes can also react with amines, ubiquitous in biological materials, to form imines, allowing for covalent linkages between the "glue" and tissues. The resulting adhesives combine the bonding forces of gecko feet and covalent bonds.

As a proof-of-concept, the covalent modification of amine-functionalized glass with oxidized dextran was tested. X-ray photoelectron spectroscopy of the surfaces verified the formation of imine bonds. Additionally, after allowing the carbohydrate derivative and the amine-modified glass to react, the oxidized dextran could not be removed by rinsing the surface. Non-oxidized dextran could be completely removed from the surface in a similar experiment, demonstrating the role of the aldehydes groups in immobilization. Furthermore, both *in vitro* and *in vivo* adhesion to tissue was studied. In addition to being biocompatible, the embossed PGSA films that were coated in oxidized dextran demonstrated significantly more adhesion than flat surfaces and films that were not coated with oxidized dextran. Tissue adhesion could be optimized by varying the dimensions of the features on the embossed PGSA films, allowing for another level of control over interfacial adhesion. Aiming to surpass the initial success of this preliminary investigation, current research is attempting to design materials for organ-specific applications that may be able to deliver drugs in addition to acting as an adhesive.

1.3.2 Methacrylated Poly[Oligo(Ethylene Glycol) Adipate]

Similar to the technique used to convert PGS into the photoactive PGSA, terminal hydroxyl groups of linear polymers can be transformed into acrylates or methacrylates. By controlling the stoichiometric ratio of the monomers, polycondensation can result in macrodiols that can eventually be acrylated or methacrylated (Figure 1.13). Employing this strategy, Dr. Jinrong Liu designed photocurable biomaterials from three common, inexpensive, and well-studied monomers: adipic acid, di(ethylene glycol), and tetra(ethylene glycol).[76] Catalyzed polycondensation was an attractive synthetic method due to the ease with which the molecular weights of the resulting polyesters can be controlled. This aspect is

critical in that the most common strategy used to alter the mechanical properties of end-capped polymers is to adjust the molecular weight. As such, polycondensation offered a relatively simple route for controlling the mechanical profiles of these polyesters. The oligo(ethylene glycol)-based polymer precursors were synthesized at 1,000, 2,000, 4,000, or 7,000 g/mol.

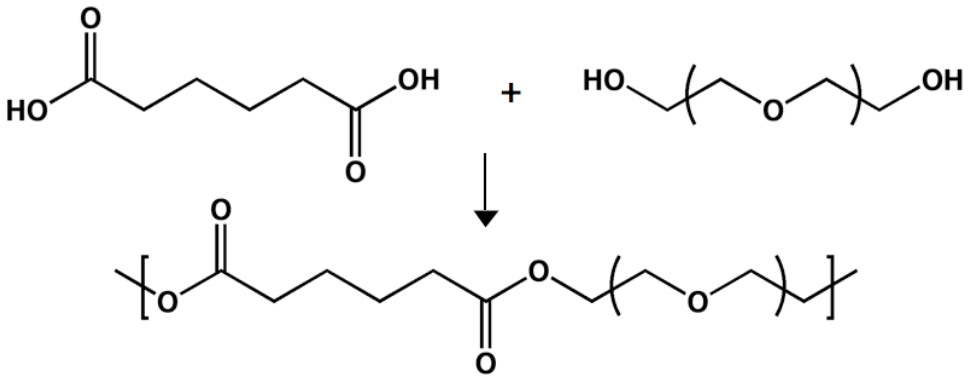

Figure 1.13. Synthesis of poly[oligo(ethylene glycol) adipate].

After methacrylation of the macrodiols, the resulting polymers were irradiated with UV light for 1 min in the presence of a photoinitiator. The ranges of YM, UTS, and RS for these polyester thermosets are 0.12 – 10.3 MPa, 0.6 – 1.5 MPa, and 15 – 165 %, respectively. These values encompass some mechanical properties of several soft tissues, including knee articular cartilage and the cerebral vein. *In vitro* degradation was also studied. Over the course of a 5-week study, these oligo(ethylene glycol)-based polymers experienced 6 – 14 % mass loss due to hydrolysis. The mechanical properties were also studied over the course of the *in vitro* degradation study. As expected due to degradation, the YM of the polyesters decreased over the course of the 5-week period.

Because these materials were designed with biomedical applications in mind, the cytotoxicity and biocompatibility were monitored. To determine how cells respond to these

samples *in vitro*, NIH 3T3 fibroblasts were seeded onto thin films. Compared to films of PLGA, fibroblasts seemed healthy with normal and spread morphologies. *In vivo* experiments were also conducted with these polyester elastomers through subcutaneous implantation. Similar to the trend observed during *in vitro* trials, the mechanical properties of the polymer samples decreased with increasing time *in vivo*. Again, this result was attributed to degradation of the polyester backbone, which led to a decrease in the cross-linking density. After 1 week of implantation, histological evaluation was performed in order to determine the response of the living system to the polymer. The presence of a fibrous capsule was noted. In general, the oligo(ethylene glycol)-based materials were determined to be suitable candidates for future biomedical studies involving polyester implants.

1.3.3 Poly(Propylene Fumarate)

Since its introduction, poly(propylene fumarate) (PPF) has been a commonly studied biomaterial (Figure 1.14).[77] The degradation products are non-toxic because PPF was composed of two resorbable monomers. Similar to several materials synthesized from thermal polycondensation, the polymer properties of PPF are dependant upon the methods used for synthesis, cross-linking, and fabrication.[78-81] The *in vitro* degradation rates of bulk and porous (70 % and 80 %) samples were first studied so that the appropriate applications could be determined. Logically, the biodegradation rate was dependent upon both the size of the pores and the overall porosity; the sample that degraded the fastest had more and larger pores. Substantial hydrolysis was observed over a 32-week study. The amount of PPF mass remaining after degradation ranged from 70 % - 85 %. After observing these degradation rates, bone tissue engineering has been the most common application for PPF. Bone was an

obvious tissue for this application due to the high degree of potential cross-linking (an alkene in each repeat unit) and the hydrophobicity of PPF.

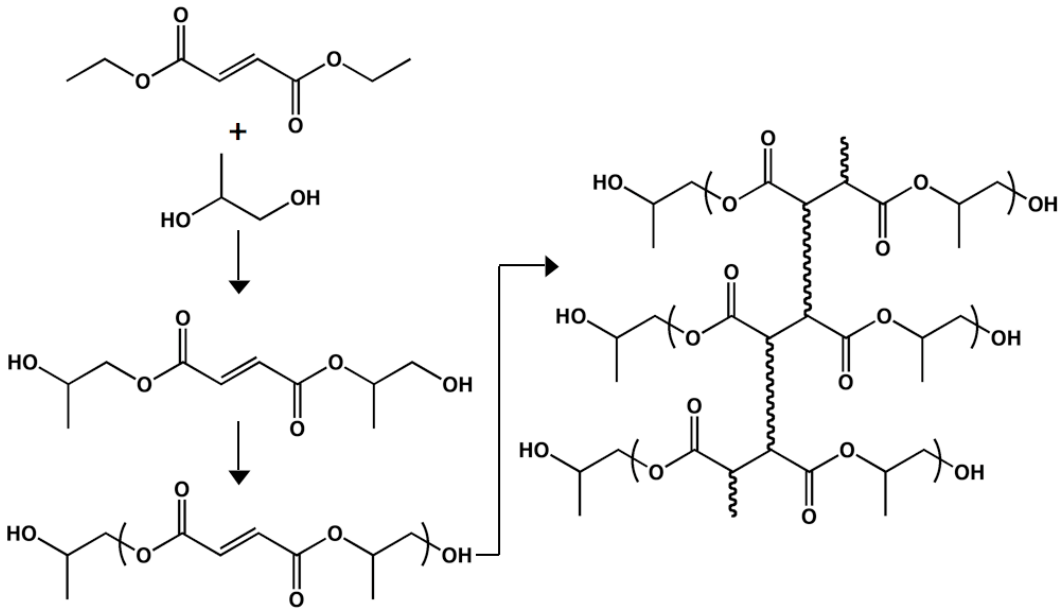

Figure 1.14. Synthesis of poly(propylene fumarate).

Because bone exists *in vivo* near soft and hard tissues, PPF was monitored in animal models to determine biocompatibility when interacting with both types of tissue.[82] For these studies, rabbits were used as the living system. Samples were implanted subcutaneously so that PPF could be observed in an environment of soft tissue. A fibrous capsule was observed surrounding the scaffolds. However, the size of the cellular encapsulation decreased as a function of time, implying that the PPF samples were minimally toxic to the rabbit. Due to surface degradation of the polyester backbone, the porosity of PPF implants increased with time throughout the study. PPF was also studied in bone engineering so that it could be monitored in hard tissue. Polyester samples were inserted into non-fatal cranial defects in the rabbits. Response of hard tissue to PPF was similar to that of soft tissues. While scaffolds contained some bone ingrowth, 40 % of the samples exhibited direct contact with bone.

Although other biomaterials have performed similarly, PPF is unique due to the slower degradation rate and the minimal thickness of the fibrous capsule.[83-86] Based on these results, PPF has been considered a promising candidate for soft and hard tissue engineering.

1.3.4 Poly(But-2-ene-1,4-diyl Malonate)

Similar to the strategy employed with PPF, another system took advantage of an internal alkene as a photoactive motif.[87] Malberg *et al.* recently described the synthesis of linear poly(but-2-ene-1,4-diyl malonate) (PBM) with a 2-step thermal polycondensation (Figure 1.15). The first step (at 110 °C) involved obtaining oligomers of malonic acid and 2-butene-1,4-diol and evacuating all observable water. The temperature was then increased to 210 °C for a second esterification step, allowing the molecular weight of the polymer to grow. Similar to other syntheses described in this chapter, no catalysts were needed in order to obtain the final polyesters. By varying the length of the second step, the molecular weight of the polyesters could be tuned (4750 – 12100 g/mol). By controlling the stoichiometry in the monomer feed, the resulting polymers were macrodiols. With hydroxyl groups at the termini of the polyester chains, PBM was combined with ε-caprolactone and L-lactide through ring-opening polymerization. The resulting co-polymers achieved molecular weights of up to 80,000 g/mol. The polydispersity indices (PDIs) of these co-polymers were very high (2.1 – 3.5) when compared to those of controlled ring-opening polymerization (< 1.2) or polycondensation (< 2). This characteristic most likely resulted from the high PDIs of the PBM macrodiols (2.6 – 4.1).

Due to the presence of alkenes along the polymer backbone, PBM was able to form thermosets through radical cross-linking. Malberg *et al.* chose benzophenone as the initiator for photocuring. Upon UV irradiation for 10 min, benzophenone degraded homolytically,

allowing radicals to cure the alkene-containing PBM chains. The co-polymers were also able to cross-link through this mechanism. The ranges of YM, UTS, and RS for PBM-based polyester thermosets are 12 – 930 MPa, 4.5 – 37 MPa, and 12 – 47 %, respectively. Currently, the future applications are directed towards the biomedical field.

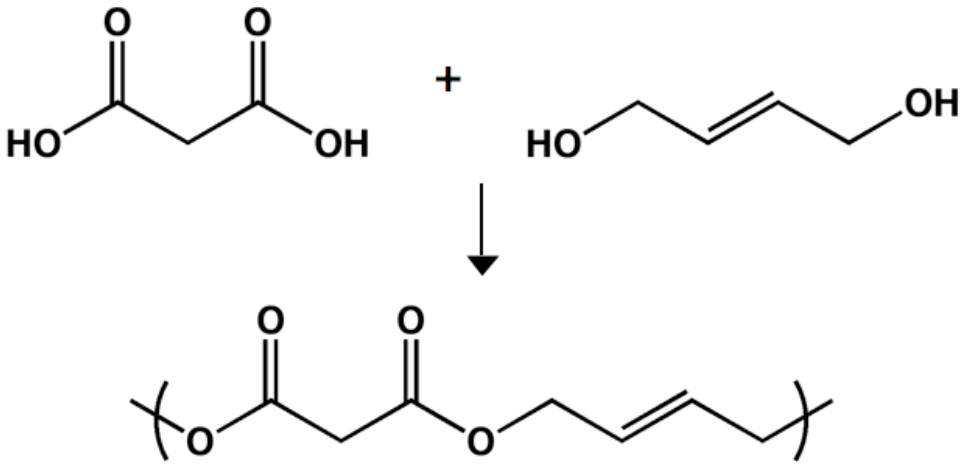

Figure 1.15. Synthesis of poly(but-2-ene-1,4-diyl malonate).

1.4 Conclusions

The materials discussed here offer tremendous potential for use in biomedical applications. A wide range of polyesters can be designed from thermal polycondensation and photocuring. Resulting in minimal toxicity, many monomers endogenous to human metabolic pathways have been selected for these polymerization strategies. The macromolecular properties of the resulting polyesters, including hydrophobicities, degradation rates, and mechanical profiles, span a range that encompasses properties displayed by a number of biological specimens. A polymer characteristic that has recently been deemed important in scaffold design is the relationship between the mechanical properties of the original tissue and those of the synthetic polymer. Finally, several of these

biomaterials have been characterized in *in vitro* and/or *in vivo* biological settings, with many being described as biocompatible.

1.5 Dissertation Organization

This dissertation is organized into six chapters. Chapter I is a general discussion of biodegradable polyesters and their biomedical applications. Chapter II describes the synthesis of novel polyesters based on erythritol, a sugar alcohol. Chapter III discusses a class of polyester thermosets based on α-ketoglutaric acid, an intermediate of the citric acid cycle. Chapter IV describes the synthesis and characterization of polyketoesters composed of 4-ketopimelic acid, citric acid, and a diol (1,4-cyclohexanedimethanol or 1,6-hexanediol). Chapter V discusses several photocurable polyester thermosets based on itaconic acid, a natural and renewable monomer. Chapter VI describes general conclusions and future research projects. Research describing the etching of poly(triol α-ketoglutarate), supplemental data for Chapters II through V, and permissions are presented in the appendices. The material discussed in Chapter V will be filed for a patent application.

1.6 References

(1) Langer, R.; Vacanti, J. P. *Science* 1993, *260*, 920-926.

(2) Yang, S.; Leong, K. F.; Du, Z.; Chua, C. K. *Injury - Int. J. Care Injured* 2008, *39*, S77-S87.

(3) Stoop, R. *Tissue Eng.* 2001, *7*, 679-689.

(4) Gosline, J.; Lillie, M.; Carrington, E.; Guerette, P.; Ortlepp, C.; Savage, K. *Philos. Trans. R. Soc. London, Ser. B* 2002, *357*, 121-132.

(5) Shepherd, D. E.; Seedhom, B. B. *Rheumatology (Oxford)* 1999, *38*, 124-132.

(6) Thambyah, A.; Nather, A.; Goh, J. *Osteoarthritis Cartilage* 2006, *14*, 580-588.

(7) Sung, H.; Chang, Y.; Chiu, C.; Chen, C.; Liang, H. *Biomaterials* 1999, *20*, 1759-1772.

(8) Dahms, S. E.; Piechota, H. J.; Dahiya, R.; Lue, T. F.; Tanagho, E. A. *Br J Urol* 1998, *82*, 411-419.

(9) Amsden, B. *Soft Matter* 2007, *3*, 1335-1348.

(10) Webb, A. R.; Yang, J.; Ameer, G. A. *Expert Opin. Biol. Ther.* 2004, *4*, 801-812.

(11) Barrett, D. G.; Luo, W.; Yousaf, M. N. *Polym. Chem.* 2010, , 296-302.

(12) Barrett, D. G.; Yousaf, M. N. *Macromolecules* 2008, *41*, 6347-6352.

(13) Shi, R.; Chen, D.; Liu, Q.; Wu, Y.; Xu, X.; Zhang, L.; Tian, W. *Int. J. Mol. Sci.* 2009, *10*, 4223-4256.

(14) Balguid, A.; Rubbens, M. P.; Mol, A.; Bank, R. A.; Bogers, A. J. J. C.; Van Kats, J. P.; De Mol, B. A. J. M.; Baaijens, F. P. T.; Bouten, C. V. C. *Tissue Eng.* 2007, *13*, 1501-1511.

(15) Gupta, B. S.; Kasyanov, V. A. *J. Biomed. Mater. Res.* 1997, *34*, 341-349.

(16) Lee, J. M.; Boughner, D. R. *Circ Res* 1985, *57*, 475-481.

(17) Monson, K. L.; Goldsmith, W.; Barbaro, N. M.; Manlet, G. T. *J. Biomech. Eng.* 2003, *125*, 288-294.

(18) Waldman, S. D.; Spiteri, C. G.; Grynpas, M. D.; Pilliar, R. M.; Kandel, R. A. *Tissue Eng.* 2004, *10*, 1323-1331.

(19) Seliktar, D.; Nerem, R. M.; Galis, Z. S. *Tissue Eng.* 2003, *9*, 657-666.

(20) Stegemann, J. P.; Nerem, R. M. *Ann. Biomed. Eng.* 2003, *31*, 391-402.

(21) Niklason, L. E.; Gao, J.; Abbott, W. M.; Hirschi, K. K.; Houser, S.; Marini, R.; Langer, R. *Science* 1999, *284*, 489-493.

(22) Barrett, D. G.; Yousaf, M. N. *Molecules* 2009, *14*, 4022-4050.

(23) Wang, Y.; Kim, Y. M.; Langer, R. *J. Biomed. Mater. Res. A.* 2003, *66*, 192-197.

(24) Wanamaker, C. L.; Tolman, W. B.; Hillmyer, M. A. *Biomacromolecules* 2009, *10*, 443-448.

(25) Pitt, C. G.; Gratzl, M. M.; Kimmel, G. L.; Surles, J.; Schindler, A. *Biomaterials* 1981, *2*, 215-220.

(26) Storey, R. F.; Hickey, T. P. *Polymer* 1994, *35*, 830-838.

(27) Wang, Y.; Ameer, G. A.; Sheppard, B. J.; Langer, R. *Nat. Biotechnol.* 2002, *20*, 602-606.

(28) Engelmayr, G. C.,Jr; Cheng, M.; Bettinger, C. J.; Borenstein, J. T.; Langer, R.; Freed, L. E. *Nat. Mater.* 2008, *7*, 1003-1010.

(29) Bruggeman, J. P.; Bettinger, C. J.; Nijst, C. L. E.; Kohane, D. S.; Langer, R. *Adv. Mater. (Weinheim, Ger.)* 2008, *20*, 1922-1927.

(30) Bruggeman, J. P.; de Bruin, B.; Bettinger, C. J.; Langer, R. *Biomaterials* 2008, *29*, 4726-4735.

(31) Bettinger, C. J.; Bruggeman, J. P.; Borenstein, J. T.; Langer, R. S. *Biomaterials* 2008, *29*, 2315-2325.

(32) Bettinger, C. J.; Kulig, K. M.; Vacanti, J. P.; Langer, R.; Borenstein, J. T. *Tissue Eng. Part A.* 2009, *15*, 1321-1329.

(33) Bettinger, C. J.; Bruggeman, J. P.; Borenstein, J. T.; Langer, R. *J. Biomed. Mater. Res. A.* 2009, *91*, 1077-1088.

(34) Roy, D. R.; Parthasarathi, R.; Maiti, B.; Subramanian, V.; Chattaraj, P. K. *Bioorg. Med. Chem.* 2005, *13*, 3405-3412.

(35) Yang, J.; Webb, A. R.; Ameer, G. A. *Adv. Mater. (Weinheim, Ger.)* 2004, *16*, 511-516.

(36) Yang, J.; Webb, A. R.; Pickerill, S. J.; Hageman, G.; Ameer, G. A. *Biomaterials* 2006, *27*, 1889-1898.

(37) Yang, J.; Motlagh, D.; Allen, J. B.; Webb, A. R.; Kibbe, M. R.; Aalami, O.; Kapadia, M.; Carroll, T. J.; Ameer, G. A. *Adv. Mater. (Weinheim, Ger.)* 2006, *18*, 1493-1498.

(38) Yang, J.; Motlagh, D.; Webb, A. R.; Ameer, G. A. *Tissue Eng.* 2006, *11*, 1876-1886.

(39) Yang, J.; Motlagh, D.; Webb, A. R.; Ameer, G. A. *Tissue Eng.* 2005, *11*, 1876-1886.

(40) Roeder, R.; Wolfe, J.; Lianakis, N.; Hinson, T.; Geddes, L. A.; Obermiller, J. *J. Biomed. Mater. Res.* 1999, *47*, 65-70.

(41) Ma, P. X.; Zhang, R. *J. Biomed. Mater. Res.* 2001, *56*, 469-477.

(42) Eagleton, M. J.; Ouriel, K.; Shortell, C.; Green, R. M. *Surgery* 1999, *126*, 759-765.

(43) Xue, L.; Greisler, H. P. *J. Vasc. Surg.* 2003, *37*, 472-480.

(44) Noh, I.; Goodman, S. L.; Hubbell, J. A. *J. Biomater. Sci. , Polym. Ed.* 1998, *9*, 407-426.

(45) Herring, M. B.; Dilley, R.; Jersild, R. A.,Jr; Boxer, L.; Gardner, A.; Glover, J. *Ann Surg* 1979, *190*, 84-90.

(46) Motlagh, D.; Allen, J.; Hoshi, R.; Yang, J.; Lui, K.; Ameer, G. *J. Biomed. Mater. Res. A*. 2007, *82*, 907-916.

(47) Heijnen, H. F. G.; Schiel, A. E.; Fijnheer, R.; Geuze, H. J.; Sixma, J. J. *Blood* 1999, *94*, 3791-3799.

(48) Gorbet, M. B.; Sefton, M. V. *Biomaterials* 2004, *25*, 5681-5703.

(49) Lee, S.; Brennan, F. R.; Jacobs, J. J.; Urban, R. M.; Ragasa, D. R.; Glant, T. T. *J. Orthop. Res.* 1997, *15*, 40-49.

(50) Heil, T. L.; Volkmann, K. R.; Wataha, J. C.; Lockwood, P. E. *J. Oral Rehabil.* 2002, *29*, 401-407.

(51) Zhang, X. Q.; Tang, H.; Hoshi, R.; De Laporte, L.; Qiu, H.; Xu, X.; Shea, L. D.; Ameer, G. A. *Biomaterials* 2009, *30*, 2632-2641.

(52) Zhao, H.; Serrano, M. C.; Popowich, D. A.; Kibbe, M. R.; Ameer, G. A. *J. Biomed. Mater. Res. A.* 2009, *93A*, 356-363.

(53) Ding, T.; Liu, Q.; Shi, R.; Tian, M.; Yang, J.; Zhang, L. *Polym. Degrad. Stab.* 2006, *91*, 733-739.

(54) Migneco, F.; Huang, Y. C.; Birla, R. K.; Hollister, S. J. *Biomaterials* 2009, *30*, 6479-6484.

(55) Liu, G.; Hinch, B.; Beavis, A. D. *J Biol Chem* 1996, *271*, 25338-25344.

(56) Grego, A. V.; Mingrone, G. *Clin Nutr* 1995, *14*, 143-148.

(57) Mortensen, P. B. *Biochim. Biophys. Acta, Lipids Lipid Metab.* 1981, *664*, 349-355.

(58) Mortensen, P. B.; Gregersen, N. *Biochim. Biophys. Acta, Lipids Lipid Metab.* 1981, *666*, 394-404.

(59) Lee, L. Y.; Wu, S. C.; Fu, S. S.; Zeng, S. Y.; Leong, W. S.; Tan, L. P. *Eur. Polym. J.* 2009, *45*, 3249-3256.

(60) Liu, Q. Y.; Tan, T. W.; Weng, J. Y.; Zhang, L. Q. *Biomed. Mater.* 2009, *4*, 025015.

(61) Liu, Q. Y.; Wu, S. Z.; Tan, T. W.; Weng, J. Y.; Zhang, L. Q.; Liu, L.; Tian, W.; Chen, D. F. *J. Biomater. Sci.* 2009, *20*, 1567-1578.

(62) Liu, Q. Y.; Tian, M.; Ding, T.; Shi, R.; Feng, Y. X.; Zhang, L. Q.; Chen, D. F. *J. Appl. Polym. Sci* 2007, *103*, 1412-1419.

(63) Liu, Q. Y.; Tian, M.; Ding, T.; Shi, R.; Zhang, L. Q. *J. Appl. Polym. Sci* 2005, *98*, 2033-2041.

(64) Liu, Q. Y.; Tian, M.; Shi, R.; Zhang, L. Q.; Chen, D. F.; Tian, W. *J. Appl. Polym. Sci* 2007, *104*, 1131-1137.

(65) Liu, Q.; Wu, J.; Tan, T.; Zhang, L.; Chen, D.; Tian, W. *Polym. Degrad. Stab.* 2009, *94*, 1427-1435.

(66) Lei, L.; Ding, T.; Shi, R.; Liu, Q.; Zhang, L.; Chen, D.; Tian, W. *Polym. Degrad. Stab.* 2007, *92*, 389-396.

(67) Lei, L.; Li, L.; Zhang, L.; Chen, D.; Tian, W. *Polym. Degrad. Stab.* 2009, *94*, 1494-1502.

(68) Djordjevic, I.; Choudhury, N. R.; Dutta, N. K.; Kumar, S. *Polymer* 2009, *50*, 1682-1691.

(69) Gratton, S. E. A.; Williams, S. S.; Napier, M. E.; Pohlhaus, P. D.; Zhou, Z.; Wiles, K. B.; Maynor, B. W.; Shen, C.; Olafsen, T.; Samulski, E. T.; DeSimone, J. M. *Acc. Chem. Res.* 2008, *41*, 1685-1695.

(70) Htay, T.; Liu, M. W. *Vasc Health Risk Manag* 2005, *1*, 263-276.

(71) Nijst, C. L.; Bruggeman, J. P.; Karp, J. M.; Ferreira, L.; Zumbuehl, A.; Bettinger, C. J.; Langer, R. *Biomacromolecules* 2007, *8*, 3067-3073.

(72) Gerecht, S.; Townsend, S. A.; Pressler, H.; Zhu, H.; Nijst, C. L.; Bruggeman, J. P.; Nichol, J. W.; Langer, R. *Biomaterials* 2007, *28*, 4826-4835.

(73) Mahdavi, A., et al *Proc. Natl. Acad. Sci. U. S. A.* 2008, *105*, 2307-2312.

(74) Lee, H.; Lee, B. P.; Messersmith, P. B. *Nature* 2007, *448*, 338-341.

(75) Geim, A. K.; Dubonos, S. V.; Grigorieva, I. V.; Novoselov, K. S.; Zhukov, A. A.; Shapoval, S. Y. *Nat. Mater.* 2003, *2*, 461-463.

(76) Liu, J. Synthesis, Characterization and Applications of New Photocurable and Biodegradable Elastomers, University of North Carolina at Chapel Hill, Chapel Hill, NC, 2008.

(77) Peter, S. J.; Yaszemski, M. J.; Suggs, L. J.; Payne, R. G.; Langer, R.; Hayes, W. C.; Unroe, M. R.; Alemany, L. B.; Engel, P. S.; Mikos, A. G. *J. Biomater. Sci. , Polym. Ed.* 1997, *8*, 893-904.

(78) Fisher, J. P.; Holland, T. A.; Dean, D.; Engel, P. S.; Mikos, A. G. *J Biomater Sci Polym Ed* 2001, *12*, 673-687.

(79) Fisher, J. P.; Holland, T. A.; Dean, D.; Mikos, A. G. *Biomacromolecules* 2003, *4*, 1335-1342.

(80) Fisher, J. P.; Timmer, M. D.; Holland, T. A.; Dean, D.; Engel, P. S.; Mikos, A. G. *Biomacromolecules* 2003, *4*, 1327-1334.

(81) Timmer, M. D.; Ambrose, C. G.; Mikos, A. G. *J. Biomed. Mater. Res. Part A* 2003, *66*, 811-818.

(82) Fisher, J. P.; Vehof, J. W. M.; Dean, D.; Van der Waerden,Jan Paul C.M.; Holland, T. A.; Mikos, A. G.; Jansen, J. A. *J. Biomed. Mater. Res.* 2002, *59*, 547-556.

(83) Ibim, S. M.; Uhrich, K. E.; Bronson, R.; El-Amin, S. F.; Langer, R. S.; Laurencin, C. T. *Biomaterials* 1998, *19*, 941-951.

(84) Jansen, J. A.; de Ruitjter, J. E.; Janssen, P. T. M.; Paquay, Y. C. G. J. *Biomaterials* 1995, *16*, 819-827.

(85) Solheim, E.; Sudmann, B.; Bang, G.; Sudmann, E. *J Biomed Mater Res* 2000, *49*, 257-263.

(86) Van der Elst, M.; Klein, C. P. A. T.; De Blieck-Hogervorst, J. M.; Patka, P.; Haarman, H. J. T. M. *Biomaterials* 1998, *20*, 121-128.

(87) Malberg, S.; Plikk, P.; Finne-Wistrand, A.; Albertsson, A. -. *Chem. Mater.* 2010, *22*, 3009-3014.

Chapter II

ALIPHATIC POLYESTER ELASTOMERS DERIVED FROM ERYTHRITOL AND α,ω-DIACIDS

Barrett, D. B.; Luo, W.; Yousaf, M. N. *Polym. Chem.* (in press; DOI: 10.1039/b9py00226j).

2.1 Introduction

The demand for biodegradable polymers in medical applications, such as tissue engineering and drug delivery, has motivated the materials community to develop new polymers.[1-3] Recently, elastomeric materials have become popular for soft tissue scaffolds due to their mechanical similarities to blood vessels, heart valves, cartilage, and other soft tissues.[4, 5] While several examples of polyester scaffolds have shown extensive promise, many of these materials suffer from complex or expensive synthetic designs.[4] A simple and facile synthesis would allow easy scale-up for industrial or medical applications.

Within the class of polyester scaffolds, many examples of both thermoplastics and thermosets have been described.[5] Thermosets offer a number of advantages for biomedical applications when compared to thermoplastic materials. For example, thermoplastic elastomers often have crystalline regions, causing heterogeneous degradation and a non-linear loss of mechanical strength.[6, 7] Additionally, the three-demensional (3D) geometry of a thermoplastic material is commonly lost during the hydrolysis period.[8] Alternatively, thermosets can be designed from completely amorphous precursors, allowing for linear degradation and a predictable loss of mechanical strength. Polyester thermosets degrade by a combination of bulk and surface erosion, which often results in the retention of the 3D structure throughout the hydrolytic process.[8]

We believe that the ideal polymer for biomedical applications should possess several characteristics. Biocompatibility and biodegradation are critical to minimize negative biological reactions to the material. The polymer should also be a thermoset with a glass transition temperature that is lower than physiological temperature so that no crystalline regions are present, minimizing the chances of heterogeneous degradation. Also, a wide

range of degradation rates and mechanical properties should be accessible from a single facile and inexpensive design strategy. This would allow the ability to tailor a material's properties to best mimic those of the natural tissue.

This chapter describes the synthesis and characterization of the poly(erythritol dicarboxylate) family of elastomers (PErD). Poly(erythritol glutarate) (PErGl), poly(erythritol adipate) (PErAd), poly(erythritol pimelate) (PErPi), poly(erythritol suberate) (PErSu), poly(erythritol azelate) (PErAz), poly(erythritol sebacate) (PErSe), poly(erythritol dodecanedioate) (PErDo), and poly(erythritol tetradecanedioate) (PErTe) were designed by thermal polycondensation of erythritol and 5-, 6-, 7-, 8-, 9-, 10-, 12-, and 14-carbon α,ω-diacids, respectively. By varying the length of the diacid, the rigidity and hydrophobicity of the resulting materials can be tuned, allowing for control over mechanical properties and degradation rates. The non-cured pre-polymers are easily melted or dissolved for facile processing, demonstrated by embossed films and porous scaffolds. Finally, the cytotoxicity of these materials was studied *in vitro* with human mesenchymal stem cells (hMSCs) and Swiss albino 3T3 (SA) fibroblasts.

2.2 Experimental Section

2.2.1 Materials

All chemicals were purchased from Fisher Scientific (Philadelphia, PA), and used without further purification.

2.2.2 Poly(Erythritol Dicarboxylate) Synthesis

The synthesis of PErD was performed based on methods previously reported.[9, 10] Equimolar amounts of a dicarboxylic acid (glutaric, adipic, pimelic acid, suberic, azelaic,

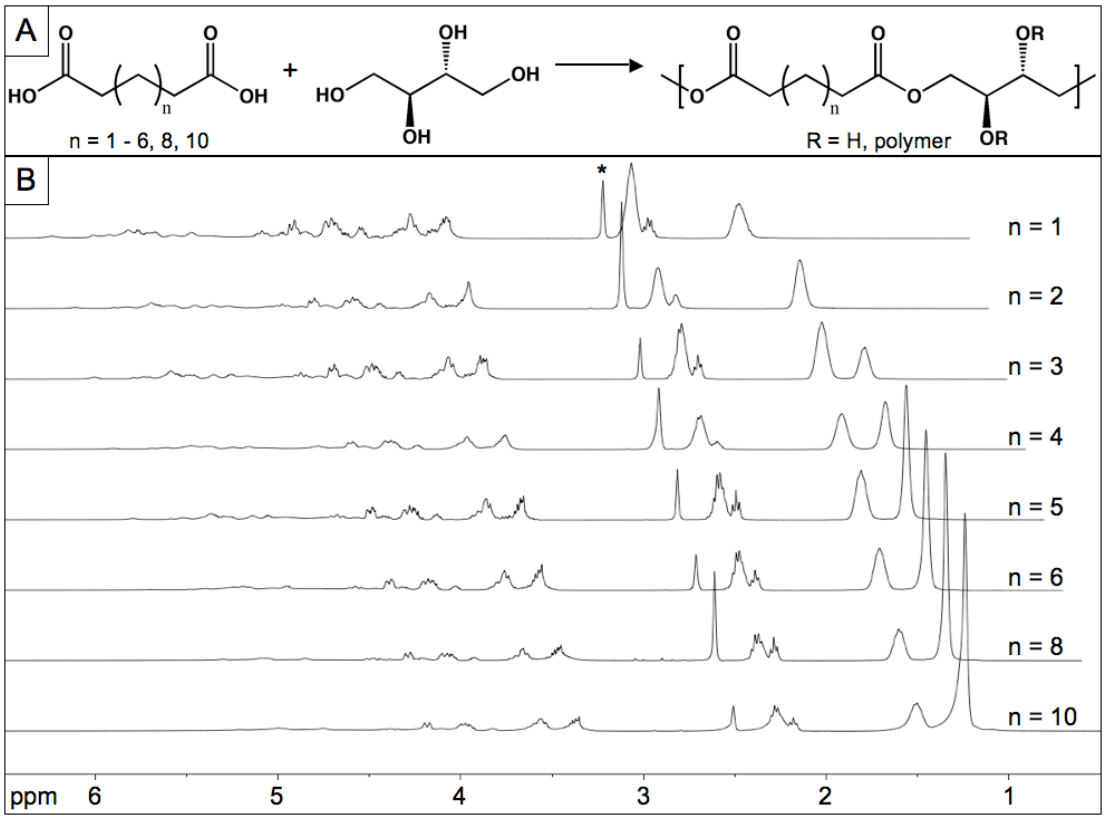

Figure 2.1. Synthesis and NMR spectra of PErD using glutaric, adipic, pimelic, suberic, azelaic, sebacic, dodecanedioic, and tetradecanedioic acids. (A) Thermal polycondensation of erythritol and dicarboxylic acids of differing lengths led to the catalyst-free design of pre-polymers. Further heating of the pre-polymers allowed for the preparation of polyester thermosets. (B) ^{1}H NMR spectra of the pre-polymers OErGl (n = 1), OErAd (n = 2), OErPi (n = 3), OErSu (n = 4), OErAz (n = 5), OErSe (n = 6), OErDo (n = 8), and OErTe (n = 10). The asterisk designates the solvent peak (d_6-DMSO).

sebacic, dodecanedioic, or tetradecanedioic acid) and erythritol were combined in a round bottom flask, which was then sealed. Under an inert environment of argon, monomers were stirred at 145 °C. After a homogenous melt formed, the mixture was stirred for an additional 2 h. The pressure was then reduced to 2 torr, and the materials continued stirring for 7 h. The round bottom flasks were immediately placed into a water bath (room temperature) to quench polycondensation. The pre-polymer was then dissolved in a minimal amount of THF, purified by precipitation in -78 °C methanol, and dried by rotary evaporation. To form elastomeric films, different procedures were followed, depending on the desired properties of

the material. Pre-polymers were cured at either 120 °C for 3 d or at 140 °C for 3 d. Additionally, oligo(erythritol glutarate) was cured at 120 °C for 2 days, resulting in an extremely flexible material.

Table 2.1. Pre-Polymer Characterization

Pre-Polymer	T_g/T_m [a] (°C)	‹M_n›[b] (g/mol)	PDI[b]
n = 1	-7.0	710	1.4
n = 2	-15.7	810	1.1
n = 3	-18.1	790	1.4
n = 4	-21.4	860	1.2
n = 5	-23.6	820	1.5
n = 6	-36.9/60.2	1020	1.6
n = 8	-41.5/63.4	1470	1.9
n = 10	-46.8/66.0	1450	2.2

[a] Determined by DSC; [b] Determined by GPC.

2.2.3 Polyester Characterization

^{1}H NMR spectra of pre-polymers were acquired on a Bruker 400 MHz AVANCE spectrometer in deuterated dimethyl sulfoxide (DMSO). Molecular weights were measured, compared to polystyrene standards, on a Waters GPC system with detection based on refractive index values. The measurements were taken at 40 °C with THF as the mobile phase on three columns in series (Waters Styragel HR2, HR4, and HR5).

Tensile tests were conducted with dry samples on an Instron 5566 at a crosshead speed of 10 mm/min at 25 °C. Samples were cured in a dog-bone-shaped mold with approximate dimensions of 10 mm x 3 mm x 1.5 mm. The Young's modulus (YM; Pa) was calculated according to the linear segment of the stress/strain curve. Three trials were performed and the average was reported. Using

$$n = YM(3RT)^{-1} \quad (1)$$

where R is the universal gas constant (8.3144 J/mol K) and T is the temperature (K), the cross-linking density (n; mmol/L) was calculated.

Table 2.2. Curing Conditions for Poly(Erythritol Dicarboxylate)

Material	Diacid	Temp (°C)	Duration (d)
1	glutaric	120	2
2	glutaric	120	3
3	adipic	120	3
4	pimelic	120	3
5	suberic	120	3
6	azelaic	120	3
7	sebacic	120	3
8	dodecanedioic	120	3
9	tetradecanedioic	120	3
10	glutaric	140	3
11	adipic	140	3
12	pimelic	140	3
13	suberic	140	3
14	azelaic	140	3
15	sebacic	140	3
16	dodecanedioic	140	3
17	tetradecanedioic	140	3

Sol-gel analysis was conducted by soaking films in THF for 24 h at room temperature. After solvent removal, the films were dried, and the percent soluble fraction (Q_s) was calculated by

$$Q_s = (m_i - m_f)m_i^{-1}(100) \quad (2)$$

where m_i and m_f represent the initial and final mass of the elastomer films, respectively. Three trials were performed and the average was reported.

Water swelling (WS) experiments were performed by swelling films in double-distilled H_2O (ddH_2O) for 24 h at room temperature. After removing surface water, the WS was calculated by

$$WS = (m_f - m_i)m_i^{-1}(100) \quad (3)$$

where m_i and m_f represent the initial and final mass of the elastomer films, respectively. Three trials were performed and the average was reported.

Contact angle measurements were obtained using flat polyester films on glass slides. Measurements were performed on a KSV CAM200 contact angle meter with water as the wetting liquid; at least four measurements were recorded.

2.2.4 Complex Film Fabrication

Porous films were prepared by previously reported methods.[11] Emobossed films were designed by adding a small amount of pre-polymer onto a glass slide and heating at 120 °C in a vacuum oven. After 10 min of reduced pressure (~ 50 torr) to remove any gas or solvent, a PFPE mold was placed directly on the pre-polymer.[12-14] The material was allowed to cure as described above, followed by the removal of the mold. To image the embossed films, a Hitachi model 2-4700 scanning electron microscope (SEM) was used after coating the polyesters in ~ 2 nm of a Pd/Au alloy (Cressington 108 auto sputter coater, Cressington Scientific Instruments Ltd.).

2.2.5 *In Vitro* Degradation

To obtain standard degradation rates, approximately 75 mg samples of elastomers were placed in scintillation vials. The elastomers were submerged in phosphate buffered saline (PBS) and samples were then stored in an incubator (37 °C). At weekly intervals, samples

were removed from the incubator, rinsed thoroughly with water, dried, and weighed again. To prevent saturation, PBS was replaced every 7 days. Values were obtained using

$$\text{Mass Loss} = (m_i - m_f)m_i^{-1}(100) \quad (4)$$

where m_i and m_f represent the initial and final mass values, respectively. Each data point was repeated in triplicate and results were reported as the average percent of the original mass lost.

2.2.6 *In Vitro* Cytotoxicity

Growth medium and hMSCs were obtained from Lonza. Stem cell culture protocol and staining were performed as described elsewhere.[15] Two different cell lines were used to assess *in vitro* cytotoxicity: hMSCs and SA fibroblasts. Medium elution tests, according to ISO 10993-5 standards, were performed with both cell lines. Briefly, elastomer samples were sterilized in ethanol for 30 min and washed in PBS for 2 h while under a germicidal lamp. Polyester segments were then added to culture medium and maintained at 37 °C in an incubator for 24 h. The medium-extract solution was then used to culture cells for at least 48 h. After the culture period, cell confluence was examined and toxicity was assessed. Fibroblasts were imaged 48 h after addition of extracted medium. hMSCs were exposed to medium/extract solution for 48 h, followed by induction of differentiation. Images were taken 10 d after addition of the differentiation induction medium using a Nikon Eclipse TE2000-E inverted microscope.

2.3 Results and Discussion

2.3.1 Motivation

We recently described the properties of the poly(triol α-ketoglutarate) (PTK) family of polyester elastomers.[16, 17] Although these materials have many interesting features, their

degradation rates were particularly of note. In terms of designing potential tissue scaffolds, the PTK series hydrolyzed in PBS too rapidly to be useful. We aimed to design similar materials with degradation rates that were more relevant to future applications in soft tissue engineering. Based on our prior experience, the critical factor to achieving this goal was to eliminate the presence of a ketone immediately adjacent to an acid in the monomer.

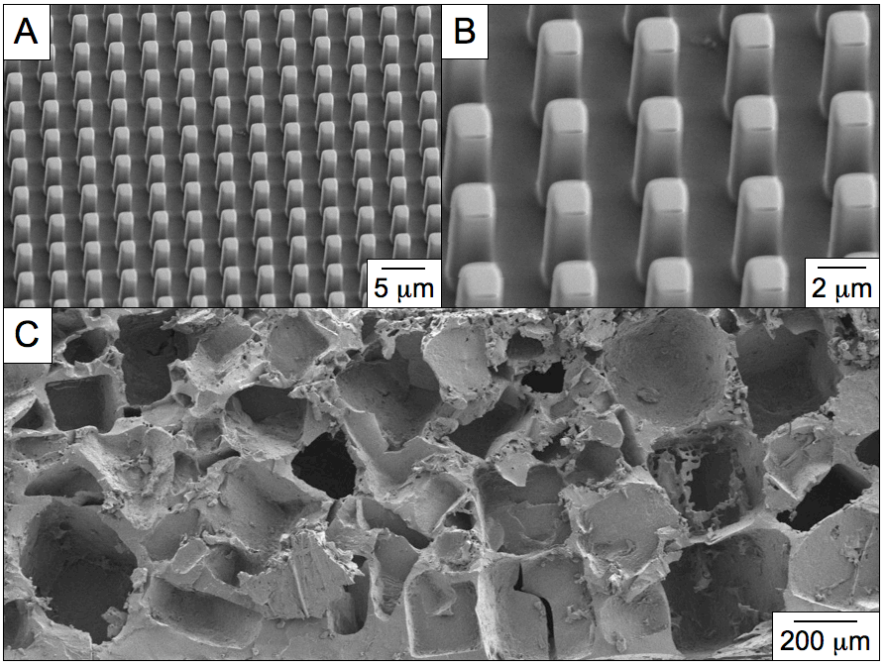

Figure 2.2. Scanning electron microscopy (SEM) images of PErD films. Curing pre-polymer in the presence of a perfluoropolyether mold allows for the facile design of micro-patterned polyester films. The pattern was (A) transferred with high fidelity, (B) creating features with an approximate dimensions of 2 μm x 2 μm x 6 μm. Additionally, porous scaffolds (C) were fabricated using standard salt-leaching techniques. Both of these fabrication methods were possible with all pre-polymers.

The foundation of our current material design is based on erythritol, a sugar alcohol that may be endogenous to the human metabolism.[18, 19] As a sugar substitute that is approved by the FDA, erythritol was an attractive monomer due to human tolerance of large amounts of the sugar alcohol with no negative side effects.[19-22] Additionally, erythritol can be

absorbed by the body and excreted unchanged, allowing normal metabolic pathways to continue unaffected.[19-22] We therefore chose several aliphatic diacids of increasing length to polymerize with erythritol: glutaric, adipic, pimelic, suberic, azelaic, sebacic, dodecanedioic, and tetradecanedioic acid. By altering the length of the diacids, the polyester elastomers were expected to achieve a range of hydrophobicities, degradation rates, and mechanical characteristics. Furthermore, several of these monomers are either naturally occurring small molecules or have previously been used in biomaterials.[23-30]

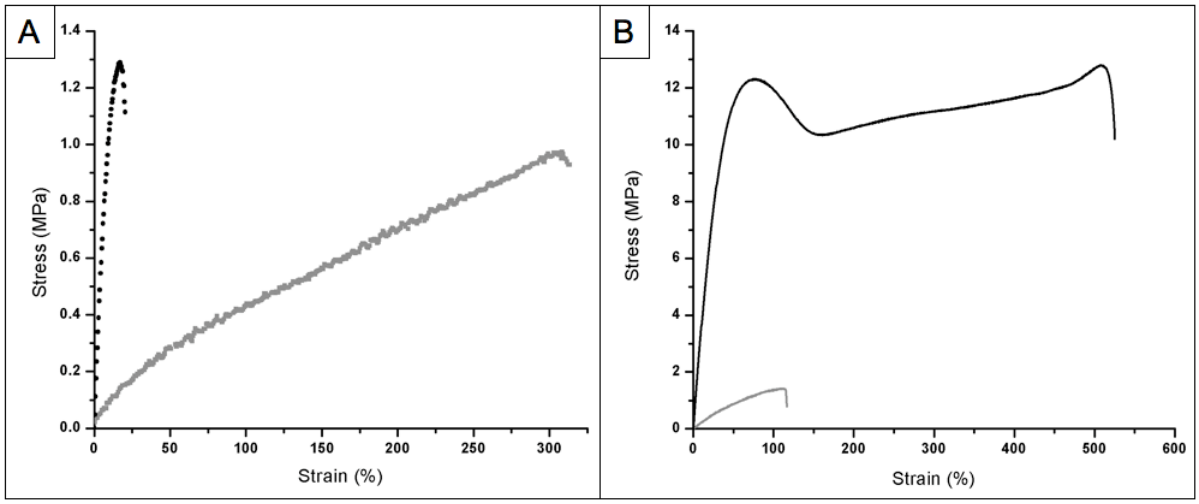

Figure 2.3. Representative stress versus strain curves for PErD. (A) For PErD films derived from odd-numbered carbon diacids, adjusting the curing temperature from 120 °C to 140 °C led to a large increase in the Young's modulus. Interestingly, the thermosets synthesized from even-numbered carbon diacids did not experience as marked of an increase in the moduli. The grey curve represents elastomer 2 while the black curve displays the stress-strain relationship for elastomer 14. (B) Semi-crystalline thermosets displayed an irregular stress-strain curves when compared to elastomeric materials. Elastomer 16 (gray) was used as the example for elastomers while material 17 (black) was shown to represent semi-crystalline thermosets. The irregular shape of the red curve (semi-crystalline materials) is most likely due to the presence of an elastomeric network containing semi-crystalline oligomers.

2.3.2 Design and Synthesis

The synthesis of the PErD series was designed for biomedical applications and, therefore, elastomers were synthesized without any catalysts or co-reagents (Figure 2.1). After forming a homogenous melt in an inert environment of argon at 145 °C, monomers were stirred while heating for 2 h. The pressure of the reaction was then reduced to ~ 2 torr for an additional 7 h, allowing random ester-based cross-linking to form pre-polymers. Materials were either amorphous or semi-crystalline, depending on the length of the diacid; diacids with less than 10 carbons combined with erythritol to form amorphous pre-polymers, while sebacic, dodecanedioic, and tetradecanedioic acids led to the synthesis of semi-crystalline materials that were solid and opaque at room temperature. The monomers were heated only to the extent of cross-linking that would create oligomeric pre-polymers with $\langle M_n \rangle \geq 500$ g/mol (Table 2.1). Thermoset formation was intended to occur during a second heating phase, enabling molding and shaping of elastomeric films.

2.3.3 Pre-Polymer Characterization

Polycondensation of erythritol and diacids (5 – 10, 12, 14 carbons) led to pre-polymers in the form of oligo(erythritol glutarate) (OErGl), oligo(erythritol adipate) (OErAd), oligo(erythritol pimelate) (OErPi), oligo(erythritol suberate) (OErSu), oligo(erythritol azelate) (OErAz), oligo(erythritol sebacate) (OErSe), oligo(erythritol dodecanedioate) (OErDo), and oligo(erythritol tetradecanedioate) (OErTe). These pre-polymers were characterized by ^{1}H NMR and GPC. The ^{1}H NMR spectra, as seen in Figure 2.1, show that all of the pre-polymers have very similar chemical signatures. The pre-polymer compositions were approximately 1:1 (erythritol:diacid), with the main difference in ^{1}H NMR spectra being the location of the methylene groups. The presence of signals around 4 and 5 ppm indicates that alcohols and acids combined to form esters; peaks d’ and e’

represent the free alcohols that did not participate in cross-linking (Appendix B). The signal associated with hydrophobic methylene groups are observed between 1.2 and 1.7 ppm. The molecular weights of the polyester networks are based on a combination of monomer reactivity and mass of the monomers. The lowest molecular weight was 710 g/mol (OErGl) while the largest was 1470 g/mol (OErDo).

Table 2.3. Mechanical Properties of Poly(Erythritol Dicarboxylate)

Material	Young's Modulus[a] (MPa)	UTS[a] (MPa)	Rupture Strain[a] (%)	n[b] (mmol/L)
1	0.21 ± 0.04	0.39 ± 0.03	418 ± 38	29 ± 5
2	0.48 ± 0.01	1.03 ± 0.17	314 ± 45	64 ± 2
3	0.39 ± 0.07	0.44 ± 0.05	208 ± 14	53 ± 10
4	0.19 ± 0.05	0.29 ± 0.07	319 ± 56	26 ± 78
5	0.22 ± 0.07	0.24 ± 0.02	315 ± 24	30 ± 9
6	0.35 ± 0.09	0.38 ± 0.07	182 ± 34	47 ± 12
7	0.08 ± 0.01	0.14 ± 0.03	466 ± 41	10 ± 2
8	46.26 ± 3.33	10.80 ± 0.44	407 ± 15	6224 ± 448
9	80.37 ± 2.85	16.65 ± 0.21	149 ± 41	10813 ± 383
10	18.36 ± 3.03	1.61 ± 0.11	63 ± 10	2470 ± 408
11	0.47 ± 0.17	0.55 ± 0.12	198 ± 4	63 ± 22
12	1.90 ± 0.26	0.86 ± 0.25	60 ± 16	256 ± 35
13	1.08 ± 0.12	0.79 ± 0.14	100 ± 8	145 ± 16
14	12.50 ± 1.46	1.31 ± 0.15	22 ± 4	1682 ± 196
15	1.92 ± 0.12	1.03 ± 0.19	85 ± 14	258 ± 17
16	1.95 ± 0.31	1.48 ± 0.06	146 ± 47	263 ± 42
17	38.89 ± 4.46	13.00 ± 0.61	446 ± 75	5232 ± 601

[a] Determined by Instron (crosshead speed of 10 mm/min); [b] Equation 1;.

2.3.4 Complex Film Design

One way to enhance the versatility of a material is to demonstrate processing compatibility with embossing of topologies and microstructures. Recent literature has focused on the importance of nano- and micro-features related to interfacial properties.[31-33]

To determine how easily embossed films could be fabricated, thermal curing was conducted in the presence of a perfluoropolyether (PFPE) mold. The molding material, PFPE, was used due to its low surface energy, allowing for simple release from the polyester film after the completion of the cross-linking period.[12-14] A small amount of the pre-polymer was placed on a glass slide and placed in an oven for 10 min, reducing the viscosity. The PFPE mold was then placed in direct contact with the pre-polymer and returned to the oven. Curing conditions were carried out as mentioned in Table 2.2. After the cross-linking period, the mold was removed and the result was a micro-embossed film (Figure 2.2). The features (2 μm x 2 μm x 6 μm) were inversely transferred from the PFPE mold with high fidelity over a large area. We will continue to explore the potential for micro-textured adhesive films or embossed tissue scaffolds to control cell behavior.

Porous materials are also commonly used in tissue engineering because they allow cells and nutrients to easily pervade the interior of scaffolds.[34-36] In order to demonstrate that micro-porous PErD thermosets could be designed, pre-polymers were dissolved in THF and combined with sieved sodium chloride (NaCl) crystals (< 400 μm). The mixture was added to a poly(tetrafluoroethylene) mold and, after solvent evaporation, the polyester-salt system was cured as described above. The cured elastomers were then swelled in ddH_2O for 96 h in order to leach out the NaCl porogen. After drying at room conditions, the films were fully dried under vacuum. We will utilize these porous scaffolds in future *in vitro* and *in vivo* biological studies.

2.3.5 Mechanical Testing

The ability to design elastomers with control over the mechanical properties is attractive for materials used in biomedical applications. Therefore, several curing conditions

Table 2.4. Physical Properties of Poly(Erythritol Dicarboxylate)

Material	T_g/T_m [a] (°C)	Q_s [b] (%)	Contact Angle (°)	WS[c] (%)
1	-4.1	37.3 ± 2.0	64.5 ± 3.3	26.4 ± 2.0
2	0.9	24.0 ± 1.3	83.1 ± 3.2	21.8 ± 2.1
3	-10.2	32.0 ± 2.0	74.9 ± 1.3	15.3 ± 2.0
4	-14.5	36.6 ± 3.3	75.9 ± 1.6	14.7 ± 1.2
5	-16.8	44.5 ± 1.8	66.9 ± 0.7	9.8 ± 0.6
6	-17.9	27.5 ± 1.6	79.7 ± 3.2	8.9 ± 1.9
7	-20.4	51.1 ± 3.4	58.6 ± 1.7	8.6 ± 0.6
8	-32.2/50.1	23.4 ± 0.9	80.9 ± 0.8	3.6 ± 0.6
9	-35.8/63.2	29.1 ± 2.2	79.8 ± 1.0	2.3 ± 1.0
10	3.8	17.1 ± 2.9	91.4 ± 1.4	20.4 ± 0.7
11	-4.7	7.4 ± 5.3	96.2 ± 1.6	13.5 ± 1.8
12	-6.6	14.9 ± 2.6	84.5 ± 0.7	10.7 ± 2.5
13	-13.5	17.3 ± 3.7	96.9 ± 2.1	9.5 ± 0.6
14	-15.9	11.6 ± 2.5	93.5 ± 2.6	5.2 ± 0.8
15	-16.6	10.8 ± 6.2	100.0 ± 2.4	5.6 ± 0.4
16	-17.0	2.7 ± 0.7	98.6 ± 1.0	3.0 ± 1.8
17	-27.4/53.8	22.4 ± 0.8	105.1 ± 0.5	2.4 ± 0.6

[a] Determined by DSC; [b] Extracted in THF for 24 h at 25 °C; equation 2. [c] Swelled in water for 24 h; equation 3.

were used to create materials with a range of structural properties (Table 2.2). With the exception of elastomer 1, all pre-polymers cured for 3 d to form thermosets (elastomer 1 cured for 2 d). As expected, cross-linking these materials at 140 °C led to more rigid materials than curing at 120 °C. The mechanical properties exhibited by various PErD elastomers varied over a wide range (Figure 2.3; Table 2.3). Elastomers 1 – 17 had YM, ultimate tensile stress (UTS), and rupture strain (RS) values of 0.08 – 80.37 MPa, 0.14 – 16.65 MPa, and 22 - 466 %, respectively.

As expected, after the stress was released, the elongated dog-bones composed of amorphous materials immediately reverted to their original dimensions. However, the three semi-crystalline polyesters (materials 8, 9, and 17) experienced semi-permanent

deformations; the original shape was not recovered unless these materials were heated above their transition temperatures. Presumably, this is due to the presence of an amorphous polyester encasing semi-crystalline oligomers. This hypothesis was strengthened after conducting the sol content analysis of these three semi-crystalline polyesters because the dried, sol-free materials were amorphous. The interesting composition of the materials 8, 9, and 17 also led to unique and reproducible stress vs. strain curves that display a local maximum, then a local minimum, and a final steady increase before rupturing (Figure 2.3). These polymers had higher YM and UTS values when compared to the amorphous polymers.

Extending the potential of PErD elastomers, the mechanical properties of several biological materials fall within the ranges observed by these materials.[4, 5] Furthermore, the design of materials with many more combinations of mechncial characteristics should be possible by adjusting the curing conditions. An advantage of using thermally cured materials is the ease with which the rigidity and flexibility can be tuned.

2.3.6 Degradation Studies

As stated previously, our earlier work included a series of polyketoester elastomers that degraded rapidly in PBS at 37 °C (complete hydrolysis in 2 – 28 d).[16, 17] The design of the PErD family of polyester elastomers was motivated by the need for biodegradable materials that hydrolyze on a timescale that is more relevant to tissue engineering applications. The only materials that were studied during *in vitro* degradation experiments were those that were amorphous, due to the need for materials that can recover from the dynamic stresses associated with *in vivo* tissue engineering. However, elastomer 7 was not studied because it turned opaque when submerged in aqueous solutions. The degradation rates of PErD seem to be controlled by two factors: the extent of cross-linking within the

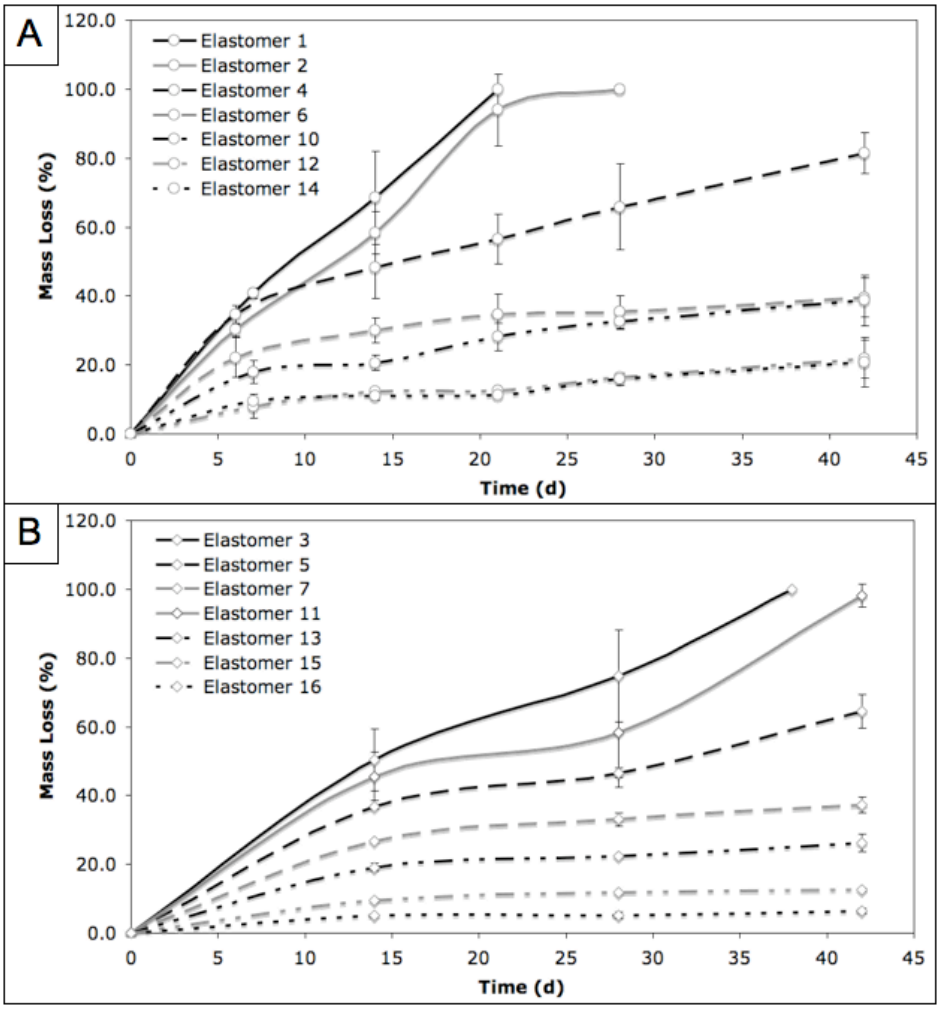

Figure 2.4. *In vitro* PErD degradation rates. Films were incubated in PBS at 37 °C for four weeks. At pre-determined time points, the percent mass loss was recorded. The PErD series achieved *in vitro* degradation ranging from 100 % in 3 weeks to 6.4 % in 6 weeks.

polymer network and the hydrophobicity of the elastomer. As such, the fastest degrading material should be soft and hydrophilic (elastomer 1), while hard, hydrophobic materials should survive longer in hydrolytic conditions (elastomers 16). This logical trend was observed in the relative rates of degradation for our materials. Due to the presence of fewer methylene groups, glutaric acid is more hydrophilic than adipic acid, which is more hydrophilic than pimelic acid, etc. Therefore, materials composed of these monomers should degrade according to their hydrophilic natures, with the fastest degrading elastomer being

composed of the most hydrophilic diacid. Also, curing at 140 °C for 3 d should lead to more extensive ester formation than cross-linking at 120 °C for 3 d. As esters are more hydrophobic than acids, the materials resulting from the 140 °C, 3 d curing should be more hydrophobic than those cross-linked at 120 °C for 3 d. By combining these two trends, intuitive deduction would suggest the following trend in degradation rates (fastest to slowest degradation): 1 > 2 > 3 > 4 > 5 > 6 > 10 > 11 > 12 > 13 > 14 > 15 > 16. As seen in Figure 2.4, the materials degrade according to the expected trend. By altering the diacid and the curing conditions, the degradation rate could be controlled, allowing for the ability to tune the hydrolysis rate to match the needs of a potential application. Overall, hydrolytic degradation rates ranged from 100 % in 3 weeks to 6.4 % in 4 weeks; the PErD series of polyesters offers a wide range of degradation rates, which could increase the versatility of these materials in regards to tissue engineering applications.

2.3.7 *In Vitro* Cytotoxicity

These materials were primarily designed for tissue engineering applications. Since biocompatibility is a requisite of tissue scaffolds, the cytotoxicity of these elastomers was studied using an elution-based method. Only those polyesters that demonstrated low water swelling values were chosen for cell studies (elastomers 4, 5, 6, 11, 12, 13, 14, 15, 16) because of potential complications that could arise from structural deformations caused by hydration. The first method consisted of culturing SA fibroblasts in polymer-extracted medium. Polyester thermosets were extracted in cell medium for 24 h at 37 °C. The medium-extract solution was then used to culture cells on tissue culture plastic that were not yet confluent. As seen in Figure 2.5, within 48 h of extract addition, cells were able to reach confluence, regardless of the polymer extract used. In the case of fibroblasts, the presence of

the extracts did not prevent the cells from achieving and maintaining confluence; all cells were viable for 1 week, at which time the study was stopped. Cells that were exposed to polymer extracts were virtually indistinguishable from cells that were not exposed to any material extracts.

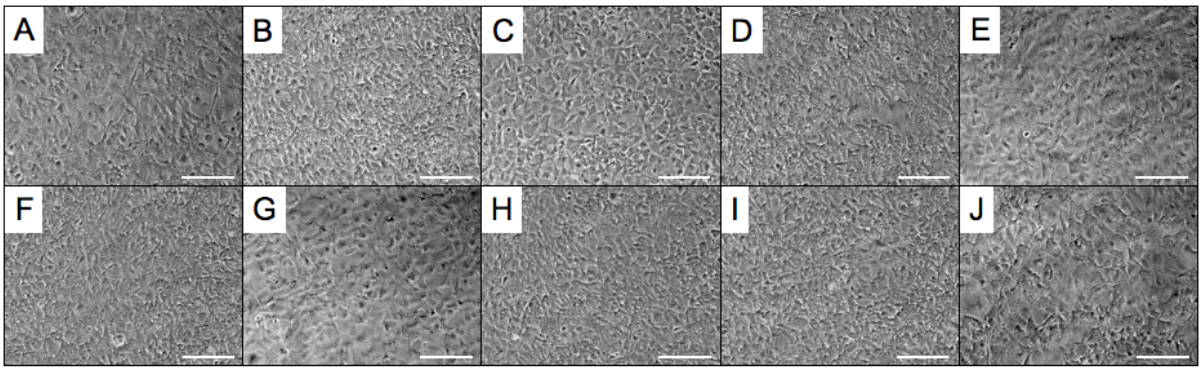

Figure 2.5. Elastomer extract-based *in vitro* cytotoxicity of PErD with fibroblasts. SA fibroblasts were cultured on tissue culture plastic in the presence of extracts from elastomer 4 (A), 5 (B), 6 (C), 11 (D), 12 (E), 13 (F), 14 (G), 15 (H), and 16 (I) for 48 h. As a positive control, cells were cultured in medium containing no polymer extracts (J). Fibroblasts were able to reach and maintain confluence, allowing these polyesters to be deemed non-cytotoxic. All scale bars represent 200 μm.

To study the effect of polymer extracts on complex cellular functions, not simply the viability, hMSCs were also cultured in the presence of the extracts . Stem cells were brought to confluence in the presence of polymer-extracted medium, followed by the addition of differentiation induction medium. hMSCs were imaged 10 d after induction of differentiation, enabling ample time for the transition from stem cells to adipocytes.[15] The presence of adipose cells can be confirmed by the formation of large lipid vacuoles. After staining with Oil Red O, the vacuoles (red) can easily be seen throughout the cells (Figure 2.6). Based on comparisons with hMSCs that were not exposed to any polymer extracts, PErD materials were deemed non-cytotoxic. The stem cells that were cultured with polymer

extracts from diacids with an even number of carbon exhibited noticeably more differentiation. As seen in Figure 2.6 (images B, D, F, H, and I), the presence of more red demonstrates that more vacuoles were produced during differentiation. Future studies will focus on further observing the relationship between differentiation and the number of carbons in the diacids.

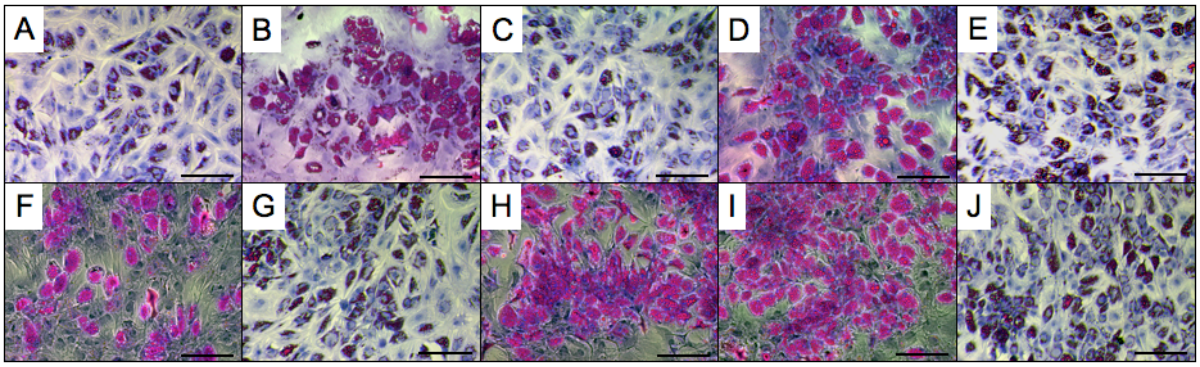

Figure 2.6. Elastomer extract-based *in vitro* cytotoxicity of PErD with stem cells. hMSCs were cultured on tissue culture plastic in the presence of extracts from elastomer 4 (A), 5 (B), 6 (C), 11 (D), 12 (E), 13 (F), 14 (G), 15 (H), and 16 (I) for 48 h. As a positive control, cells were cultured in medium containing no polymer extracts (J). After reaching confluence, induction medium was added to begin the differentiation process. As seen by the presence of vacuoles (red), hMSCs were able to differentiate into adipocytes after exposure to PErD extracts. All scale bars represent 200 μm.

2.4 Conclusions

We have designed a novel series of polyester elastomers based on aliphatic diacids and erythritol, a sugar alcohol that is FDA-approved for human consumption. Thermal polymerization offers a simple avenue for tuning the mechanical properties, hydrophobicity, and degradation rates of the PErD family of materials. Future work will focus on *in vivo* characterization and applications (tissue engineering and drug delivery) of this family of thermosets. The pre-polymers are compatible with imprint lithography and emulsions (data not shown), enabling multiple methods of obtaining particles or embossed films. We will

also continue to explore the cause of the odd-even effect and how it relates to the biocompatibility of these materials. Based on our preliminary results, we believe that the PErD series of polyester elastomers may find wide use in a range of biomedical applications.

2.5 Acknowledgements

The authors thank the Ashby and DeSimone research groups for insightful discussions, as well as Professor Wei You. This work was supported by the Carolina Center for Cancer Nanotechnology Excellence (NCI), the Burroughs Wellcome Foundation (Interface Career Award), and the National Science Foundation (Career Award).

2.6 References

(1) Okada, M. *Prog. Polym. Sci.* **2002**, *27*, 87-133.

(2) Ratner, B. D.; Bryant, S. J. *Annu. Rev. Biomed. Eng.* **2004**, *6*, 41-75.

(3) Lavik, E.; Langer, R. *Appl. Microbiol. Biotechnol.* **2004**, *65*, 1-8.

(4) Amsden, B. G. *Soft Matter* **2007**, *3*, 1335-1348.

(5) Webb, A. R.; Yang, J.; Ameer, G. A. *Expert Opin. Biol. Ther.* **2004**, *4*, 801-812.

(6) Pitt, C. G.; Gratzl, M. M.; Kimmel, G. L.; Surles, J.; Schindler, A. *Biomaterials* **1981**, *2*, 215-220.

(7) Storey, R. F.; Hickey, T. P. *Polymer* **1994**, *35*, 830-838.

(8) Wang, Y.; Kim, Y. M.; Langer, R. *J. Biomed. Mater. Res. A.* **2003**, *66*, 192-197.

(9) Bruggeman, J. P.; de Bruin, B. J.; Bettinger, C. J.; Langer, R. *Biomaterials* **2008**, *29*, 4726-4735.

(10) Bruggeman, J. P.; Bettinger, C. J.; Nijst, C. L. E.; Kohane, D. S.; Langer, R. *Adv. Mater.* **2008**, *20*, 1922-1927.

(11) Mikos, A. G.; Sarakinos, G.; Leite, S. M.; Vacanti, J. P.; Langer, R. *Biomaterials* **1993**, *14*, 323-330.

(12) Rolland, J. P.; Hagberg, E. C.; Denison, G. M.; Carter, K. R.; DeSimone, J. M. *Angew. Chem. Int. Ed.* **2004**, *43*, 5796-7599.

(13) Rolland, J. P.; Van Dam, R. M.; Schorzman, D. A.; Quake, S. R.; DeSimone, J. M. *J. Am. Chem. Soc.* **2004**, *126*, 2322-2323.

(14) Gratton, S. E. A.; Williams, S. S.; Napier, M. E.; Pohlhaus, P. D.; Zhou, Z.; Wiles, K. B.; Maynor, B. W.; Shen, C.; Olafsen, T.; Samulski, E. T.; DeSimone, J. M. *Acc. Chem. Res.* **2008**, *41*, 1685-1695.

(15) Luo, W.; Jones, S. R.; Yousaf, M. N. *Langmuir* **2008**, *24*, 12129-12133.

(16) Barrett, D. G.; Yousaf, M. N. *Macromolecules* **2008**, *41*, 6347-6352.

(17) Barrett, D. G.; Lamb, B. M.; Yousaf, M. N. *Langmuir* **2008**, *24*, 9861-9867.

(18) Touster, O.; Hecht, S. O.; Todd, W. M. *J. Biol. Chem.* **1960**, *235*, 951-953.

(19) Bernt, W. O.; Borzelleca, J. F.; Flamm, G.; Munro, I. C. *Regul. Toxicol. Pharmacol.* **1996**, *24*, S191-7.

(20) Bornet, F. R.; Blayo, A.; Dauchy, F.; Slama, G. *Regul. Toxicol. Pharmacol.* **1996**, *24*, S280-5.

(21) Tetzloff, W.; Dauchy, F.; Medimagh, S.; Carr, D.; Bar, A. *Regul. Toxicol. Pharmacol.* **1996**, *24*, S286-95.

(22) Bornet, F. R.; Blayo, A.; Dauchy, F.; Slama, G. *Regul. Toxicol. Pharmacol.* **1996**, *24*, S296-302.

(23) Pourjavadi, A.; Rezai, N.; Zohuriaan, M. J. *J. Appl. Polym. Sci.* **1998**, *68*, 173-183.

(24) Ben-Shabat, S.; Abuganima, E.; Raziel, A.; Domb, A. J. *J. Polym. Sci. A: Polym. Chem.* **2003**, *41*, 3781-3787.

(25) Okada, M.; Tsunoda, K.; Tachikawa, K.; Aoi, K. *J. Appl. Polym. Sci.* **2000**, *77*, 338-346.

(26) Siriphannon, P.; Monvisade, P.; Jinawath, S.; Hemachandra, K. *J. Biomed. Mater. Res. A*. **2007**, *81*, 381-391.

(27) Carnahan, M. A.; Grinstaff, M. W. *Macromolecules* **2006**, *39*, 609-616.

(28) Sheihet, L.; Piotowska, K.; Dubin, R. A.; Kohn, J.; Devore, D. *Biomacromolecules* **2007**, *8*, 998-1003.

(29) Liu, G.; Hinch, B.; Beavis, A. D. *J. Biol. Chem.* **1996**, *271*, 25338-25334.

(30) Grego, A. V.; Mingrone, G. *Clin. Nutr.* **1995**, *14*, 143-148.

(31) Geim, A. K.; Dubonos, S. V.; Grigorieva, I. V.; Novoselov, K. S.; Zhukov, A. A.; Shapoval, S. Y. *Nat. Mater.* **2003**, *2*, 461-463.

(32) Lee, H.; Lee, B. P.; Messersmith, P. B. *Nature* **2007**, *448*, 338-341.

(33) Mahdavi, A., et al *Proc. Natl. Acad. Sci. U. S. A.* **2008**, *105*, 2307-2312.

(34) Yang, J.; Shi, G.; Bei, J.; Wang, S.; Cao, Y.; Shang, Q.; Yang, G.; Wang, W. *J. Biomed. Mater. Res.* **2002**, *62*, 438-446.

(35) Yang, J.; Webb, A. R.; Ameer, G. A. *Adv. Mater.* **2004**, *16*, 511-516.

(36) Yang, J.; Webb, A. R.; Pickerill, S. J.; Hageman, G.; Ameer, G. A. *Biomaterials* **2006**, *27*, 1889-1898.

Chapter III

POLY(TRIOL α-KETOGLUTARATE): BIODEGRADABLE, CHEMOSELECTIVE, AND MECHANICALLY TUNABLE ELASTOMERS

Reproduced in part with permission from:
Barrett, D. G.; Yousaf, M. N. *Macromolecules* **2008**, *41*, 6347-6352.

3.1 Introduction

The development of new biomaterials with a range of functions and properties is becoming increasingly important for new and diverse applications in biomedical research, including drug delivery and tissue engineering.[1-5] For applications that require soft materials that can mimic biological tissues, much research is directed towards the design of biodegradable and bio-reducible polymers that can form biocompatible elastomeric networks.[6-12] Although this is an area of intense research, many of these materials are generated through complex syntheses or difficult engineering processes, which increases the costs of these materials and decreases the general availability to the broader research community. The design of simple, straightforward, yet diverse materials would provide faster access to the new technology and therefore enable rapid progress in evaluating new biomaterials for a variety of applications.

A traditional approach for generating new biomaterials that can be tedious and inefficient, yet powerful when it works, has been to design one polymer for one particular application. In order to streamline the discovery process, a more efficient strategy would be to design novel materials capable of successful performance in multiple diverse applications. With this approach, materials can be multifaceted in terms of mechanical characteristics and chemical functionality. Mechanical versatility implies that a single technique can achieve a spectrum of structural and strength-related properties. Chemical versatility can be defined as the ability to introduce a wide range of functional moieties into the polymer at various time points in the synthesis – during the pre-polymer stage or as a cross-linked film. A material that was multifaceted both mechanically and chemically could potentially allow for the modulation of both sets of properties independently. Mechanical and chemical versatility

could enable the properties of a specific material to be tuned in order to achieve a desired result for a particular application.

We believe, therefore, that the ideal polymer for biological or medical applications should possess several key characteristics. First, biocompatibility and biodegradation are key to ensure that there are no adverse cellular responses to the material. Second, a wide range of degradation rates and mechanical properties should be accessible from a single, facile, and inexpensive design strategy. This would allow for the ability to tailor material properties to best fit a particular application, thereby maximizing the probability of success. Third, the inclusion of a chemoselective ligand conjugation strategy would greatly increase the flexibility of a polymer in biological and medical applications.[13-17] A single strategy that incorporates all of these criteria would allow for the rapid development and testing of new biomaterials.

In this chapter, we describe the syntheses and characterization of poly(triol α-ketoglutarate) (PTK), a novel and chemoselective series of polyketoesters. Due to the unique characteristics of this polymer family, a wide range of mechanical properties and degradation rates are possible. Also, inclusion of ketones in the repeat unit allows for the mild and chemoselective functionalization of these materials. Upon reaction, and therefore conjugation, of the oxyamine-terminated cell attachment peptide glycine-arginine-glycine-aspartic acid-serine (H_2NO-GRGDS), these materials are able to support cell attachment and cellular growth.[18, 19] Because of the potential diversity of mechanical and chemical properties, PTK may be employed for a number of biomedical applications including tissue engineering and drug delivery.

3.2 Experimental Section

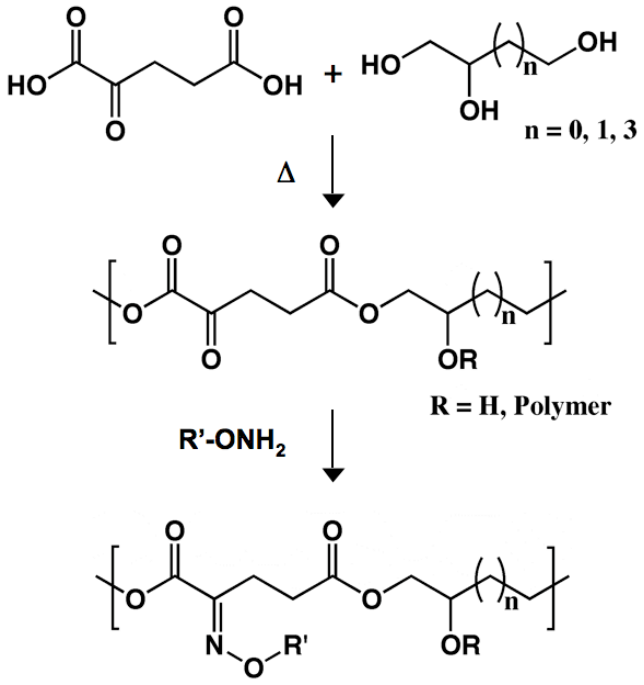

Figure 3.1. Synthesis of poly(triol α-ketoglutarate).

3.2.1 Materials

All chemicals were purchased from Sigma-Aldrich (Milwaukee, WI) or Fisher Scientific (Philadelphia, PA), and used without further purification unless otherwise noted. α-ketoglutaric acid (αKG) was recrystallized from ethyl acetate.

3.2.2 Poly(Triol α-ketoglutarate) Synthesis

Equimolar amounts of αKG and triol (glycerol, 1,2,4-butanetriol, or 1,2,6-hexanetriol) were combined in a round bottom flask. In an inert environment of N_2, monomers were stirred at 125 °C. After a homogenous melt formed, the mixture was stirred for one hour. Polymers were then precipitated in −78 °C methanol (MeOH), concentrated by rotary evaporation, and dried under vacuum at room temperature. Yields for poly(glycerol α-ketoglutarate) (PGa), poly(1,2,4-butanetriol α-ketoglutarate) (PBa), and poly(1,2,6-hexanetriol α-ketoglutarate) (PHa) were 93 %, 88 %, and 81 %, respectively. To form

elastomeric films, pre-polymers were cured at either 60 °C, 90 °C, or 120 °C for times ranging from 6 h to 7 days.

3.2.3 Polyketoester Characterization

Infrared spectra were recorded on an ASI ReactIR 1000 with THF as the solvent. Thermal properties were recorded by DSC and TGA. Using a Seiko 220C DSC, pre-polymer glass transition temperatures were measured during the second heating cycle (10 °C/min). Thermal degradation was collected with a Perkin-Elmer TGA with a heating rate of 10 °C/min in an atmosphere of N_2.

Tensile tests were conducted on an Instron 5566 at a crosshead speed of 10 mm/min at 25 °C. Samples were cured in a dog-bone-shaped mold with approximate dimensions of 10 mm x 3 mm x 1.5 mm. The Young's modulus (YM) was calculated according to the linear segment of the stress/strain curve. Three trials were performed and the average was reported. Using

$$n = \mathrm{YM}(3\mathrm{RT})^{-1} \qquad (1)$$

where R is the universal gas constant and T is the temperature in K, the cross-linking density (n) was calculated.

Sol-gel analysis was conducted by soaking films in THF for 24 h at room temperature. After solvent removal, the films were dried, and the percent soluble fraction (Q_s) was calculated by

$$Q_s = \frac{m_i - m_f}{m_i} \times 100 \qquad (2)$$

where m_i and m_f represent the initial and final mass of the elastomer films, respectively. Three trials were performed and the average was reported.

3.2.4 Film Molding

A small amount of pre-polymer was placed onto a glass slide and heated to 120 °C in a vacuum oven. After 30 min of reduced pressure (~ 50 torr) to remove any gas or solvent, a polydimethylsiloxane (PDMS) stamp, fabricated by soft lithography, was placed directly on the pre-polymer.[20] The material was allowed to cure for 24 hours, followed by the removal of the PDMS stamp. The molded elastomeric films were then coated in ~ 2 nm of a Pd/Au alloy (Cressington 108 auto sputter coater, Cressington Scientific Instruments Ltd.) and imaged using a Hitachi model 2-4700 scanning electron microscope (SEM).

3.2.5 *In Vitro* Degradation

To obtain standard degradation rates, approximately 75 mg segments of each elastomer were placed in scintillation vials. Vials were filled with phosphate buffered saline (PBS) and samples were then stored in an incubator (37 °C). At predetermined intervals, samples were removed from the incubator, rinsed thoroughly, dried, and weighed again. To prevent saturation, PBS was replaced every 7 days. Each data point was repeated in triplicate and results were reported as the average percent of the original mass lost.

3.2.6 Film Functionalization

To pattern immobilized ligands, a PDMS microfluidic cassette was placed in direct contact with a PTK film, creating a seal. Then, a 5 mM solution of an oxyamine-modified rhodamine dye (rhodamine-ONH_2) in MeOH was flowed through the channels. The surface was then rinsed with MeOH, dried with N_2, and fluorescent images were taken using a Nikon Eclipse TE2000-E inverted microscope (Nikon USA, Inc., Melville, NY). To functionalize the elastomer surface with a biospecific cell-adhesive peptide, 100 μL of a solution of H_2NO-GRGDS (1 mM in 1:1 DMSO:H_2O) were added directly to the top of the film and allowed to

Table 3.1. Curing Conditions for Poly(Triol α-ketoglutarate)

Polyketoester	Triol	Temp. (°C)	Duration
1A	glycerol	60	7 d
2A	butanetriol	60	7 d
3A	hexanetriol	60	7 d
1B	glycerol	90	2 d
2B	butanetriol	90	2 d
3B	hexanetriol	90	2 d
1C	glycerol	120	1 d
2C	butanetriol	120	1 d
3C	hexanetriol	120	1 d
3D	hexanetriol	120	6 h
3E	hexanetriol	120	12 h
3F	hexanetriol	120	18 h

react for 5 hours. The elastomers were then rinsed in PBS and dried in a vacuum chamber at room temperature.

3.2.7 *In Vitro* Biocompatibility

Polyketoester films were soaked in bovine calf serum-containing Dulbecco's modified eagle medium (Sigma, St. Louis, MO) for 24 hours to remove any soluble or degraded portions of the materials. Cytotoxicity was then examined by two methods. First, the serum-containing medium with the elastomer extraction was added to a confluent layer of 3T3 Swiss Albino mouse fibroblasts on tissue culture plastic. After 48 hours, cells were examined by light microscopy and cytotoxicity was determined based on cell morphology, monolayer confluence, and the ability to continue sub-culturing cells (compared to cells cultured on tissue culture plastic). Second, small fragments of the materials were added to a confluent layer of fibroblasts on tissue culture plastic. After 48 hours, cells were examined by light microscopy and cytotoxicity was determined as compared to cells not treated on tissue culture plastic.

Fibroblasts were next added directly to GRGDS-presenting films and incubated in Dulbecco's modified Eagle's medium with 10% bovine calf serum and 1% penicillin/streptomycin at 37 ºC with 5% CO_2. The cells were added at a density of ~ 80,000 cells/mL. Phase-contrast images were taken 24 h after seeding using a Nikon Eclipse TE2000-E inverted microscope.

3.3 Results and Discussion

3.3.1 Motivation

The motivation for designing PTK was influenced by several criteria. First, the development of materials with a facile post-polymerization modification strategy was critical. The use of αKG satisfied this particular requirement due to the presence of a ketone group. Oxyamines, hydrazines, and hydrazides can react rapidly and chemoselectively with ketones at physiological conditions without catalysts or co-reagents, allowing for easy ligand conjugation by forming stable oxime linkages.[13-15, 21-23] Second, since biomedical applications are targeted for these PTKs, biocompatibility was required and, therefore, at least one natural product was used in each material to minimize potential cytotoxicity. αKG is a ubiquitous metabolite required for the citric acid cycle, while glycerol is a key component in the synthesis of phospholipids.[24, 25] Third, the ability to generate a wide range of elastomer properties with a simple and cost efficient synthesis would greatly enhance the versatility of PTK. By thermally curing the polyesters with varying temperatures and/or durations, the extent of cross-linking can be easily controlled for a range of mechanical properties. Fourth, due to the potential need for consistent degradation profiles, linear degradation of the PTK was desired. By using ester linkages for both polymerization and cross-linking, consistent and uniform degradation could be achieved. With these criteria,

Table 3.2. Mechanical Characteristics of Poly(Triol α-ketoglutarate)

Polyketoester	Mass Loss (°C)[a] 5%	YM[b] (MPa)	UTS[b] (MPa)	YM[b] (%)	n[b] (mmol/L)	Q_s[c] (%)	Complete Degradation (days)[d]
1A	*NA*[e]	*NA*	*NA*	*NA*	*NA*	*NA*	*NA*
2A	259	1.95	1.0	583	262.3	48.5	2
3A	267	0.1	0.3	395	13.45	59.0	4
1B	239	459.4	9.3	121	61790	41.9	3
2B	260	161.3	4.7	418	21690	32.5	7
3B	293	2.5	2.1	176	336.3	16.3	14
1C	255	499.7	16.7	43	67210	28.5	8
2C	285	381.9	8.1	95	51370	4.4	17
3C	307	657.4	30.8	22	88420	3.5	28
3D	268	0.1	0.2	379	13.45	60.9	4
3E	288	1.3	1.2	151	174.9	14.8	12
3F	293	4.2	2.2	200	566.2	14.5	13

[a] Determined by TGA in N_2, 10 °C/min. [b] Determined by Instron (crosshead speed of 10 mm/min). [c] Extracted in THF for 24 h at 25 °C. [d] Degradation was monitored in PBS at 37 °C. [e] Incomplete curing at given conditions.

αKG was combined with glycerol, 1,2,4-butanetriol, and 1,2,6-hexanetriol to generate PGa, PBa, and PHa, respectively – a series of chemoselective and biodegradable polymers with a range of mechanical and chemical properties. Furthermore, because all four monomers are inexpensive and the pre-polymer synthesis can be performed in bulk, PTKs are available for potential large-scale applications.

3.3.2 Polyketoester Pre-Polymer Synthesis and Characterization

The synthesis of PTK was designed for biological applications and, therefore, the elastomers were generated without any potential contaminating catalysts or co-reagents (Figure 3.1). After forming a homogenous melt at 125 °C, monomers were stirred while heating for 1 h. Random cross-linking proceeds rapidly without the use of reduced pressure or a catalyst, allowing for purification by precipitation in −78 °C MeOH. The pre-polymers were heated only to the extent of cross-linking that would enable purification – the majority

of the heating and cross-linking was intended to occur during a second heating phase, allowing for the molding and shaping of elastomeric films.

To determine the influence on mechanical effects of a ketone adjacent to one of the acids in αKG, two control pre-polymers were synthesized based on glutaric acid and diethyl β-ketoglutarate. The use of glutaric acid would allow for the determination of the effects of the presence of a ketone while diethyl β-ketoglutarate, which contains a ketone in the beta position relative to both carbonyl groups, would help to determine the role of the location of a ketone. However, under identical reaction conditions as were used with αKG, these controls did not sufficiently polymerize due to the lower reactivity of the two control molecules. Furthermore, pre-polymers were unable to form from glutaric acid or diethyl β-ketoglutarate after approximately three hours of reaction at 125 °C. These results suggest that the rapid cross-linking of PTK is due to the presence of a ketone moiety in the alpha position to the acid group in αKG.

PTK pre-polymers were then characterized by IR and DSC. The IR spectra of all three pre-polymers show an intense carbonyl stretch at ~ 1740 cm^{-1} due to the formation of multiple ester linkages (Appendix C, Figures C1-C3). DSC was used to calculate the glass transition temperatures (T_g) of PGa, PBa, and PHa (–22.5 °C, –33.4 °C, and –38.4 °C, respectively). With all T_g values less than 0 °C, PGa, PBa, and PHa are completely amorphous at room temperature. Furthermore, the three pre-polymers are soluble in several common organic solvents, including acetone, chloroform, dimethyl sulfoxide (DMSO), N,N-dimethylformamide, dioxane, ethanol, MeOH, DCM, and THF. The range of organic solvents can facilitate a variety of potential functionalization reactions as well as diverse processing techniques.

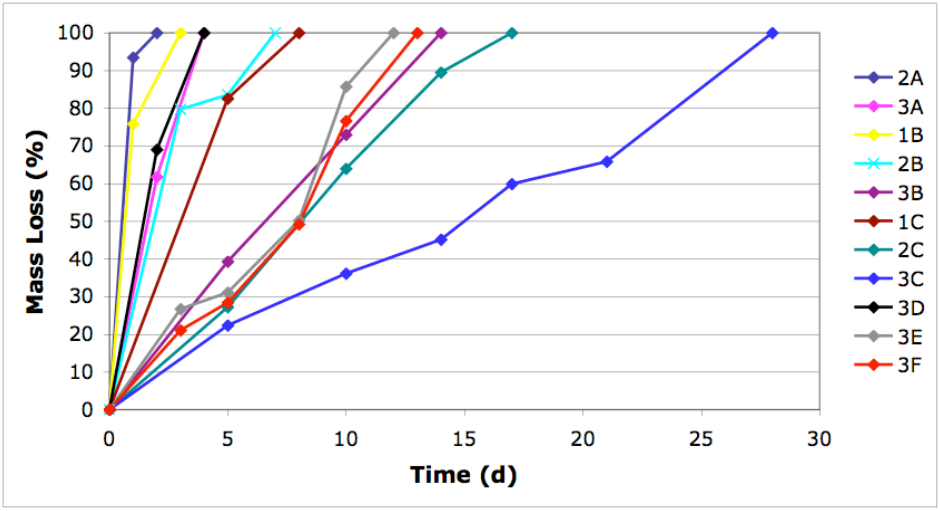

Figure 3.2. Degradation rate profiles for polyketoesters 2A – 3F. Due to the ease with which the extent of cross-linking and the hydrophobicity of the triol could be controlled, PTK films were able to hydrolytically degrade at varying rates. Complete mass loss was observed in as rapidly as 2 days (2A) and as long as 28 days (3C).

3.3.3 Polyketoester Cross-Linking and Mechanical Properties

The ability to design elastomers with a wide variety of mechanical properties was directly related to the ease with which the extent of cross-linking could be controlled. Therefore, several curing conditions were used to create materials with a range of structural properties (Table 3.1). Cross-linking the pre-polymers at lower temperatures for longer time periods (60 °C, 7 days) led to very soft, elastic materials while shorter curing periods at higher temperatures (120 °C, 1 day) produced hard, glassy materials.

TGA gave insight into the thermal stability of the eleven elastomers that were produced (Table 3.2). All eleven elastomers exhibited 5 % mass loss at temperatures of at least 239 °C. In addition, eight of the materials experienced 10 % mass loss at temperatures above 300 °C. A general trend became apparent in that the triol used, not the curing conditions, influenced the thermal stability of the elastomeric films. For example, material 3D, which was only cured for 6 h, exhibited higher thermal stability than four other materials

(2A, 1B, 2B, 1C) that were cured for at least 24 h. The main difference between these materials is that 3D is derived from PHa, while the other four are derived from PGa (1B, 1C) or PBa (2A, 2B).

The mechanical properties exhibited by various PTK elastomers were dispersed over a wide range (Table 3.2). Several unique combinations of YM, ultimate tensile stress (UTS), and rupture strain (RS) were present in these materials. For example, materials 1B and 2B were fairly rigid with correspondingly large YM values (YM = 459.4 MPa and YM = 161.4 MPa, respectively) and UTS values (UTS = 9.3 MPa and UTS = 4.7 MPa, respectively) when compared to the other materials. However, both were also capable of extreme elongation, at least doubling in length (RS = 121 % and RS = 418 %, respectively). In addition, typical soft and elastic materials were also produced. Materials 3A and 3D both had a YM value of 0.1 MPa, UTS values under 0.5 MPa (0.3 MPa and 0.2 MPa, respectively), and RS values over 350 % (395 % and 379 %, respectively). Overall, the YM varied by three orders of magnitude (0.1 MPa < YM < 657 MPa), the UTS varied by two orders of magnitude (0.2 MPa < UTS < 30 MPa), and the RS varied by one order of magnitude (22 % < RS < 583 %).

These pre-polymers could also be cured at physiological temperature (37 °C). However, the duration of the cross-linking process was dramatically increased (2 – 4 weeks). Temperature-sensitive cargo could therefore potentially be entrapped in the branched polyketoester network. Biopolymers such as proteins and nucleic acids, which can denature upon heating, may be able to survive the curing process at 37 °C, allowing for the potential delivery and release of natural therapeutics. Experiments are being pursued to fully determine the flexibility of curing materials at physiological temperatures.

Extending the potential for the success of PTK as a biomaterial is the fact that the mechanical properties of many biological materials fall within the ranges achieved by these materials. For example, elastin from bovine ligaments exhibits a YM of 2 MPa, an UTS of 1.1 MPa, and an RS of 150 %.[26] All of these values fall within the spectrum of material properties of PTK, due to the ease with which the cross-linking density can be controlled. Also, collagen can recover from deformations of up to 20 %, while arteries and veins can achieve RS of up to 260 %.[27-31] Furthermore, due to the ease with which the mechanical properties can be finely tuned, PTK could potentially be used for applications requiring a combination of flexibility and strength or for applications necessitating strength and rigidity.

3.3.4 *In Vitro* Degradation

Based on the alpha location of the ketone relative to the acid in PTK, electron-withdrawing effects should increase the electrophilic character of the carbonyl carbon in the adjacent ester. Accordingly, we expected these polyketoesters, which are also hydrophilic, to have rapid *in vitro* degradation rates. As expected, PGa, PBa, PHa exhibited 100 % mass loss in relatively short periods of time (< 28 days). However, since the curing conditions led to varying extents of cross-linking, a range of degradation rates were obtained (Table 3.2, Figure 3.2). The rates seem to be controlled by two factors: the extent of cross-linking within the polymer network and hydrophobicity of the elastomer. Therefore, the fastest degrading material should be soft and hydrophilic (1A) while the slowest degradation rate should be associated with a material that is hard and hydrophobic (3C). The only exception to this

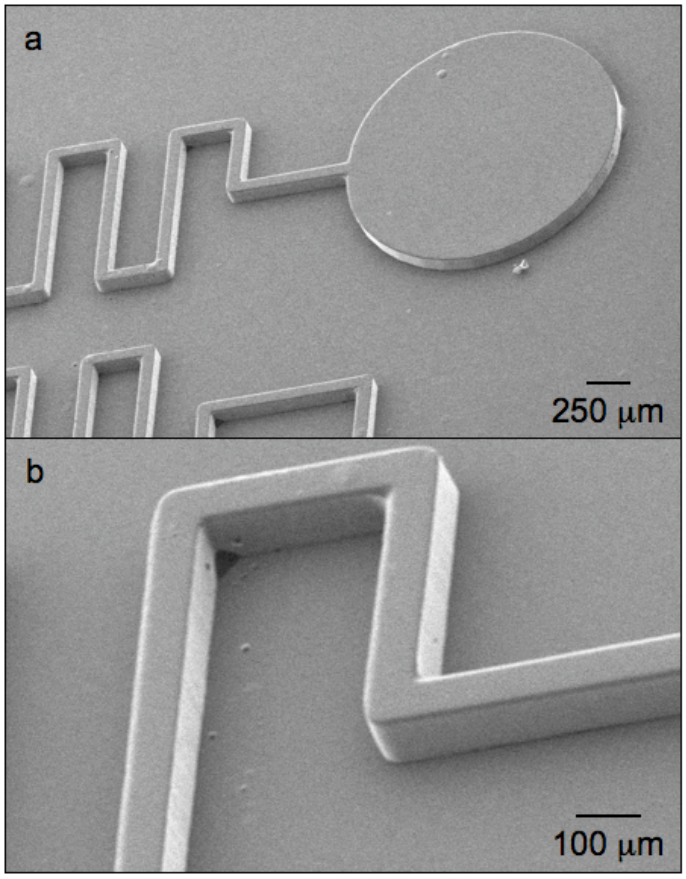

Figure 3.3. Scanning electron microscopy (SEM) images of thermally cured PHa. After partially curing PHa on a glass slide, a PDMS stamp was applied in order to pattern the elastomeric film. After the curing process ended, the stamp was removed, revealing the molded polyketoester film. The pattern was (a) transferred with high fidelity, (b) creating features with an approximate height of 70 μm.

general trend was material 1A – curing for 7 days at 60 °C led to insufficient cross-linking, producing a pseudo-amorphous material. For the remaining eleven materials, complete hydrolytic degradation occurred in as little as 2 days (elastomer 2A) and as many as 28 days (elastomer 3C). The other nine materials were dispersed between these two, allowing for the potential to tune the desired degradation rate or release profile of a particular material.

3.3.5 Film Micro-Molding

One way to enhance the versatility of a material is to allow for the patterning of topologies and microstructures. Imprint lithography was used to easily generate features in

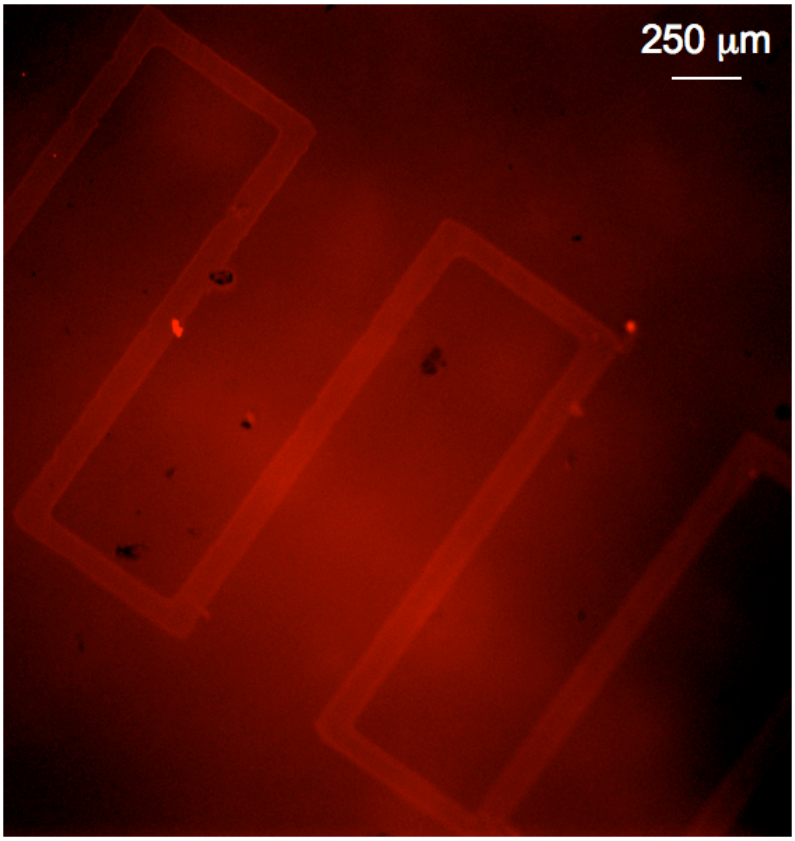

Figure 3.4. PHa patterned with a fluorescent dye. Using microfluidics, a solution of an oxyamine-modified rhodamine in MeOH was patterned on a flat PHa surface. After rinsing the surface, the fluorescent pattern is clearly visible against the non-modified PHa background.

PTK. After placing a small amount of pre-polymer on a glass slide in a vacuum oven at 120 °C, the pressure was reduced for 30 min to remove any residual solvent or gas. Using a patterned PDMS stamp, designed features were inversely transferred to polyketoester films by placing the stamp directly in contact with the pre-polymer. The pressure was reduced for an additional 20 min to remove trapped air. After a total curing period of 24 h, the PDMS stamp was removed. The elastomeric film was able to receive the inverse pattern of the PDMS stamp with high fidelity (Figure 3.3). This micro-molding strategy has the potential to create microfluidic devices or complex 3D microstructures for cell scaffolds.

3.3.6 Film Functionalization

The main factor for developing these PTKs was the desire to include a simple and mild functionalization strategy in a biomaterial. Using monomers that contain ketones accomplishes this through the ability to form stable oximes upon reaction with oxyamine-tethered molecules. Previous work has shown that ketones could survive extended periods of time at temperatures up to 170 °C during polymer synthesis.[32, 33] Therefore, the ketones in the polyketoesters should be able to survive curing processes at temperatures of 120 °C or less, allowing for mild post-polymerization modifications.

To demonstrate the covalent immobilization of ligands, an oxyamine-modified fluorescent dye was coupled to the surface of a polyketoester film. After placing a PDMS microfludic cassette in direct contact with a film of PHa, a liquid-tight seal was created. By flowing a MeOH solution containing an oxyamine-modified rhodamine through the device, spatial control of ligand immobilization was controlled. As seen in Figure 3.4, the fluorescent pattern is easily visible through the background fluorescence from the polyester film. Therefore, the ketones are still capable of reacting with oxyamine-containing ligands. As a control, a fluorescent dye without an oxyamine was flowed through the apparatus; no fluorescent pattern was observed. Since oxyamines are easily incorporated into a wide range of molecules, including peptides and carbohydrates, PTKs have the potential to be modified for biospecific tissue engineering and targeted delivery applications.

3.3.7 *In Vitro* Biocompatibility

To determine biocompatibility, cells were cultured in the presence of both PTK degradation by-products and pieces of elastomer films. None of the eleven films produced were deemed cytotoxic, as determined by cell morphology, monolayer confluence, and the ability to continue sub-culturing cells. A non-cytotoxic result was expected, as two of the

four monomers are naturally occurring metabolites. The fact that materials 2C and 3C are non-cytotoxic may also be due to their low sol-gel fractions (4.4 % and 3.5 %, respectively).

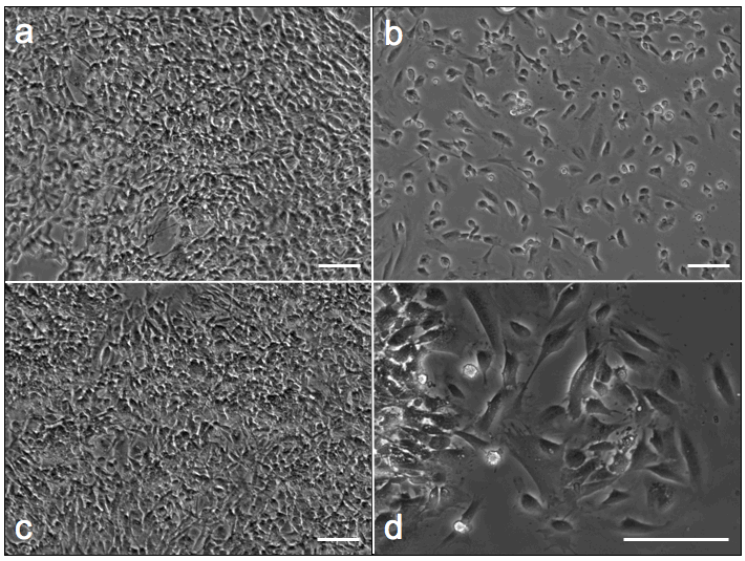

Figure 3.5. Poly(triol α-ketoglutarate) as cell scaffolds. 3T3 Swiss Albino fibroblasts were seeded onto elastomer films to determine their ability to act as cell scaffolds. Films were functionalized with H_2NO-GRGDS. On material 2C, cells were able to create a lawn (a) as well as take extended morphologies when space was available (b). Cells were also able to form a lawn (c) and take extended morphologies (d) on material 3C. The scale bars represent 50 μm.

A second method for determining biocompatibility was conducted by seeding cells on elastomers 1C, 2C, and 3C. Cells were unable to attach or proliferate on any of these three materials. However, when H_2NO-GRGDS peptide was coupled to the surface (1 mM, 5 hr), cells were able to recognize the peptide ligand and attach to the elastomer surface (Figure 3.5, Appendix C, Figure C4). The RGD peptide sequence is the minimal cell adhesive ligand found in the extracellular matrix protein fibronectin.[18, 19] After 48 h of division and migration, a lawn of contact inhibited cells was formed on materials 2C and 3C. Interestingly, although cells were able to attach to 1C after immobilization of H_2NO-GRGDS, PGa degraded too rapidly and did not allow for cellular division and migration.

3.4 Conclusions

Poly(triol α-ketoglutarate) was produced from the condensation of α-ketoglutaric acid and either glycerol, 1,2,4-butanetriol, or 1,2,6-hexanetriol. Altering the triol, the curing temperature, or the duration of the curing period allowed for control over the mechanical and degradation properties. A wide range of strengths and elasticities were easily achieved, producing materials that were strong and flexible, strong and inflexible, or weak and flexible. In addition, the ketone in the repeat unit is capable of reacting with oxyamine-terminated ligands, allowing for facile modification of polyester films. By immobilizing the cell adhesive peptide GRGDS, these materials were able to support cell adhesion through a receptor-ligand interaction without any cytotoxicity from the degradation byproducts. We believe that PTK may be applied to a wide range of tissue engineering and drug delivery applications. Attempts to extend the versatility of this strategy to include the design of new cell scaffolding materials, such as polyketoamides, are currently underway.

3.5 Acknowledgements

The authors thank the Ashby and DeSimone research groups for insightful discussions. This work was supported by the Carolina Center for Cancer Nanotechnology Excellence, grants from the NIH to M.N.Y., and the Burroughs Wellcome Foundation (Interface Career Award).

3.6 References

(1) Liu, H.; Webster, T. J. *Biomaterials* **2007**, *28*, 354-369.

(2) Kumar, M. N. V. R. *React. Funct. Polym.* **2000**, *46*, 1-27.

(3) Shastri, V. P. *Pharm. Biotechnol.* **2003**, *4*, 331-337.

(4) Shin, H.; Jo, S.; Mikos, A. G. *Biomaterials* **2003**, *24*, 4364.

(5) Jagur-Grodzinski, J. *Polym. Adv. Technol.* **2006**, *17*, 395-418.

(6) Odelius, K.; Plikk, P.; Albertsson, A. - C. *Biomacromolecules* **2005**, *6*, 2718-2725.

(7) Olson, D. A.; Gratton, S. E.; DeSimone, J. M.; Sheares, V. V. *J. Am. Chem. Soc.* **2006**, *128*, 13625-13633.

(8) Brown, A. H.; Sheares, V. V. *Macromolecules* **2007**, *40*, 4848-4853.

(9) Younes, H. M.; Bravo-Grimaldo, E.; Amsden, B. G. *Biomaterials* **2004**, *25*, 5261-5269.

(10) Yang, J.; Webb, A. R.; Ameer, G. A. *Adv. Mater.* **2004**, *16*, 511-516.

(11) Wang, Y.; Ameer, G. A.; Sheppard, B. J.; Langer, R. *Nat. Biotechnol.* **2002**, *20*, 602-606.

(12) Nijst, C. L.; Bruggeman, J. P.; Karp, J. M.; Ferreira, L.; Zumbuehl, A.; Bettinger, C. J.; Langer, R. *Biomacromolecules* **2007**, *8*, 3067-3073.

(13) Yang, S. K.; Weck, M. *Macromolecules* **2008**, *41*, 346-351.

(14) Taniguchi, I.; Mayes, A. M.; Chan, E. W. L.; Griffith, L. G. *Macromolecules* **2005**, *38*, 216-219.

(15) Van Horn, B. A.; Iha, R. K.; Wooley, K. L. *Macromolecules* **2008**, *41*, 1618-1626.

(16) Riva, R.; Schmeits, S.; Jerome, C.; Jerome, R.; Lecomte, P. *Macromolecules* **2007**, *40*, 796-803.

(17) Zugates, G. T.; Anderson, D. G.; Little, S. R.; Lawhorn, I. E. B.; Langer, R. *J. Am. Chem. Soc.* **2006**, *128*, 12726-12734.

(18) Pierschbacher, M. D.; Ruoslahti, E. *Nature* **1984**, *309*, 30-33.

(19) Ruoslahti, E. *Annu. Rev. Cell Dev. Biol.* **1996**, *12*, 697-715.

(20) Sanda, F.; Endo, T. *J. Polym. Sci. , Part A: Polym. Chem.* **2001**, *39*, 265-276.

(21) Chan, E. W. L.; Yousaf, M. N. *J. Am. Chem. Soc.* **2006**, *128*, 15542-15546.

(22) Lazny, R.; Nodzewska, A.; Sienkiewicz, M.; Wolosewicz, K. *J. Comb. Chem.* **2005**, *7*, 109-116.

(23) Mahal, L. K.; Yarema, K. J.; Bertozzi, C. R. *Science* **1997**, *276*, 1125-1128.

(24) He, W.; Miao, F. J.; Lin, D. C.; Schwander, R. T.; Wang, Z.; Gao, J.; Chen, J. L.; Tian, H.; Ling, L. *Nature* **2004**, *429*, 188-193.

(25) Lee, D. P.; Deonarine, A. S.; Kienetz, M.; Zhu, Q.; Skrzypczak, M.; Chan, M.; Choy, P. C. *J. Lipid Res.* **2001**, *42*, 1979-1986.

(26) Kim, Y. -.; Kim, H. K.; Nishida, H.; Endo, T. *Macromol. Mater. Eng.* **2004**, *289*, 923-926.

(27) Chung, I. S.; Matyjaszewski, K. *Macromolecules* **2003**, *36*, 2995-2998.

(28) Barrett, D. G.; Yousaf, M. N. *Biomacromolecules* **2008**, *9*, 2029-2035.

(29) Barrett, D. G.; Yousaf, M. N. *Molecules* **2009**, *14*, 4022-4050.

(30) Webb, A. R.; Yang, J.; Ameer, G. A. *Expert Opin. Biol. Ther.* **2004**, *4*, 801-812.

(31) Amsden, B. *Soft Matter* **2007**, *3*, 1335-1348.

(32) Risse, W.; Sogah, D. Y. *Macromolecules* **1990**, *23*, 4029-4033.

(33) Wang, F.; Chen, T.; Xu, J. *Macromol. Rapid. Commun.* **1998**, *19*, 135-137.

Chapter IV

KETONE-CONTAINING POLYESTER ELASTOMERS CAPABLE OF OXIME-BASED FUNCTIONALIZATION

4.1 Introduction

Recently, thermal polyesterification has become a popular strategy for synthesizing versatile polyester thermosets for biomedical applications.[1-6] By employing starting materials with an average functionality greater than two, esterification occurs and polymer chains interconnect, forming cross-linked materials. Several factors have led to the increased use of this polymerization strategy: ease, versatility, and the resulting polyesters. The ease of this synthetic methodology is difficult to match; the monomers are heated and stirred in a partial vacuum. Depending on the monomers and the desired macromolecular properties, the duration of the cross-linking period can vary between an hour and several days.[6-10] The end result is a cured polyester. As no complex synthesis is required, detailed training in organic reactions is not necessary, allowing a wide range of scientists the ability to develop these biomaterials. Thermal polycondensation also offers versatility in the polyester design. The choice of monomers can be made in an effort to impart application-specific properties on the final material; for example, hydrophobicity, crystallinity, rigidity, and degradation rates can be controlled.[1,2,11,12] The mechanical properties of the resulting polyesters can also be tuned by adjusting the curing conditions, allowing for one precursor to result in several materials that vary between rigid and flexible.[7,8,13,14] Finally, the polyesters designed with thermal polycondensation are simple and effective. The potential of these thermosets in biomedical and biotechnological fields continues to expand.[15-20]

Previous polyester elastomers have been designed with thermal polycondensation to incorporate a wide range of starting materials.[1,2] With the goal of biocompatibility, several polymers have been synthesized from monomers that are endogenous to human metabolic pathways.[1] The use of molecules that are naturally present in the human metabolism offers a

potential strategy to minimize cytotoxic effects. During degradation, such polymers can hydrolyze and release small molecules that the body can resorb, metabolizing them in various physiological pathways. Similarly, some research has focused on the thermal polymerization of the starting materials from other known biomaterials.[1,2,8,11,12,21-23]

In addition to a simple and versatile synthetic strategy, the installation of an efficient methodology for chemical modifications would further increase the potential success of a polymer.[7,24-27] As discussed above, thermal polycondensation offers a route to create mechanically diverse materials by adjusting the monomer feed composition and the curing conditions. However, to date, no conjugation strategy has been demonstrated to be compatible with polymerization technique. The inclusion of an immobilization reaction would impart the resulting biomaterial with chemical versatility, the ability to introduce a wide range of functional moieties into a polymer at various time points in the synthesis – during the pre-polymer stage or as a cross-linked film.

Several characteristics are critical to the success of a polymer in biomedical applications. For a material to be a successful polymer in biomedical applications, the polymer should be biocompatible and biodegradable in order to minimize adverse biological side-effects. Related to degradation, a biomaterial should be completely amorphous at physiological conditions so that hydrolysis proceeds linearly and homogeneously.[28-30] Also, a single, facile, and inexpensive synthetic strategy should allow access to a wide range of macromolecular properties (mechanical profiles, degradation rates, hydrophobicities, etc.). This would allow for the ability to tailor material properties to best fit a particular application, thereby maximizing the probability of success. Furthermore, while several immobilization strategies exist, the inclusion of a ketone would introduce two key benefits: a

chemoselective handle for conjugation and a location that can act as an anchor between the material and the tissue. Ketones are able to react specifically with oxyamine- and hydrazide-terminated ligands.[31-34] Similar to aldehydes, ketones can also act as a covalent anchor between biomaterials and tissue through the formation of imines due to the ubiquitous nature of amines in biological environments.[19] A recent study indicates that covalent attachment between materials and tissue enables strong adhesion without causing negative biological responses *in vivo*.[35,36]

In this chapter, we describe the syntheses and characterization of poly(diol 4-ketopimelate -*co*- diol citrate) (PDKDC), a novel and chemoselective series of polyketoesters. Two diols were employed in the syntheses of PDKDC: 1,4-cyclohexanedimethanol or 1,6-hexanediol. Varying the diol and the curing conditions led to the design of several elastomers with a range of physical and mechanical properties. The PDKDC materials described here displayed Young's moduli (YM), ultimate tensile stress (UTS), and rupture strain (RS) values of 0.39 – 1.13 MPa, 0.27 – 1.04 MPa, and 108 - 426 %, respectively. Additionally, the incorporation of the ketone from 4-ketopimelic acid imparted these materials with two advantages: a handle for covalent functionalization through oxime formation and a site for covalent anchoring to the surrounding tissue through imine linkages. In order to assess the full potential of these polyketoesters, biocompatibility was studied both *in vitro* and *in vivo*. Finally, the systemic *in vivo* response caused by PDKDC elastomers was evaluated by blood analysis. Preliminary results indicate that these polyketoesters are excellent candidates for biomaterials.

4.2 Experimental Section

4.2.1 Materials

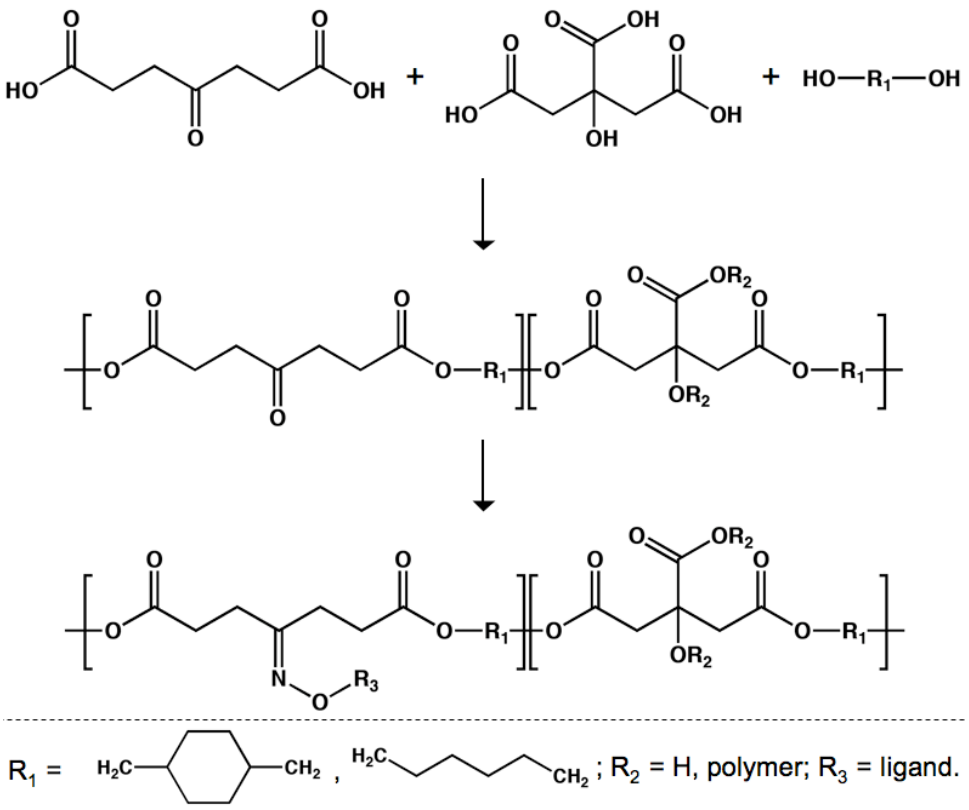

Figure 4.1. Synthesis of poly(diol 4-ketopimelate -co- diol citrate). Thermal polycondensation of 4-ketopimelic acid, citric acid, and either 1,4-cyclohexanedimethanol or 1,6-hexanediol led to the catalyst-free design of pre-polymers. Further heating of the pre-polymers allows for the preparation of elastomeric polyester thermosets. The inclusion of a ketone allowed for post-polymerization modifications through oxime formation.

All chemicals were used without further purification. Citric acid (CA), 4-Ketopimelic acid (4KP), 1,6-hexanediol (HD), 1,4-cyclohexanedimethanol (CHDM), and solvents were purchased from Fisher Scientific (Philadelphia, PA). *O*-Allylhydroxylamine hydrochloride, poly(DL-lactide-*co*-glycolide), and poly(ε-caprolactone) (PCL) were purchased from Sigma-Aldrich (Milwaukee, WI).

4.2.2 Poly(CHDM 4-ketopimelate -co- CHDM citrate) Synthesis

Polymerizations were performed based on previous description.[9,10] Briefly, 4-ketopimelic acid, citric acid, and 1,4-cyclohexanedimethanol were combined in a round

bottom flask in a molar ratio of 1:1:2. The mixture was heated at 135 °C until a homogenous melt was formed, stirred for 2 h in an environment of argon, and finally stirred at ~ 2 torr for 45 min. To form elastomeric thermosets, the pre-polymers were cured for 3 d at 100 °C, 120 °C, or 140 °C.

4.2.3 Poly(HD 4-ketopimelate -co- HD citrate) Synthesis

4-Ketopimelic acid, citric acid, and 1,6-hexanediol were combined in a round bottom flask in a molar ratio of 1:1:2. The mixture was heated at 135 °C until a homogenous melt was formed, stirred for 2 h in an environment of argon, and finally stirred for 2 h at a reduced pressure of ~ 2 torr. To form elastomeric thermosets, the pre-polymers were cured for 3 d at 120 °C or 140 °C.

4.2.4 Polyketoester Characterization

^{1}H NMR spectra of pre-polymers were acquired on a Bruker 400 MHz AVANCE spectrometer in deuterated dimethyl sulfoxide (DMSO). Molecular weights were measured compared to polystyrene standards on a Waters gel permeation chromatography (GPC) system with detection based on refractive index values. The measurements were taken at 40 °C with tetrahydrofuran (THF) as the mobile phase on three columns in series (Waters Styragel HR2, HR4, and HR5). Thermal properties were recorded by differential scanning calorimetry (DSC) and thermogravimetric analysis (TGA). Pre-polymer and polymer glass transition temperatures were measured during the second heating cycle (10 °C/min) on a TA Instruments Q200 DSC. Thermal degradation was collected with a Perkin-Elmer TGA with a heating rate of 10 °C/min in an atmosphere of N_2.

Tensile tests were conducted on an Instron 5566 at a crosshead speed of 10 mm/min at 37 °C. Samples were cured in a dog-bone-shaped mold with approximate dimensions of 10

mm x 3 mm x 1.5 mm, swelled in ddH_20 at 37 °C for 24 h, and then tested. The Young's modulus (*YM*; Pa) was calculated according to the linear segment of the first 5 % of the stress/strain curve. Three trials were performed and the average was reported. Using

$$n = \mathrm{YM}(3\mathrm{RT})^{-1} \quad (1)$$

where R is the universal gas constant (8.3144 J mol^{-1} K^{-1}) and T is the temperature in K, the cross-linking density (*n*; mmol L^{-1}) was calculated.

Water swelling (WS) experiments were performed by swelling films in ddH_2O for 24 h at room temperature. After removing surface water, the WS was calculated by

$$WS = \frac{m_f - m_i}{m_i} \times 100 \quad (2)$$

where m_i and m_f represent the initial and final mass of the elastomer films, respectively. Three trials were performed and the average was reported.

Sol-gel analysis was conducted by soaking films in THF for 24 h at room temperature. After solvent removal, the films were dried, and the percent soluble fraction (Q_s) was calculated by

$$Q_s = \frac{m_i - m_f}{m_i} \times 100 \quad (3)$$

where m_i and m_f represent the initial and final mass of the elastomer films, respectively. Three trials were performed and the average was reported.

Contact angle measurements were recorded on a KSV CAM200 contact angle meter with water as the wetting liquid.

4.2.5 Pre-Polymer Functionalization

Pre-polymer was added to a round-bottom flask and dissolved in a 4:1 solution (v/v) of methanol (MeOH) and dimethylformamide (DMF). A 2-fold molar excess of *O*-

allylhydroxylamine was added to the solution, which was stirred at room temperature for 24 h. Following the reaction, the solvent was removed by rotary evaporation. After dissolving the resulting residue in dichloromethane, the organic solution was washed with water, dried over $MgSO_4$, filtered, and concentrated *in vacuo*.

4.2.6 Film Molding

A small amount of pre-polymer was placed onto a glass slide and heated to 140 °C in a vacuum oven. After 30 min of reduced pressure (~ 50 torr) to remove any gas or solvent, a perfluoropolyether (PFPE) mold was placed directly on the pre-polymer.[37-39] The material was allowed to cure for 3 d, followed by the removal of the mold. The molded elastomeric films were then coated in ~ 2 nm of a Pd/Au alloy (Cressington 108 auto sputter coater, Cressington Scientific Instruments Ltd.) and imaged using a Hitachi model 2-4700 scanning electron microscope (SEM).

4.2.7 Polymer Functionalization

The pre-polymer based on 1,6-hexanediol was dissolved in 1,4-dioxane and added to glass slides. After solvent evaporation, curing proceeded at 140 °C for 3 d. Films were then submerged for 5 h in a 100 mM solution of the ligand in a solvent system of 9:1 (v/v) methanol-to-water. After rinsing the thin films and drying *in vacuo*, ligand immobilization was characterized with contact angle measurements.

4.2.8 *In Vitro* Degradation

To obtain standard degradation rates, ~ 50 mg segments of each elastomer were placed in scintillation vials. Vials were filled with phosphate buffered saline (PBS) and samples were then stored in a water bath at 37 °C. At predetermined intervals, samples were

removed, rinsed thoroughly with ddH_2O, dried, and weighed again. To prevent saturation, PBS was replaced every 7 days. Values were obtained using

$$Mass\ Loss = \frac{m_i - m_f}{m_i} \times 100 \quad (4)$$

where m_i and m_f represent the initial and final mass values, respectively. Each data point was repeated in triplicate and results were reported as the average percent of the original mass lost.

4.2.9 *In Vitro* Cytotoxicity

To test cell viability, Swiss albino 3T3 fibroblasts (SAFs) were plated in 24-well plates at a density of approximately 40,000 cells per well and incubated for 18h at 37 °C in a humidified 5% CO_2 atmosphere. After incubation, each polymer sample [~ 50 mg; sterilized in 70 % ethanol (EtOH) and washed in PBS under a germicidal lamp for 2 h] was placed within a cell culture insert with 3 μm pores (PET track etched membrane, Becton Dickinson), placed in a well, and covered with complete culture medium. SAFs and materials were continuously incubated for 72h. Cell viability was estimated at 24 h and 72 h by quantification of intracellular ATP using the CellTiter-Glo™ Luminescent Cell Viability Assay (Promega) following the manufacturer's suggested protocol. Luminescence was measured with a Molecular Devices SpectraMax M5 microplate reader (Molecular Devices Laboratories). The viability of the cells exposed to polymer samples was expressed as a percentage of the viability of cells grown in the absence of polymers.

4.2.10 *In Vivo* Biocompatibility

Pre-polymers were dissolved in 1,4-dioxane and cast into a mold of poly(tetrafluoroethylene) (PTFE). After the solvent was removed with reduced pressure, cross-linking was performed as previously described and the film was removed from the

mold. PLGA was dissolved in methylene chloride and cast into a PTFE mold. After solvent evaporation, the film was removed from the mold. All samples were cut into 10 mm x 2 mm x 1 mm samples for use in live-animal studies. Polyester thermosets were sterilized in EtOH for 30 min and washed in PBS for 2 h while under a germicidal lamp. PLGA control samples were exposed to 365 nm light for 10 min.

For the live-animal studies, 7-week old female Sprague-Dawley rats (7-weeks old, Harlan Laboratories) were anesthetized under isoflurane and O_2 and shaved of all hair on the dorsal portions of the right and left sides. The surgical areas were prepared with alternating applications of a 10 % povidone/iodine solution and 70 % EtOH. Four 1-cm longitudinal incisions were made for implantation of the polymer samples. The incisions were closed with sterile 5-0 surgical sutures, followed by a subcutaneous injection of bupreorphine (0.05 mg/kg) every 12 h for a total of 24 h. The animals were cared for in accordance with UNC and NIH regulations. At predetermined time points, 7 rats were euthanized with CO_2; as a secondary method of euthanasia, animals were decapitated using a standard small animal guillotine and the trunk blood was collected in 50 mL conical tubes (Falcon, Franklin Lakes, NJ). Blood samples were allowed to clot at room temperature for 2 h before being centrifuged at 200 rpm for 15 min at room temperature. Plasma samples were collected, aliquoted, and stored at -80 °C for further analysis. All polyester samples were harvested in the surrounding tissue for histological evaluation.

Biocompatibility was assessed by two different methods. First, the local response of the host system was studied by histological evaluation. As previously stated, polymer samples were harvested with the surrounding tissue intact. The tissue was fixed for 36 h in 10 % formalin, washed with ddH_2O, and stored in 70 % EtOH. Tissue blocks were

dehydrated stepwise in 80 % EtOH, 95 % EtOH, 100 % EtOH, and xylene. After dehydration, the samples were embedded in paraffin and sectioned into 5 μm thin films. Slides were stained with hematoxylin (H&E) and Masson's trichrome stain. Images were recorded on a Nikon Eclipse TE2000-E inverted microscope with Metamorph software.

As a second method, the systemic biocompatibility was monitored though blood analysis. Plasma concentrations of pro-inflammatory cytokines Interleukin-1 (IL-1), Interleukin-6 (IL-6), and Tumor Necrosis Factor alpha (TNF-α) were quantified using commercially available ELISA kits (R&D Systems, Inc., Minneapolis, MN). Plates were read on an EL-800x microplate reader and analyzed with KC Junior Software (Biotek Instruments, Winooski, VT). Briefly, a monoclonal antibody specific for the cytokine of interest was pre-coated onto a microplate. Standards and plasma samples were added into the wells and the immobilized antibody bound cytokines contained in the sample. After washing away unbound substances, an enzyme-linked polyclonal antibody specific for the cytokine of interest was added to the wells. Following a wash to remove any unbound antibody-enzyme reagent, a substrate solution was added to the wells and color developed in proportion to the amount of bound cytokine in the initial step.

4.3 Results and Discussion

4.3.1 Motivation

We recently described the poly(triol α-ketoglutarate) (PTK) family of polyester elastomers.[7,40] Although these materials demonstrated many interesting macromolecular properties, their degradation rates were particularly noteworthy. In terms of designing potential tissue scaffolds, the PTK series hydrolyzed in PBS too rapidly to be useful; the reduction in pH associated with ester hydrolysis was too drastic. The current work aimed to

design similar materials with degradation rates that were more appropriate for future applications in tissue engineering. Prior experience suggested that the critical factor to achieving this goal was to alter the location of the ketone in the monomer.[24,40]

Initially, 4KP was polymerized with a number of sugar alcohols, which acted as the cross-linking agent. However, ^{1}H NMR results indicated that another linkage was forming (data not shown). We believe that ketals were being synthesized in addition to esters; the reaction contained ketones, vicinal diols, and acid, three common components used to obtain ketals. Ketals were undesired as they reduced the number of ketones that could act as a site for immobilization. Therefore, the current work involved a synthetic strategy that did not include any vicinal diols. Citric acid acted as the cross-linking agent for the polymerization of 4KP and either CHDM or HD. All four of these monomers have previously been incorporated into non-cytotoxic biomaterials.[10,25,41,42] By altering the diol and the curing conditions, a wide range of macromolecular characteristics (hydrophobicity, degradation rate, mechanical profile, etc.) were achieved.

4.3.2 Pre-Polymer Synthesis and Characterization

The synthesis of PDKDC was designed to be as mild as possible because these polyketoesters will be evaluated for future biomedical applications. These elastomers were generated without the use of any catalysts or co-reagents in an attempt to minimize the presence of potentially toxic species (Figure 4.1). The monomers (molar ratio of 4KP:CA:diol = 1:1:2) were melted at 135 °C and stirred for 2 h in an inert environment of argon. The pressure was then reduced for an additional heating period (45 min or 2 h). The pre-polymers were esterified only to the extent of cross-linking that would enable purification in –78 °C MeOH. The majority of heating and cross-linking occurred during a

Table 4.1. Pre-Polymer Characterization

Pre-Polymer	T_g (°C)	M_n (g/mol)	PDI
PP-CHDM	- 34.4	1140	1.3
PP-HD	- 36.9	960	1.2

second heating phase, which allowed for elastomers to be molded and shaped. The resulting oligomers were named according to the diol used in the formulation: PP-CHDM or PP-HD.

The pre-polymers were characterized in order to verify that esterification was the only reaction that occurred. The ^{1}H NMR spectra, as seen in Figures D1 and D2, show similar chemical signatures. Both pre-polymers contain equal molar equivalents of 4KP and CA, resulting in the peaks located between 2 ppm and 3 ppm. The differences arise from the use of different diols in the pre-polymer formulations. CHDM produces signals between 0.75 ppm and 1.75 ppm; HD results in peaks located between 1.25 ppm and 1.75 ppm. The presence of signals around 4 ppm indicates that alcohols and acids combined to form esters. The most important aspect of both of these spectra is the presence of peaks 'a' and 'b', which are associated with the ketone. These peaks provide evidence that the ketones survive the synthetic conditions.

Additionally, the pre-polymers were characterized by GPC and DSC (Table 4.1). The number-average molecular weights of PP-CHDM and PP-HD were determined by GPC to be 1140 g/mol and 960 g/mol, respectively. The glass transition temperature (T_g) of PP-CHDM was 34.4 °C while that of PP-HD was 36.9 °C. These pre-polymers are soluble in common polar organic solvents such as acetone, DMSO, DMF, 1,4-dioxane, EtOH, MeOH, and THF.

4.3.3 Pre-Polymer Functionalization

Table 4.2. Curing Conditions for Poly(Diol 4-Ketopimelate -*co*- Diol Citrate)

Elastomer	Diol	Temp. (°C)	Duration
1	CHDM	100	3 d
2	CHDM	120	3 d
3	CHDM	140	3 d
4	HD	120	3 d
5	HD	140	3 d

Due to the presence of a ketone in the repeat unit, post-polymerization modifications were possible.[7,25,40] To demonstrate the covalent immobilization of ligand to the PDKDC backbone, an oxyamine-containing small molecule was conjugated to each pre-polymer. *O*-allylhydroxylamine (OAH) was dissolved in a solution of MeOH and DMF (4:1 v/v). PP-CHDM or PP-HD was dissolved in the solution such that the molar ratio of oxyamine-to-ketone was 2:1. After stirring for 24 h at room temperature, complete conversion of ketones to oximes was observed by ^{1}H NMR (Figure D3 and D4). OAH was chosen as the ligand due to the diagnostic peaks associated with the vinyl protons: h and i. Additionally, the peak that represents the methylene unit adjacent to the ketone (peak b in Figures D1 and D2) shifted once the transition to oximes was complete (peak b in Figures D3 and D4). Therefore, the ketones are still capable of reacting with oxyamine-containing ligands. Since oxyamines are easily incorporated into a wide range of molecules, including peptides and carbohydrates, PDKDC has the potential to be modified for biospecific tissue engineering.

4.3.4 Polyketoester Curing and Mechanical Properties

One of the attractive qualities of thermal polycondensation is the ability to design different mechanical profiles by altering the curing conditions. Therefore, several curing conditions were used to create materials with a range of structural properties (Table 4.2). All

thermosets were prepared by curing pre-polymers for 3 d; the degree of cross-linking was controlled by varying the curing temperature (100 °C, 120 °C or 140 °C). CHDM was chosen as the diol when a rigid material was desired; the cyclic structure of CHDM limited the flexibility of the polyester thermosets. Conversely, softer polymers were developed from HD, which has a linear structure that promotes flexibility. This hypothesis was realized upon characterization of the mechanical profiles of these elastomers (Table 4.3). Overall, these materials achieved YM, UTS, and RS values of 0.39 – 1.13 MPa, 0.27 – 1.04 MPa, and 108 - 426 %, respectively. The range of these mechanical properties encompasses several anatomical materials.[28,43] Additionally, recent literature has suggested that the surface topology of tissue scaffolds can play an important role in their performance. Therefore, we demonstrated that the PDKDC series of polyesters can be molded. By curing in the presence of a PFPE mold, materials 3 and 5 were embossed with micron-scale features (Figure D5).

Table 4.3. Macromolecular Properties of Poly(Diol 4-Ketopimelate -*co*- Diol Citrate)

Elastomer	T_g [a] (°C)	Young's Modulus [b] (MPa)	UTS [b] (MPa)	Rupture Strain [b] (%)	n [c] (mmol/L)	Contact Angle (°)
1	19.1	0.39 ± 0.02	0.35 ± 0.07	426 ± 85	53 ± 3	77.9 ± 1.1
2	21.4	0.85 ± 0.01	0.44 ± 0.03	160 ± 2	114 ± 1	78.8 ± 0.4
3	19.5	1.13 ± 0.12	1.04 ± 0.20	158 ± 17	152 ± 16	94.9 ± 1.0
4	- 25.7	0.43 ± 0.10	0.27 ± 0.01	153 ± 22	58 ± 14	77.6 ± 1.3
5	- 21.1	0.62 ± 0.12	0.39 ± 0.11	108 ± 5	83 ± 17	88.1 ± 0.5

[a] determined by DSC on second heating cycle (10 °C/min); [b] determined with hydrated samples by Instron (10 mm/min crosshead speed) at 37 °C; [c] determined from eq. 1.

4.3.5 Polymer Characterization

Certain macromolecular properties were directly linked to the choice of diol and to the curing conditions of the PDKDC polyketoesters. As such, the soluble fractions, water

swelling, and contact angles were determined. The extent of cross-linking increased as the curing temperature increased from 100 °C to 140 °C due to further esterification of alcohols and acids. Therefore, as the polyester chains became covalently linked, the amount of polymer that remained free decreased; the amount of sol in these materials was indirectly related to the curing temperature (Figure 4.2). Interestingly, the water swelling was independent of the material composition, remaining relatively constant at ~ 5 %. The contact angle followed a trend similar to the soluble fraction. As cross-linking became more extensive, the hydrophobicity of the PDKDC materials increased due to the loss of alcohols and acids. Also, with similar synthetic conditions, HD produced more hydrophilic materials. As seen in Table 4.3, the contact angles of materials 1 – 5 were 77.9 °C, 78.8 °C, 94.9 °C, 77.6 °C, 88.1 °C. These values agree with intuitive hypotheses based on the above factors.

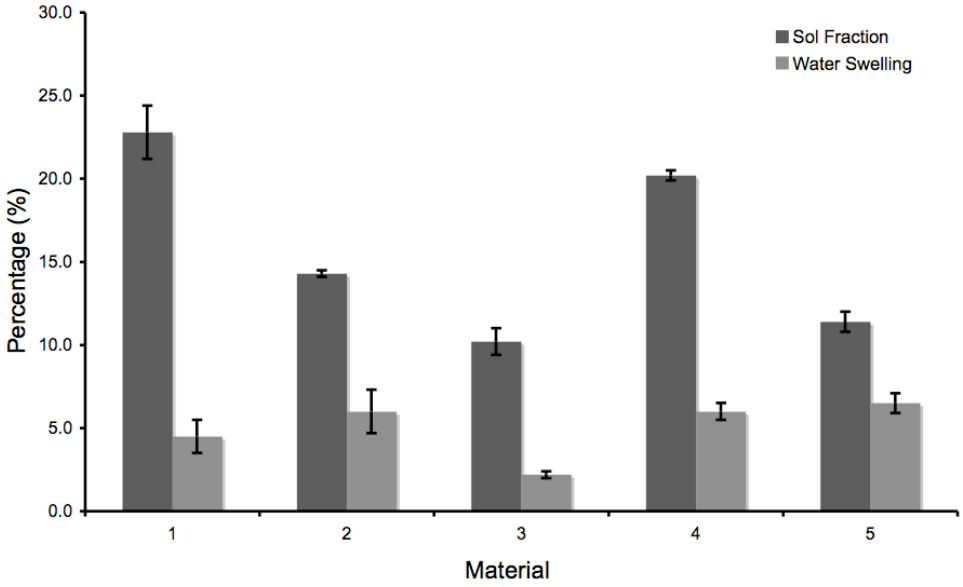

Figure 4.2. Sol fraction and water swelling of materials 1 – 5.

TGA offered insight into the thermal stability of PDKDC elastomers that were synthesized (Table D1). Materials 1 – 5 all exhibited 5 % mass loss at temperatures of at least 290 °C; in addition, 10 % mass loss occurred at temperatures exceeding 323 °C. Between 428 °C and 446 °C, only 50 % of the original mass of the PDKDC materials remained. After observing the data, trends emerged with respect to material composition. Thermal stability seemed to be related to choice of diol; all CHDM-based polyketoesters were more thermally stable than the HD-based materials. Additionally, assuming a constant choice of diol, the curing temperature was also directly related to the stability of these polymers at high temperatures. As the curing temperature increased, the temperatures associated with 5 %, 10 %, and 50 % mass remaining also increased.

Due to the free ketone in the repeat unit of all PDKDC materials, ligands can be conjugated through oxime or hydrazone moieties. To demonstrate the covalent immobilization of ligands, oxyamine- or hydrazide-containing ligands were immobilized to the surface of thin films of material 5 (Figure D6). Ligands 1 – 4 vary in terms of their hydrophobicities due to different terminal functionalities. Material 5 has a contact angle of 88.10 °. After immobilizing ligands, the contact angles of the modified PDKDC film were reduced by at least 10 ° (Table D2). These results were expected because the ligands contain functional groups that are more hydrophilic than the hydrophobic polyester backbone of material 5. As oxyamines and hydrazides are easily incorporated into a wide range of molecules, including peptides and carbohydrates, PDKDC thermosets have the potential to be modified for various biomedical applications.

4.3.6 *In Vitro* Degradation

Due to the gamma-location of the ketone, relative to the esters in PDKDC, the reactivity of the ester carbon should be unaffected, allowing degradation rates that are comparable to similarly synthesized materials.[24,25,40] As the curing conditions led to varying extents of cross-linking, a range of degradation rates were obtained (Table 4.3, Figure 4.3). Because CHDM and HD are similarly hydrophobic, the hydrolysis rates were primarily controlled by the extent of cross-linking within the polymer network. Degradation was observed over a 4-week period in PBS at 37 °C. The polyesters that degraded most rapidly also achieved the lowest cross-linking densities (materials 1 and 4), while the most cross-linked material displayed the slowest degradation rate (material 3). Overall, 10 – 31 % hydrolytic degradation was observed over the 4-week study; the degradation rates of the five materials were distributed within this range.

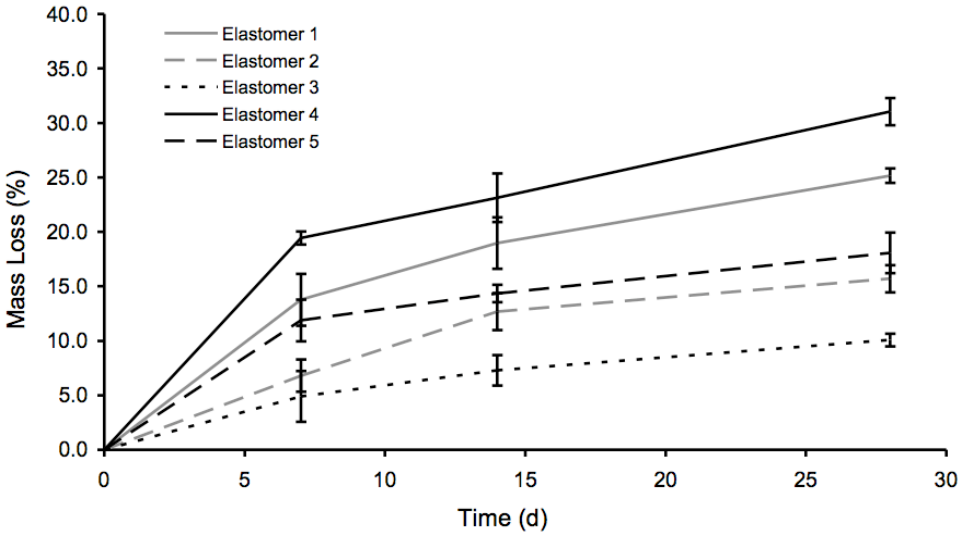

Figure 4.3. *In vitro* degradation of PDKDC. Polyester samples were incubated in PBS at 37 °C for four weeks. At pre-determined time points, the percent mass loss was recorded. After 4 weeks, the PDKDC series achieved *in vitro* degradation ranging from 10 % to 31 %.

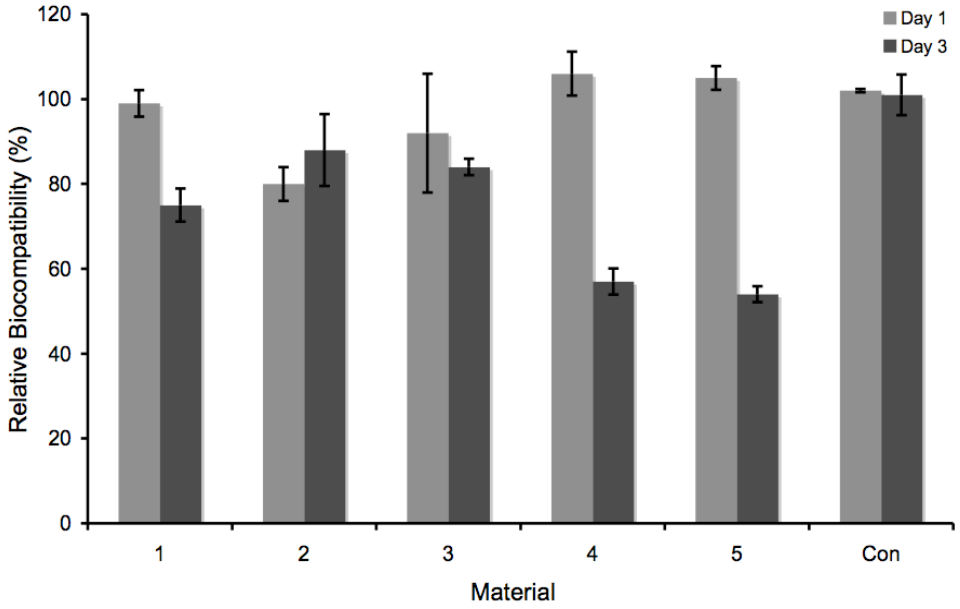

Figure 4.4. *In vitro* cytotoxicity of PDKDC based on an ATP-luminescence assay. SAFs were cultured on tissue culture plastic in the presence of itaconate-based polyesters. As a positive material control, cells were cultured in the presence of PCL (Con). The viability of the cells exposed to polymer samples was expressed as a percentage of the viability of cells grown in the absence of polymers.

4.3.7 *In Vitro* Cytotoxicity

The PDKDC series of polyesters was designed for tissue engineering and other biomedical applications. As such, the cytotoxicity of these thermosets was studied by monitoring the intracellular concentration of ATP. Polyester samples were sterilized in EtOH and washed in PBS under a germicidal lamp. SAFs were cultured in a 24-well plate that contained transparent and permeable inserts. Due to preliminary data suggesting that viability could be limited by polymer samples resting directly on cells, PDKDC samples were placed in the inserts in order to eliminate direct contact between polyesters and cells. Because of the permeability of the inserts, the cells were exposed to the soluble fraction of the polyesters and any degradation products during culture. Two positive controls were utilized during the course of these studies: cells were exposed to no polyester elastomers and

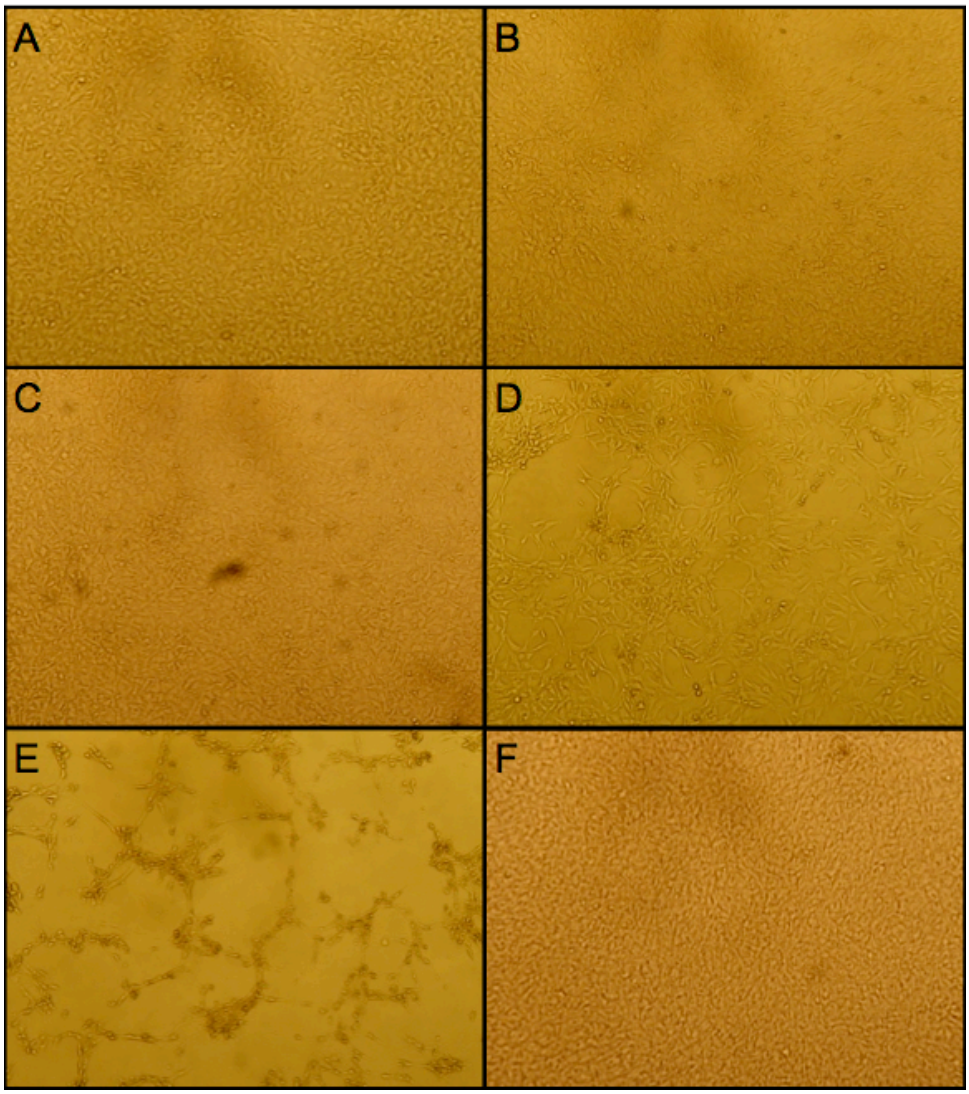

Figure 4.5. Optical micrographs of cells from *in vitro* cytotoxicity assay. SAFs were imaged after 72 h of culture with materials 1 (A), 2 (B), 3 (C), 4 (D), and 5 (E). As a control, cells were cultured with samples of PCL (F). Materials 4 and 5, the polymers based on 1,6-hexanediol, displayed toxicity towards SAFs.

to PCL. The cytotoxicity was evaluated after 24 h and 72 h. As seen in Figure 4.4, SAFs showed little negative response to the polyesters after a day of culture. However, materials 4 and 5 – both of which contain HD as the diol – displayed toxic characteristics after 3 d of culture (Figure 4.5). During the study, the color of culture medium exposed to materials 4 and 5 changed from red to yellow; this change indicated a drop in pH, which could

potentially explain the negative biological responses. Compared to cells that were not exposed to polymer samples, cell cultured in the presence of materials 1 – 3 (CHDM-based materials) were able to proliferate well (≥75 % viability). These preliminary biological data indicate that PDKDC polyesters warrant further exploration as potential biomaterials.

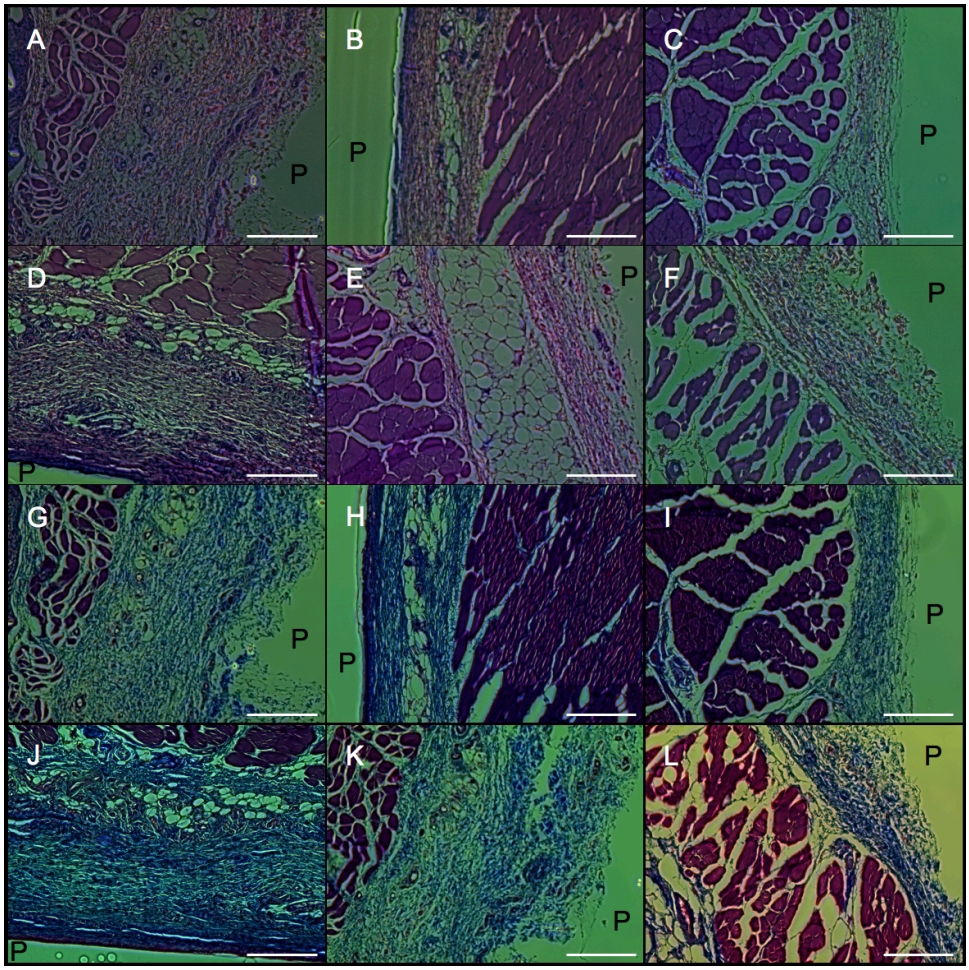

Figure 4.6. *In vivo* histological evaluation of PDKDC after two weeks of implantation. Material 1 (A,G), Material 2 (B,H), Material 3 (C,I), Material 4 (D,J), Material 5 (E,K), and PLGA (F,L) were subcutaneously implanted in rats. Tissue sections were stained with hematoxylin and eosin (A – F) or Masson's trichrome (G – L). The polymers in the images are labeled with a "P". All scale bars represent 200 μm.

4.3.8 *In Vivo* Biocompatibility

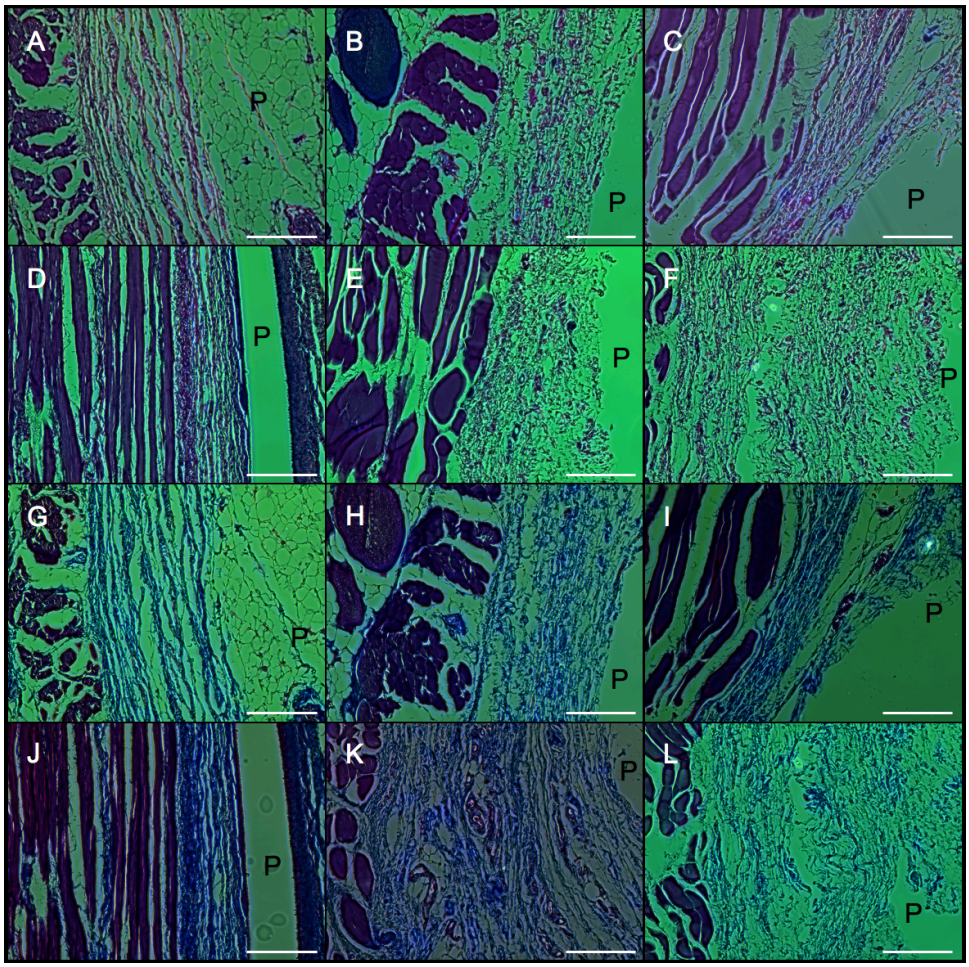

Figure 4.7. *In vivo* histological evaluation of PDKDC after four weeks of implantation. Material 1 (A,G), Material 2 (B,H), Material 3 (C,I), Material 4 (D,J), Material 5 (E,K), and PLGA (F,L) were subcutaneously implanted in rats. Tissue sections were stained with hematoxylin and eosin (A – F) or Masson's trichrome (G – L). The polymers in the images are labeled with a "P". All scale bars represent 200 μm.

The clinical use of novel biomaterials requires a thorough understanding and examination of the biological processes that occur when cells and tissues are exposed to these materials.[44] Thus, both *in vitro* and *in vivo* biocompatibility testing are useful in determining the clinical utility of biomaterials. The *in vivo* response to PDKDC polyketoesters was evaluated by subcutaneous implantation in rats. Fourteen days after implantation, the inflammatory response exhibited by rats was mild for materials 1 – 5 (Figure 4.6). The

fibrous capsules encompassing the implants were of similar thickness as those that surrounded the material control (PLGA samples). Assessment after 28 d *in vivo* exposed thicker fibrous capsules around PDKDC implants when compared to the 14 d samples (Figure 4.7). Again, though, these thicknesses were similar to that of the capsule surrounding the PLGA implant at similar time points. These results are comparable to other soft thermoset elastomers.[4-6,9,10]

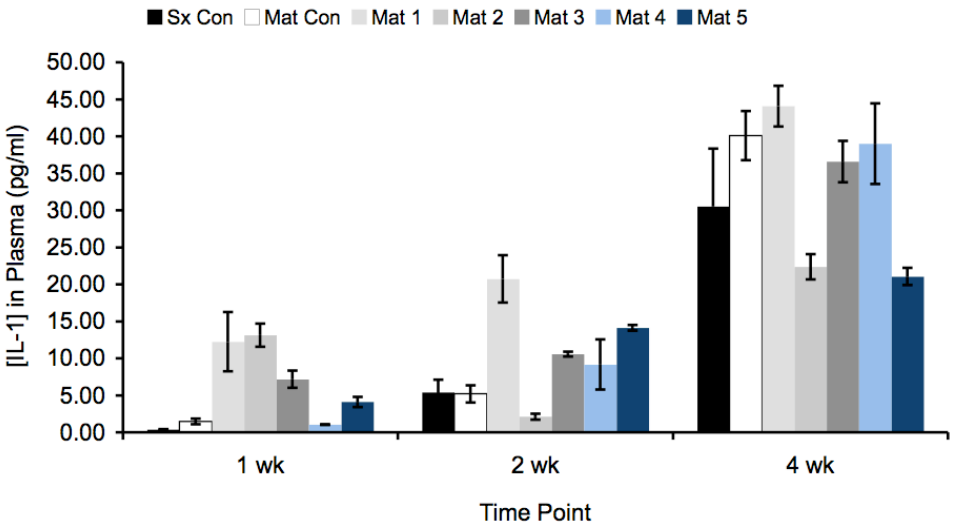

Figure 4.8. Plasma IL-1 concentrations. The concentration of IL-1, a blood-based marker of stress, was calculated in order to understand the systemic consequences of PDKDC implantation. The mean concentration ± standard deviation is shown from three replicates per sample (1 sample/treatment group). 'Sx Con' represents the surgery control with no implantation and 'Mat Con' is a material control of PLGA.

Although histological evaluations are common in the evaluation of *in vivo* biomaterials, they only offer a local view of the inflammatory response elicited by material implants. Therefore, a systemic approach was combined with histological data in order to understand how the entire animal reacted to the polymer samples. From an inflammatory perspective, the most biocompatible materials are those that produce the least amount of

inflammation for the shortest period of time. Assessment of the quality or intensity of inflammation can be characterized in different ways, including quantification of cytokine expression, quantification and phenotypic characterization of cellular infiltrates, and measurement of chemokines and matrix metalloproteinases.[44-49] For these initial studies, we chose to characterize circulating plasma concentrations of pro-inflammatory cytokines associated with acute inflammation. When animals were sacrificed in order to procure tissue samples, trunk blood was collected. Both material and surgery controls were analyzed in addition to materials 1 – 5. PLGA again served as a materials control. A surgery control was used in order to differentiate between inflammation caused by surgeries from that which resulted due to the implanted polymers. Blood plasma samples were tested for the presence of several cytokines that are associated with inflammation: IL-1, IL-6, and TNF-α.[44,50-52] Surgical controls exhibited a plasma IL-6 concentration of 1.56 pg/mL and a plasma TNF-α concentration of 1.75 pg/mL. No differences in the concentrations of plasma IL-6 or TNF-α were noted among experimental groups when compared to sham surgery controls at any time point (data not shown).

Interestingly, quantification of plasma IL-1 revealed several differences (Figure 4.8). Across time points, surgical controls (Sx) exhibited an increasing level of IL-1 over time from 1 week (0.39 pg/mL) to 4 weeks (30.53 pg/mL). PLGA controls and material 4 exhibited similar levels of plasma IL-1 across all time points (PLGA: 1.45-40.11 pg/mL; material 4: 1.05-39 pg/mL). In contrast, at week 1, animals that received implants of materials 1, 2, and 3 exhibited increased levels of IL-1 compared to Sx or PLGA controls (12.25, 13.13, and 7.18 pg/mL, respectively). To a lesser extent, the animal treated with material 5 exhibited an elevated level of plasma IL-1, with 4.10 pg/mL. By week 2, the

concentration of IL-1 associated with material 2 had decreased, while all others remained elevated compared to SX or PLGA. By week 4, all groups had decreased to levels at or below that of Sx or PLGA controls.

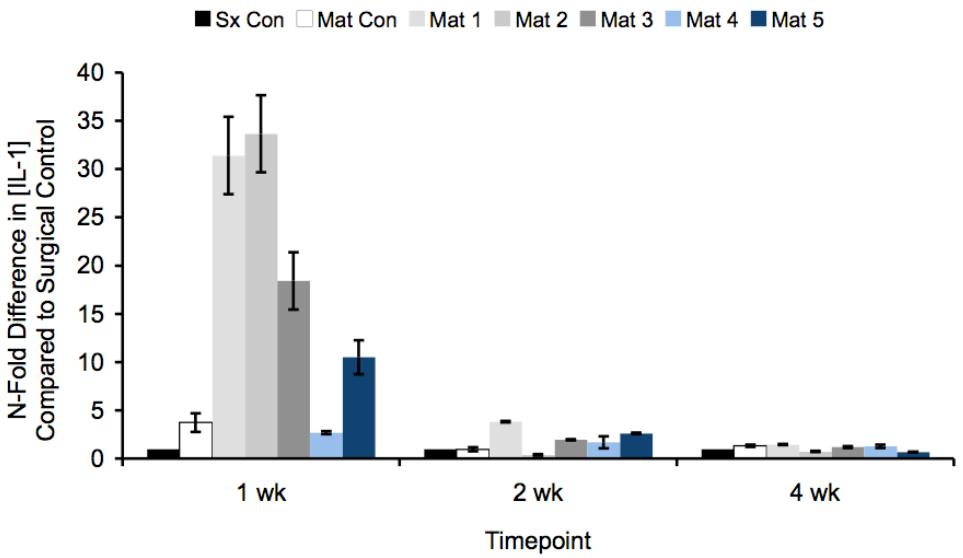

Figure 4.9. Plasma IL-1 concentrations expressed as n-fold differences relative to the surgical control. N-fold differences ± standard deviation compared to mean concentration of surgical controls at each time point (3 replicates per sample, 1 sample/treatment group) is displayed. 'Sx Con' represents the surgery control with no implantation and 'Mat Con' is a material control of PLGA.

Plasma IL-1 concentrations were also calculated as n-fold differences compared to surgical controls (Figure 4.9). CHDM-based materials caused an 18- to 34-fold difference compared to Sx controls at week 1. However, these differences returned to levels comparable with Sx or PLGA controls by week 4. Material 5 initially exhibited a 10.5-fold increase compared to Sx controls at week 1, but this effect dropped significantly by weeks 2 and 4. In general, the plasma levels of IL-1 associated with materials 1 – 5 returned to the levels of Sx and PLGA controls by week 4.

The induction of pro-inflammatory IL-1, but not IL-6 or TNF-α is consistent with the current literature. Previous studies have found that TNF-α levels did not differ in response to different biomaterials, irrespective of hydrophobicity and ionic state.[44] Other studies demonstrated that IL-1 and IL-6 responses could increase or decrease based on the chemical properties of the biomaterial. With respect to the duration of elevated cytokine concentrations, IL-1 concentrations were elevated at week 4 in both control and experimental groups. However, levels were generally comparable to that of sham surgery controls, indicating that the increase in IL-1 specifically associated with the biomaterial had been attenuated.

These *in vivo* data are interesting when compared to the *in vitro* biocompatibility results. CHDM-based materials, which showed relative consistency in biocompatibility from day 1 to day 3, were among the most detrimental materials from an inflammatory perspective, relative to Sx controls. This inconsistency between *in vitro* and *in vivo* biocompatibility data is further highlighted when material 4 is examined. At day 3 *in vitro*, material 4 demonstrated less than 60 % biocompatibility. However, material 4 produced a minimal inflammatory response *in vivo*. Taken together, these findings highlight the importance of considering both *in vitro* and *in vivo* biocompatibility data. With respect to the experimental materials that were tested, material 4 appeared to induce a minimal inflammatory response while materials 1 and 2 induced the most robust inflammatory response. Future studies will focus on long-term *in vivo* studies with a larger population of animals.

4.4 Conclusions

Poly(diol 4-ketopimelate -co- diol citrate) was synthesized from the polycondensation of 4-ketopimelic acid, citric acid, and either 1,4-cyclohexanedimethanol or 1,6-hexanediol. Thermal polycondensation offers a facile route to tune the mechanical properties, hydrophobicity, and the degradation rates of the PDKDC family of thermosets. The liquid pre-polymers are compatible with imprint lithography and salt-leaching techniques, enabling the fabrication of embossed films or porous scaffolds. By including a ketone in the repeat unit, these materials can covalently link to biological tissue through imines or to soluble ligands through oximes. The ketone-oxyamine conjugation strategy can be manipulated to covalently attach a wide range of biomolecules and/or nanomaterials to polyketoester films. *In vitro* and *in vivo* biocompatibility studies suggest that the non-functionalized thermosets are suitable candidates for tissue scaffolds. A cytokine, IL-1, was also identified as a potential blood-based marker of systemic inflammation that is sensitive to subtle differences in material composition. Future work will focus on the synthesis of novel polymer by altering the diol and the monomer feed ratios. Additionally, long-term *in vivo* observation will focus on non-functionalized and oxime-modified polyester samples. Our lab has experience synthesizing oxyamine-tethered molecules such as carbohydrates, peptides, and poly(ethylene glycol), all of which could be useful in biological studies. Based on these preliminary studies, we believe that the PDKDC series of polyester elastomers may be appropriate for tissue engineering applications.

4.5 Acknowledgement

The authors are grateful to Charlene Ross and the UNC Animal Studies Core as well as Janine Weaver and the Histopathology Lab. The authors thank the Ashby and DeSimone research groups for insightful discussions. This work was supported by the Carolina Center

for Cancer Nanotechnology Excellence (MNY), the NSF (MNY), and the Charles Lee Raper Dissertation Fellowship (DGB).

4.6 References

(1) Barrett, D. G.; Yousaf, M. N. *Molecules* **2009**, *14*, 4022-4050.

(2) Shi, R.; Chen, D.; Liu, Q.; Wu, Y.; Xu, X.; Zhang, L.; Tian, W. *Int. J. Mol. Sci.* **2009**, *10*, 4223-4256.

(3) Bettinger, C. J.; Bruggeman, J. P.; Borenstein, J. T.; Langer, R. S. *Biomaterials* **2008**, *29*, 2315-2325.

(4) Bruggeman, J. P.; Bettinger, C. J.; Nijst, C. L. E.; Kohane, D. S.; Langer, R. *Adv. Mater.* **2008**, *20*, 1922-1927.

(5) Bruggeman, J. P.; de Bruin, B. J.; Bettinger, C. J.; Langer, R. *Biomaterials* **2008**, *29*, 4726-4735.

(6) Wang, Y.; Ameer, G. A.; Sheppard, B. J.; Langer, R. *Nat. Biotechnol.* **2002**, *20*, 602-606.

(7) Barrett, D. G.; Yousaf, M. N. *Macromolecules* **2008**, *41*, 6347-6352.

(8) Barrett, D. G.; Luo, W.; Yousaf, M. N. *Polym. Chem.* **2010**, , 296-302.

(9) Yang, J.; Webb, A. R.; Ameer, G. A. *Adv. Mater.* **2004**, *16*, 511-516.

(10) Yang, J.; Webb, A. R.; Pickerill, S. J.; Hageman, G.; Ameer, G. A. *Biomaterials* **2006**, *27*, 1889-1898.

(11) Djordjevic, I.; Choudhury, N. R.; Dutta, N. K.; Kumar, S. *Polymer* **2009**, *50*, 1682-1691.

(12) Ding, T.; Liu, Q.; Shi, R.; Tian, M.; Yang, J.; Zhang, L. *Polym. Degrad. Stab.* **2006**, *91*, 733-739.

(13) Migneco, F.; Huang, Y. C.; Birla, R. K.; Hollister, S. J. *Biomaterials* **2009**, *30*, 6479-6484.

(14) Lee, L. Y.; Wu, S. C.; Fu, S. S.; Zeng, S. Y.; Leong, W. S.; Tan, L. P. *Eur. Polym. J.* **2009**, *45*, 3249-3256.

(15) Motlagh, D.; Yang, J.; Lui, K. Y.; Webb, A. R.; Ameer, G. A. *Biomaterials* **2006**, *27*, 4315-4324.

(16) Motlagh, D.; Allen, J.; Hoshi, R.; Yang, J.; Lui, K.; Ameer, G. *J. Biomed. Mater. Res. A.* **2007**, *82*, 907-916.

(17) Kibbe, M. R.; Martinez, J.; Popowich, D. A.; Kapadia, M. R.; Ahanchi, S. S.; Aalami, O. O.; Jiang, Q.; Webb, A. R.; Yang, J.; Carroll, T.; Ameer, G. A. *J. Biomed. Mater. Res. A.* **2009**, *93A*, 314-324.

(18) Kang, Y.; Yang, J.; Khan, S.; Anissian, L.; Ameer, G. A. *J. Biomed. Mater. Res. A.* **2006**, *77*, 331-339.

(19) Mahdavi, A., et al *Proc. Natl. Acad. Sci. U. S. A.* **2008**, *105*, 2307-2312.

(20) Engelmayr, G. C.,Jr; Cheng, M.; Bettinger, C. J.; Borenstein, J. T.; Langer, R.; Freed, L. E. *Nat. Mater.* **2008**, *7*, 1003-1010.

(21) Liu, Q. Y.; Tan, T. W.; Weng, J. Y.; Zhang, L. Q. *Biomed. Mater.* **2009**, *4*, 025015.

(22) Liu, Q. Y.; Wu, S. Z.; Tan, T. W.; Weng, J. Y.; Zhang, L. Q.; Liu, L.; Tian, W.; Chen, D. F. *J. Biomater. Sci.* **2009**, *20*, 1567-1578.

(23) Lei, L.; Ding, T.; Shi, R.; Liu, Q.; Zhang, L.; Chen, D.; Tian, W. *Polym. Degrad. Stab.* **2007**, *92*, 389-396.

(24) Barrett, D. G.; Yousaf, M. N. *Chembiochem* **2008**, *9*, 62-66.

(25) Barrett, D. G.; Yousaf, M. N. *Biomacromolecules* **2008**, *9*, 2029-2035.

(26) Li, H.; Riva, R.; Jerome, R.; Lecomte, P. *Macromolecules* **2007**, *40*, 824-831.

(27) Riva, R.; Schmeits, S.; Jerome, C.; Jerome, R.; Lecomte, P. *Macromolecules* **2007**, *40*, 796-803.

(28) Amsden, B. *Soft Matter* **2007**, *3*, 1335-1348.

(29) Wang, Y.; Kim, Y. M.; Langer, R. *J. Biomed. Mater. Res. A.* **2003**, *66*, 192-197.

(30) Amsden, B. G.; Tse, M. Y.; Turner, N. D.; Knight, D. K.; Pang, S. C. *Biomacromolecules* **2006**, *7*, 365-372.

(31) Chan, E. W. L.; Yousaf, M. N. *J. Am. Chem. Soc.* **2006**, *128*, 15542-15546.

(32) Hoover, D. K.; Lee, E. J.; Chan, E. W. L.; Yousaf, M. N. *Chembiochem* **2007**, *8*, 1920-1923.

(33) Westcott, N. P.; Pulsipher, A.; Lamb, B. M.; Yousaf, M. N. *Langmuir* **2008**, *24*, 9237-9240.

(34) Pulsipher, A.; Westcott, N. P.; Luo, W.; Yousaf, M. N. *J. Am. Chem. Soc.* **2009**, *131*, 7626-7632.

(35) Bilic, G.; Brubaker, C.; Messersmith, P. B.; Mallik, A. S.; Quinn, T.; Done, E.; Gucciardo, L.; Zeisberger, S. M.; Zimmermann, R.; Deprest, J.; Zisch, A. H. *American Journal of Obstetrics and Gynecology* **2010**, *202*, 85.e1-85.e9.

(36) Brubaker, C. E.; Kissler, H.; Wang, L. -.; Kaufman, D. B.; Messersmith, P. B. *Biomaterials* **2010**, *31*, 420-427.

(37) Rolland, J. P.; Van Dam, R. M.; Schorzman, D. A.; Quake, S. R.; DeSimone, J. M. *J. Am. Chem. Soc.* **2004**, *126*, 2322-2323.

(38) Rolland, J. P.; Maynor, B. W.; Euliss, L. E.; Exner, A. E.; Denison, G. M.; DeSimone, J. M. *J. Am. Chem. Soc.* **2005**, *127*, 10096-10100.

(39) Rolland, J. P.; Hagberg, E. C.; Denison, G. M.; Carter, K. R.; DeSimone, J. M. *Angew. Chem. Int. Ed.* **2004**, *43*, 5796-7599.

(40) Barrett, D. G.; Lamb, B. M.; Yousaf, M. N. *Langmuir* **2008**, *24*, 9861-9867.

(41) Yang, J.; Motlagh, D.; Webb, A. R.; Ameer, G. A. *Tissue Eng.* **2005**, *11*, 1876-1886.

(42) Won, C. -.; Chu, C. -.; Yu, T. -. *Macromol. Rapid Commun.* **1996**, *17*, 653-659.

(43) Webb, A. R.; Yang, J.; Ameer, G. A. *Expert Opin. Biol. Ther.* **2004**, *4*, 801-812.

(44) Anderson, J. M.; Rodriguez, A.; Chang, D. T. *Sem. Immunol.* **2008**, *20*, 86-100.

(45) Mosser, D. M. *J. Leuk. Biol.* **2003**, *73*, 209-212.

(46) Gordon, S. *Nat. Rev. Immunol.* **2003**, *3*, 23-35.

(47) Fenton, M. J.; Buras, J. A.; Donnelly, R. P. *J. Immunol.* **1992**, *149*, 1283-1288.

(48) Chizzolini, C.; Rezzonico, R.; De Luca, C.; Burger, D.; Dayer, J. -. *J. Immunol.* **2000**, *164*, 5952-5960.

(49) Mantovani, A.; Sica, A.; Sozzani, S.; Allavena, P.; Vecchi, A.; Locati, M. *TRENDS Immunol.* **25**, *2004*, 677-686.

(50) Hata, H.; Sakaguchi, N.; Yoshitomi, H.; Iwakura, Y.; Sekikawa, K.; Azuma, Y.; Kanai, C.; Moriizumi, E.; Nomura, T.; Nakamura, T.; Sakaguchi, S. *J. Clin. Invest.* **2004**, *114*, 582-488.

(51) Pereira, B. J. G.; Shapiro, L.; King, A. J.; Falagas, M. E.; Strom, J. A.; Dinarello, C. A. *Kidney Int.* **1994**, *45*, 890-896.

(52) Suzuki, K.; Nakaji, S.; Yamada, M.; Totsuka, M.; Sato, K.; Sugawara, K. *Exerc. Immunol. Rev.* **2002**, *8*, 6-48.

Chapter V

ONE-STEP SYNTHESES OF PHOTOCURABLE POLYESTERS BASED ON A RENEWABLE RESOURCE

5.1 Introduction

The need for novel biodegradable polymers in biomedical fields, such as drug delivery and tissue engineering, has motivated the biomaterials community to develop new polymers.[1-3] Aliphatic polyesters are of particular interest due to their biodegradable and non-toxic properties. Currently, a tremendous portion of polyester research for biomedical applications has focused on polymers derived from lactide, glycolide, and ε-caprolactone.[4] However, their utility is limited because the resulting polymers are often difficult to synthesize or hard and brittle at physiological conditions. Therefore, the evolution of polyester design must continue in order to develop facile syntheses of elastomeric materials.

Many examples of both thermosets and thermoplastics have been described in literature. [1-3,5] When compared to thermoplastic materials, amorphous thermosets offer a number of advantages for biomedical applications. Thermoplastic elastomers often contain crystalline regions, which result in heterogeneous degradation and a non-linear loss of mechanical strength.[1,6] Additionally, the three-demensional (3D) geometry of thermoplastic materials is commonly altered throughout the course of hydrolysis.[6] In contrast to thermoplastics, thermosets can be synthesized from precursors that are completely amorphous, enabling a predictable loss of mechanical properties and linear degradation.[1] In terms of biomaterials, the ability of a thermoset to retain its 3D structure is critical for various implants, including stents, tissue scaffolds, grafts, and sutures.

Although both photocurable and thermally cured thermosets continue to be the focus of a significant portion of biomaterial research, the ability to cross-link biodegradable materials with light offers many benefits over thermal gelation. One benefit is that significantly faster curing periods (minutes versus days) and lower curing temperatures

(room temperature versus 80 – 150 °C) are easily accessible. As such, photocuring provides a less harsh route to curing process than thermal cross-linking procedures. Therefore, fragile cargos, which include drugs and proteins, can be encapsulated in thermosets that are cured with light; this characteristic enables the design of drug releasing particles, stents, and sutures.[7, 8]

We believe that the ideal polymer for biomedical applications should possess several characteristics. Biocompatibility and biodegradation are requisites in order to minimize the stress that is imposed upon living systems by the material. The polymer should also be a completely amorphous thermoset with no crystalline regions present, minimizing heterogeneous degradation. A wide range of macromolecular properties should also be accessible from a facile and inexpensive strategy. This would allow for the ability to tailor a material's properties to best suit a particular application. Finally and most importantly, the resulting polyesters should be photocurable after a single step while maintaining a simple synthetic scheme. This requirement would allow for curing to take place in several minutes and eliminate the need for post-polymerization modifications that can degrade or alter the labile polyester backbone.

In this chapter, we describe the synthesis and characterization of several photocurable polyesters based on itaconic acid (IA), a photoactive, biocompatible, and renewable monomer.[9] IA is an ideal monomer and/or co-monomer for thermal polycondensation, a polymerization strategy that has recently gained popularity in biomaterial synthesis.[2,3,5] IA was combined with adipic acid (AA) and trimethylolpropane (TMP) in order to obtain hyperbranched, photocurable polyesters. A similar pre-polymer was synthesized by the polyesterification of IA, succinic acid (SA), and sorbitol. Additionally, dimethyl itaconate

(DMI) is compatible with enzymatic polyester synthesis, catalyzed by Novozyme 435 – Lipase B from *Candida Antarctica* (CALB). In order to demonstrate versatility, linear polyesters were generated by combining DMI with various diols. The rigidity and strength of the resulting materials can be tuned by varying the cross-linking density through the initial monomer feed ratio, allowing for control over mechanical properties. Additionally, the non-cured pre-polymers are easily melted and/or dissolved for easy processing, demonstrated by micron-scale particles, embossed films, and porous scaffolds. Finally, *in vitro* cytotoxicity of the materials toward Swiss albino 3T3 fibroblasts (SAFs) was studied due to future biomedical applications.

5.2 Experimental Section

5.2.1 Materials

All chemicals were used without further purification. TMP, CALB, N,N'-dicyclohexylcarbodiimide (DCC), N-hydroxysuccinimide (NHS), poly(ethylene glycol) (PEG; 400 g/mol), 3-methyl-1,5-pentanediol (MPD), poly(ethylene glycol) methyl ether methacrylate (PEGMEM; 475 g/mol), and 2-(methacryloyloxy)ethyl acetoacetate (MEA) were purchased from Sigma-Aldrich (Milwaukee, WI). IA, DMI, AA, SA, 1,4-cyclohexanedimethanol (CHDM), sorbitol, diethoxyacetophenone (DEAP), and all solvents were purchased from Fisher Scientific (Philadelphia, PA). Amine-functionalized rhodamine was purchased from Invitrogen (Carlsbad, CA).

5.2.2 Poly(Trimethylolpropane Itaconate -*co*- Trimethylolpropane Adipate) Synthesis

The synthesis was similar to methods previously reported.[10-12] All polymerizations were performed on a scale of ≥ 15 g. The total diacid content was combined with an equimolar amount of TMP in a round bottom flask. The ratios of diacids, IA:AA, used were

1:0, 1:3, and 1:9. In an inert environment of argon, monomers were stirred at 145 °C. After a homogenous melt formed, the mixture was stirred for 2 h. The pressure was then reduced to 2 torr, and the materials continued stirring for 6.5, 7.5, or 8.5 h (see Table 5.1). The round bottom flasks were immediately placed into a water bath (room temperature) to stop polycondensation. Pre-polymers were precipitated in -78 °C methanol and dried under vacuum. To form thermosets, pre-polymers were combined with 0.1 wt % DEAP and irradiated with 365 nm light for 10 min in an Electro-Cure-500 UV curing chamber (Electro-Lite Corporation, Bethel, CT).

5.2.3 Poly(Sorbitol Itaconate -*co*- Sorbitol Succinate) Synthesis

The synthesis of sorbitol-based pre-polymers was similar to the above procedure. The polymerization was performed on a scale of ≥ 15 g. The total diacid content was combined with an equimolar amount of sorbitol in a round bottom flask. The ratio of diacids, IA:SA, used was 2:3. In an inert environment of argon, the monomers were stirred at 150 °C. After a homogenous melt formed, the mixture was stirred for 2 h. The pressure was then reduced to 2 torr, and the materials continued stirring for 5 h. The round bottom flasks were immediately placed into a water bath (room temperature) to stop polycondensation. Pre-polymers were precipitated in -78 °C methanol and dried under vacuum. To form thermosets, pre-polymers were combined with 0.1 wt % DEAP and irradiated with 365 nm light for 10 min in an Electro-Cure-500 UV curing chamber (Electro-Lite Corporation, Bethel, CT).

5.2.4 Linear Poly(Diol Itaconate) Synthesis

Similar syntheses have been described elsewhere.[13] All polymerizations were performed on a scale of ≥ 15 g. For materials 5 and 6, DMI was combined with an equimolar

amount of a diol (CHDM or PEG) and Novozyme 435 (10 wt % of the total monomer weight) in an inert environment of argon and heated to 90 °C in oil bath. For material 7, the procedure was identical except that a different monomer feed ratio was used: DMI (0.25 molar equivalents), AA (0.75 equivalents), MPD (1 molar equivalent), and Novozyme 435 (10 wt % of the total monomer weight). After a homogenous melt was formed, the mixture was stirred for 2 h. The pressure was then reduced to 200 torr for 10 h, to 125 torr for 12 h, and to 5 torr for the final 24 h of the reaction. Upon completion, the mixture was diluted with methylene chloride and the enzyme was removed by filtration. Following rotary evaporation, polymers were precipitated in -78 °C methanol and dried under vacuum. To form thermosets, pre-polymers were combined with 0.1 wt % DEAP and irradiated with 365 nm light for 10 min.

5.2.5 Polyester Characterization

^{1}H NMR spectra of pre-polymers were acquired on a Bruker 400 MHz AVANCE spectrometer in deuterated chloroform; pre-polymer 4 was dissolved in deuterated dimethyl sulfoxide (DMSO). Molecular weights were measured compared to polystyrene standards on a Waters gel permeation chromatography (GPC) system with detection based on refractive index values. The measurements were taken at 40 °C with tetrahydrofuran as the mobile phase on three columns in series (Waters Styragel HR2, HR4, and HR5). Pre-polymer and polymer glass transition temperatures were measured during the second heating cycle (10 °C/min) on a TA Instruments Q200 DSC.

Tensile tests were conducted on an Instron 5566 at a crosshead speed of 10 mm/min at room temperature. Samples were cured in a dog-bone-shaped mold with approximate dimensions of 10 mm x 3 mm x 1.5 mm. Dog-bones were either tested dry or after swelling

in ddH_2O at room temperature for 24 h. The Young's modulus (YM; Pa) was calculated according to the linear segment of the stress/strain curve. Three trials were performed and the average was reported. Using

$$n = \mathrm{YM}(3\mathrm{RT})^{-1} \quad (1)$$

where R is the universal gas constant (8.3144 J/mol K) and T is the temperature (K), the cross-linking density (n; mmol/L) was calculated.

Sol-gel analysis was conducted by soaking films in isopropanol (IPA) for 24 h at room temperature. After solvent removal, the films were dried, and the percent soluble fraction (Q_s) was calculated by

$$Q_s = \frac{m_i - m_f}{m_i} \times 100 \quad (2)$$

where m_i and m_f represent the initial and final mass of the elastomer films, respectively. Three trials were performed and the average was reported.

Water swelling (WS) experiments were performed by swelling films in ddH_2O for 24 h at room temperature. After removing surface water, the WS was calculated by

$$WS = \frac{m_f - m_i}{m_i} \times 100 \quad (3)$$

where m_i and m_f represent the initial and final mass of the elastomer films, respectively. Three trials were performed and the average was reported.

Contact angle measurements were obtained on flat polyester films cured on glass slides. Measurements were performed on a KSV CAM200 contact angle meter with water as the wetting liquid.

5.2.6 Polyester Molding

Particles of material 5 were fabricated as previously described.[7] To generate embossed films, a small amount of pre-polymer 1 was placed onto a glass slide, heated to reduce viscosity, and molded by direct contact with a perfluoropolyether (PFPE) mold.[14-16] The material was cured as described above, followed by removal of the mold. Imaging of 3D polyester samples was conducted on a Hitachi model 2-4700 scanning electron microscope (SEM) after coating with ~ 2 nm of a Pd/Au alloy (Cressington 108 auto sputter coater, Cressington Scientific Instruments Ltd.).

5.2.7 Porous Films

Porous films were prepared based on previously reported methods.[17] Briefly, material 3 was used as a cross-linking agent for a thermoset composed primarily of a methacrylated monomer (PEGMEM or MEA). A polymer formulation was developed by dissolving material 3 (10 wt %) and DEAP (1 wt %) in the methacrylate (89 wt %). The solution was combined with 87.5 wt % sieved NaCl and cured as described above. The porogen was removed by swelling the films in ddH_2O for 4 d, replacing the water every 12 h. After drying the porous scaffold in a vacuum oven (60 °C), SEM images were recorded as described above.

5.2.8 Particle Functionalization

Particles of material 2 (3 μm x 3 μm x 1 μm) were fabricated as described earlier.[7] Particles were dispersed in N'N-dimethylformamide (DMF) containing excess NHS and DCC. After stirring for 30 min, an excess amount of an amine-modified rhodamine dye was added to the particles.[18, 19] After 5 h, conjugation was halted by centrifuging the particles and decanting the supernatant solution. The particles were repeatedly re-suspended in acetone, centrifuged, and decanted until the remaining acetone was clear, indicating removal of the

rhodamine solution. The container was wrapped in aluminum foil in order to minimize exposure to light. Optical and fluorescent images were obtained on a Zeiss Axio Imager D.1M equipped with a Zeiss AxioCam MRm camera.

5.2.9 *In Vitro* Cytotoxicity

To test cell viability, SAFs were plated in 24-well plates at a density of approximately 40,000 cells per well and incubated for 18 h at 37 °C in a humidified 5% CO_2 atmosphere. After incubation, each polymer sample (~ 50 mg; sterilized in 70 % ethanol and washed in PBS under a germicidal lamp for 2 h) was placed within a cell culture insert with 3 μm pores (PET track etched membrane, Becton Dickinson), placed in a well, and covered with complete culture medium. SAFs and materials were continuously incubated for 72 h. Cell viability was estimated at 24 h and 72 h by quantification of intracellular ATP using the CellTiter-Glo™ Luminescent Cell Viability Assay (Promega) following the manufacturer's suggested protocol. Luminescence was measured with a Molecular Devices SpectraMax M5 microplate reader (Molecular Devices Laboratories). The viability of the cells exposed to polymer samples was expressed as a percentage of the viability of cells grown in the absence of polymers.

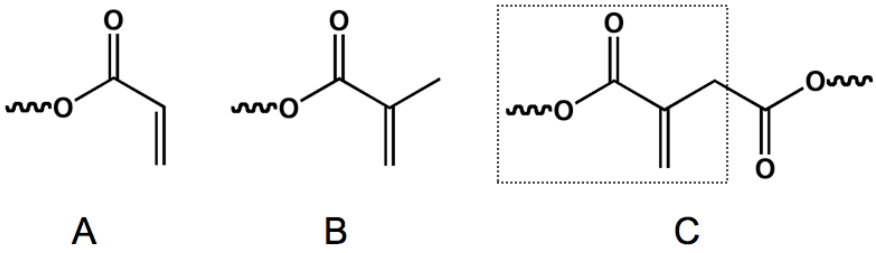

Figure 5.1. Common photocurable functional groups. The structural similarities in (A) acrylates and (B) methacrylates are also found in (C) itaconates. Itaconic acid is commonly polymerized through radical activation of the alkene. However, it is also a suitable monomer for the condensation polymerization of polyesters.

5.3 Results and Discussion

5.3.1 Motivation

Aliphatic polyesters are both strengthened and limited by their inherently biodegradable linkages. They are able to hydrolyze under physiological conditions, allowing for the design of medical devices and delivery vectors that do not require surgical removal. However, these relatively fragile linkages are not ideal in some common post-polymerization reaction conditions, including the use acidic and basic reagents. Therefore, including any desired functionality of the final material into the initial polymerization strategy would be beneficial. For example, terminal and pendant hydroxyl units are often converted into acrylates or methacrylates to create photocurable polyesters. The results are often reported to be 'without significant degradation', even though the complete absence of degradation is desired. We believe that the ideal photocurable polyester would involve one synthetic step that encompasses both the polycondensation and the introduction of acrylate-like moieties.

Table 5.1. Pre-Polymer Synthetic Conditions

Pre-Polymer	Synthesis	Reaction (h)	Temp. (°C)	Topology	Polyol[a]	Other Monomer	IA:DA[b]
PP1	thermal	10.5	145	branched	TMP	—[c]	1.0
PP2	thermal	9.5	145	branched	TMP	AA	0.25
PP3	thermal	8.5	145	branched	TMP	AA	0.1
PP4	thermal	7	150	branched	Sorb	SA	0.4
PP5	enz.	48	90	linear	CHDM	—[c]	1.0
PP6	enz.	48	90	linear	PEG	—[c]	1.0
PP7	enz.	48	90	linear	MPD	AA	0.25

[a] TMP = trimethylolpropane; Sorb = sorbitol; CHDM = 1,4-cyclohexanedimethanol; PEG = poly(ethylene glycol); MPD = 3-methyl-1,5-pentanediol. [b] Molar ratio of itaconate in total diacid/diester content in monomer feed. [c] Homopolymer.

The polymers described herein are based on monomers that have been utilized in previously studied biomaterials: IA, DMI, AA, TMP, sorbitol, SA, CHDM, PEG, and MPD (Table 5.1).[20-27] While all of the starting materials are biocompatible, our novel polyesters are based on IA, which provides an attractive foundation for polymers (Figure 5.1). IA is a completely renewable resource and can be isolated from bacterial fermentation and the distillation of citric acid.[28-30] Many classes of biomaterials have been based on itaconates, including hydrogels and glass ionomer cements.[20,31,32] These materials are synthesized through radical polymerization of the alkene in the itaconate monomer. As opposed to radical polymerizations, this report focuses on designing itaconate-based materials through polyesterification.

5.3.2 Poly(Trimethylol Itaconate -*co*- Trimethylol Adipate)

Hyperbranched polyesters were synthesized by thermal polycondensation. This technique is gaining in popularity due to its simplicity. Polyols and polyacids react to form esters under conditions of heat (120 – 150 °C) and vacuum without catalysts or co-reagents, making this polymerization strategy especially attractive for biomaterials. TMP was combined with IA and AA in various ratios, generating pre-polymers with different concentrations of the photocurable moiety (Figure 5.2). Pre-polymers 1, 2, and 3 (PP1, PP2, and PP3) contained IA, AA, and TMP in ratios of 1:0:1, 1:3:4, and 1:9:10, respectively. The monomers were heated only to the extent of cross-linking that would create oligomeric pre-polymers; thermal cross-linking was avoided in order to obtain soluble pre-polymers. The molecular weights of these oligomers were relatively small, with PP1, PP2, and PP3 having $\langle M_n \rangle$ values of 1140, 2200, and 1170 g/mol (Table 5.2). Additionally, all of the pre-polymers were amorphous, with glass transition (T_g) temperatures ranging from -28.8 °C – -

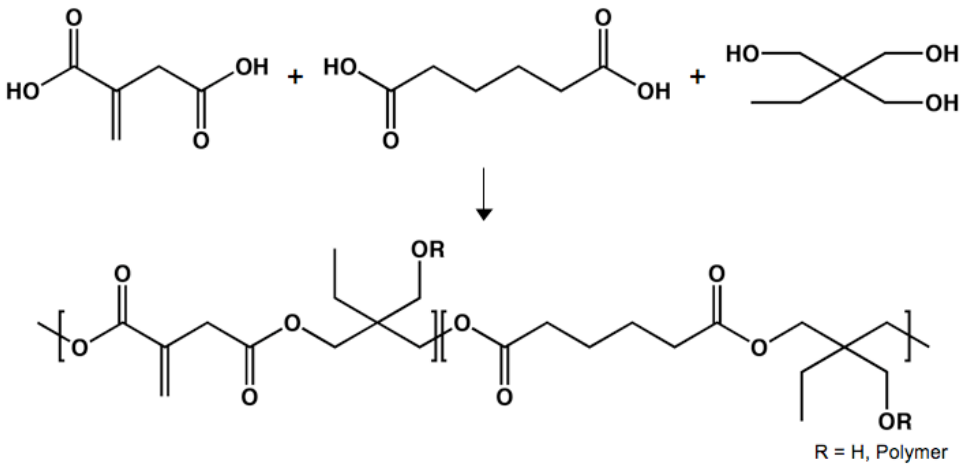

Figure 5.2. Thermal Synthesis of Poly(Trimethylolpropane Itaconate -*co*- Trimethylolpropane Adipate).

7.4 °C. The inclusion of larger amounts of AA caused lower T_g values, most likely due to the resulting decrease in cross-linking density.

In addition to GPC and DSC, PP1, PP2, and PP3 were characterized by ^{1}H NMR. The ^{1}H NMR spectra of PP1, PP2, and PP3 were very similar due to the use of common monomers (Figure E1). The main differences between the pre-polymers were caused by different monomer feed ratios. PP1 is a homopolymer, poly(TMP itaconate), where as PP2 and PP3 are copolymers, poly(TMP itaconate -*co*- TMP adipate). The spectra associated with PP1 does not display the peaks at 1.6 and 2.3 ppm that correspond to the adipate structure. All three of these pre-polymers contained at least 10 % itaconic acid in the monomer feed. As such, all of the NMR spectra have alkene peaks at approximately 5.8 and 6.2 ppm. The presence of these peaks is crucial because they support the observation that cross-linking did not occur during the synthesis. The absence of these peaks would imply that the alkene was altered, preventing it from participating in the photocuring process. Previous studies were unable to polymerize IA without the addition of radical inhibitors such as hydroquinone.[33]

Table 5.2. Pre-Polymer Characterizations

Pre-Polymer	T_g (°C)[a]	‹M_n› (g/mol)[b]	PDI[b]
PP1	-7.4	1140	1.3
PP2	-23.2	2200	1.7
PP3	-28.8	1170	1.3
PP4	39.8	940	1.1
PP5	-25.4	2030	1.3
PP6	-50.8	6650	1.3
PP7	-57.6	11900	1.6

[a] Determined by DSC on second heating cycle (10 °C/min). [b] Determined by GPC.

All three of the pre-polymers were cured upon exposure to UV light in the presence of the photoinitiator, DEAP. Thermosets were formed by exposing PP1, PP2, or PP3 with 0.1 wt % DEAP to 365 nm light for 10 min. As the concentration of the cross-linking moiety was controlled by the ratio of IA:AA in the monomer feed, the mechanical properties of these polymers could be controlled (Table 5.3). Material 1, poly(TMP itaconate), was a strong and brittle polymer, with a Young's modulus (YM), ultimate tensile stress (UTS), and rupture strain (RS) of approximately 200 MPa, 18 MPa, and 23 %, respectively. However, by increasing the amount of AA in the monomer feed, the resulting polyesters were weaker and much more flexible. Material 2 (IA:AA = 1:3) displayed YM, UTS, and RS values of 2 MPa, 1 MPa, and 65 %, respectively; material 3 (IA:AA = 1:9) was far more elastic, with a YM of 0.2 MPA, an UTS of 0.2 MPa, and a RS of 200 %. Between materials 1 – 3, the YM varied over 3 orders of magnitude, the UTS varied over 2 orders of magnitude, and the RS varied over 1 order of magnitude.

Table 5.3. Mechanical Properties of Photocured Itaconate-Based Polyesters

Material	Pre-Polymer	Young's Modulus [a] (MPa)	UTS [a] (MPa)	Rupture Strain [a] (%)	n [b] (mmol/L)
1	PP1	201.66 ± 37.14	18.20 ± 0.10	23 ± 6	27131 ± 4996
2	PP2	2.03 ± 0.24	1.14 ± 0.32	65 ± 14 [d]	273 ± 33
3	PP3	0.19 ± 0.02	0.22 ± 0.02	198 ± 28 [d]	26 ± 3
4	PP4	11.22 ± 1.22	2.05 ± 0.33	119 ± 19	1509 ± 164
5	PP5	378.82 ± 53.03	16.59 ± 4.52	6 ± 2	50964 ± 7134
6	PP6	7.49 ± 0.55	2.70 ± 0.80	45 ± 16	1008 ± 74
7	PP7	2.45 ± 0.17	2.04 ± 0.33	99 ± 11 [d]	329 ± 22
1 [c]	PP1	186.32 ± 20.11	7.64 ± 2.02	5 ± 1	25067 ± 2707
2 [c]	PP2	1.40 ± 0.17	0.46 ± 0.09	40 ± 10 [d]	189 ± 23
3 [c]	PP3	0.17 ± 0.02	0.12 ± 0.03	111 ± 32 [d]	22 ± 3
4 [c]	PP4	0.88 ± 0.25	0.11 ± 0.05	23 ± 6	118 ± 34
5 [c]	PP5	398.14 ± 6.62	15.04 ± 3.00	6 ± 1	53564 ± 891
6 [c]	PP6	13.85 ± 0.43	0.97 ± 0.38	12 ± 1	1863 ± 58
7 [c]	PP7	2.40 ± 0.14	1.89 ± 0.64	99 ± 11 [d]	323 ± 18

[a] Determined by Instron (crosshead speed of 10 mm/min). [b] Equation 1. [c] Samples were hydrated in H_2O at room temperature for 24 h before testing. [d] Samples were cut by Instron clamps before tearing due to strain.

The hydrophobicity of these polyesters was also investigated by determining the contact angle of water on thin polymeric films (Table 5.4). The contact angles increased by including larger amounts of AA in the starting formulations due to the longer hydrocarbon portion of AA relative to IA. The contact angle values for materials 1, 2, and 3 were 42.7 °, 52.7 °, and 64.5 °, respectively. The soluble fraction of the thermosets was also calculated (Figure 5.3). This characteristic followed a logical pattern, with the soluble fraction increasing as the relative concentration of IA decreased; comparable trends have been

observed with similar materials.[34] The results concerning the degree of swelling in water were unexpected (Figure 5.3). Although materials 1 – 3 are hyperbranched and contain free carboxylic acids, the water swelling values were low. Of these polyesters, elastomer 1 exhibited the largest degree of swelling in water at 7.5 %. As the amount of AA in the monomer feed increased, the amount of swelling in water decreased. This trend is logical as AA contains more hydrophobic methylene units than IA.

Table 5.4. Physical Properties of Photocured Itaconate-Based Polyesters

Material	Pre-Polymer	T_g [a] (°C)	Contact Angle (°)
1	PP1	18.4	42.7 ± 1.2
2	PP2	-18.4	52.7 ± 1.3
3	PP3	-25.6	64.5 ± 0.9
4	PP4	4.0	29.4 ± 0.7
5	PP5	8.1	79.5 ± 0.8
6	PP6	-36.7	87.4 ± 0.5
7	PP7	-62.4	96.0 ± 0.9

[a] Determined by DSC on second heating cycle (10 °C/min).

5.3.3 Poly(Sorbitol Itaconate -*co*- Sorbitol Succinate)

In order to demonstrate that the macromolecular properties of the cross-linked elastomers could be further tuned, a hyperbranched pre-polymer was synthesized from the polycondensation of IA, SA, and sorbitol. The synthesis of pre-polymer 4 (PP4) was very similar to those of the TMP-based materials (Figure 5.4). Again, the monomers were heated only to the extent of cross-linking that would create oligomeric pre-polymers. PP4 was amorphous (T_g = 39.8 °C) with ‹M_n› = 940 g/mol (Table 5.2). Additionally, as sorbitol

contains six hydroxyl groups, this pre-polymer should be very hydrophilic when compared to PP 1 – 3. This hypothesis was supported by the fact that PP4 was soluble in water, along with other polar organic solvents (DMSO, DMF, methanol, ethanol, etc); PP1 – PP3 were soluble in organic solvents that were much more non-polar, such as chloroform and methylene chloride.

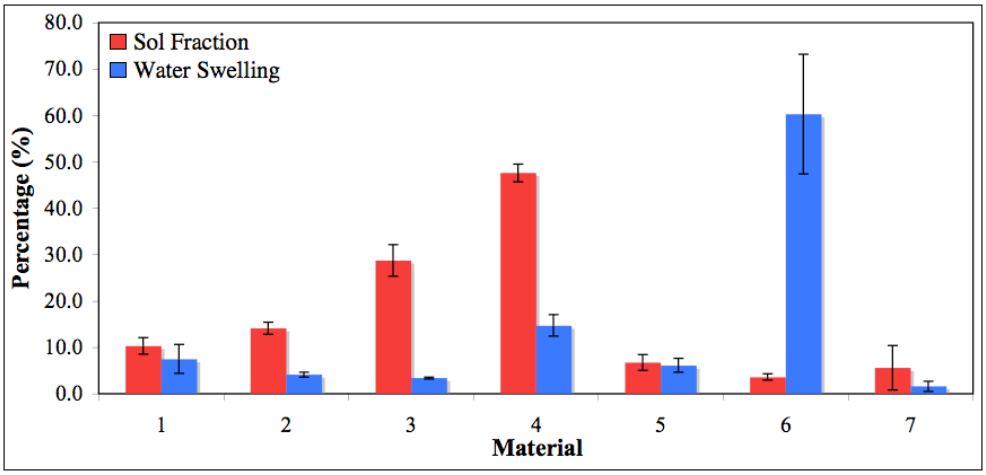

Figure 5.3. Sol fraction and water swelling of UV-cured itaconate-based polyesters.

The ^{1}H NMR spectrum of PP4 is similar to that of other pre-polymers based on sugar alcohols (Figure E2).[35] The peaks from esters and alcohols corresponding to sugar alcohols are broad, spanning from 3.3 to 6.3 ppm. The signals that represent esters formed from secondary alcohols are located at higher end of this range (3.3 – 4.3 ppm). The esters formed by primary alcohols and the remaining unreacted alcohols produce peaks from 4.3 to 6.3 ppm. Common to PP1 – PP3, the peaks associated with the pendant alkene are found at approximately 5.8 and 6.2 ppm, indicating that cross-linking did not occur during the reaction. Also, the spectrum contains peaks at 2.5 ppm that result from the use of succinic acid as a co-monomer.

Succinic acid was included in the monomer feed of material 4 in an attempt to dilute the cross-linking density and design a flexible elastomer (Table 5.3). This goal was realized, as polymer 4 displayed a YM, UTS, and RS of approximately 11 MPa, 2 MPa, and 120 %, respectively (Table 5.3). In the hydrated state, these values changed to 0.88 MPa (YM), 0.11 MPa (UTS), and 23 % (RS). Material 4 experienced the greatest loss of mechanical properties as a result of hydration. We believe that these results are due to the fact that polymer 4 is best able to interact with water because of the large number of free hydroxyl groups from sorbitol and the presence of free acids.

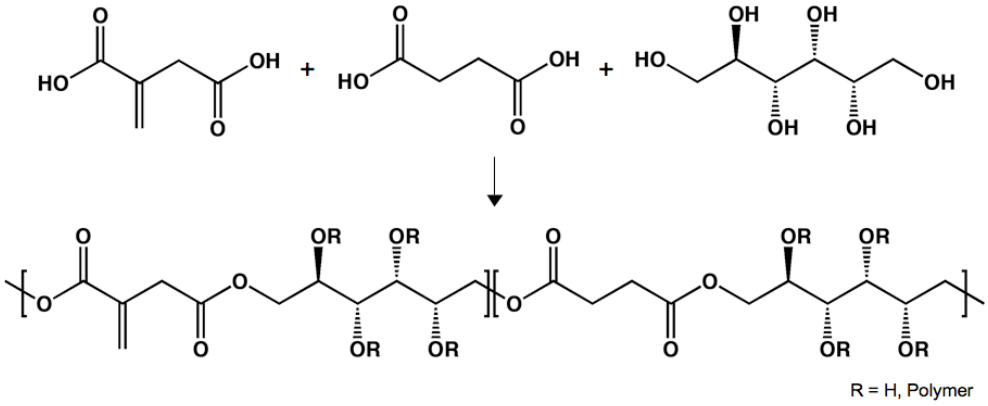

Figure 5.4. Thermal Synthesis of Hydrophilic Poly(Sorbitol Itaconate -*co*- Sorbitol Succinate).

The hydrophobicity of material 4 was determined by contact angle measurements. Polymer 4 was expected to display significant hydrophilic character due to the presence of 6 hydroxyl groups in sorbitol. This hypothesis was verified when the contact angle for material 4 was determined to be 29.4 ° (Table 5.4). The soluble portion of this polyester was surprisingly large at 47.6 % (Figure 5.3). This result may be due to the reactivity of the hydroxyl groups in sorbitol relative to those in TMP. Although sorbitol contains 6 alcohol moieties, four are secondary. TMP contains 3 primary hydroxyl groups, which are more

reactive than their secondary counterparts. The soluble fraction may be higher in polymers dependent upon esterification involving secondary alcohols because fewer ester bonds are formed. This conclusion is also supported by the fact that PP4 achieved the lowest molecular weight out of all of the hyperbranched pre-polymers (Table 5.2). The degree of swelling in water for polyester 4 was 14.7 %. The use of such a hydrophilic monomer facilitated the design of a polymer with many free acids and alcohols that experienced at least twice as much swelling in water as materials 1 – 3.

5.3.4 Poly(1,4-Cyclohexanedimethanol Itaconate) and Poly(PEG Itaconate)

The versatility of itaconic acid would be increased greatly if linear polymers could also be synthesized. Initially, tin (II) 2-ethylhexanoate was employed as the catalyst in order to obtain poly(CHDM itaconate); however, the reaction gelled within hours. We therefore catalyzed all linear polymerizations with CALB, an enzyme isolated from a species of thermophilic bacteria (Figure 5.5).[36] PP5 and PP6, both homopolymers, were designed by combining DMI with CHDM and PEG, respectively. In the presence of 10 wt % CALB, polymerizations occurred at 90 °C for 48 h under a partial vacuum for the final 46 h. PP5 and PP6 achieved molecular weights of 2030 g/mol and 6650 g/mol, respectively (Table 5.2). The choice of diol had a large impact on the thermal properties. PP5, composed of the cyclic diol CHDM, had the largest T_g of all linear materials (-25.4 °C). The T_g of PP6 was -50.8 °C, much lower due to the use of PEG as the diol.[37]

The ^{1}H NMR spectra of PP5 and PP6 are much easier to distinguish than the spectra of hyperbranched PP1 – PP3 (Figure E3 and E4). The peaks representing the pendant alkene of the itaconate group were easily distinguished at 5.8 and 6.2 ppm. The methylene from the itaconate structure produces a singlet at 3.3 ppm. In Figure S3, the ester peaks are present at

approximately 4.0 ppm, with the rest of the spectrum resulting from the hydrophobic protons of the cyclic CHDM group. The peaks corresponding to the protons adjacent to the ester groups in PP6 are located at 4.2 ppm. The major peak at 3.6 ppm represents the large number of ethylene glycol units in the PEG diol.

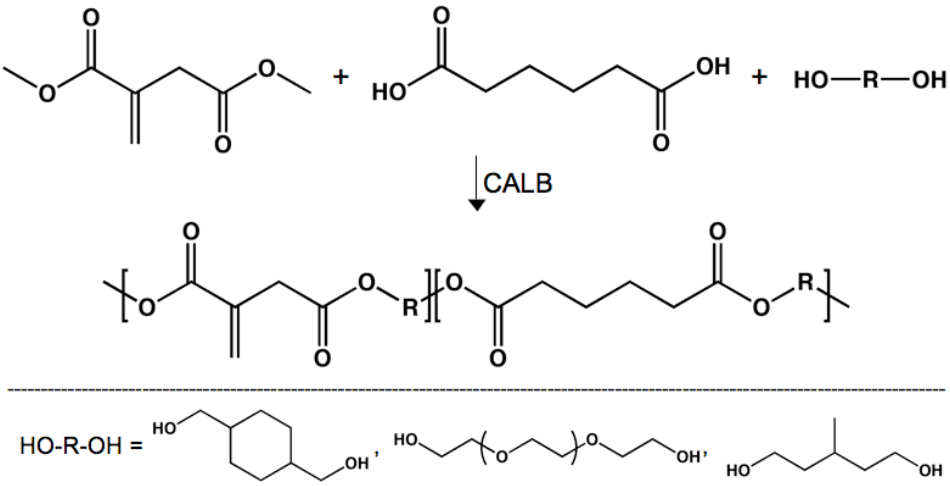

Figure 5.5. Enzymatic Synthesis of Photocurable Linear Poly(Diol Itaconate -*co*- Diol Adipate).

Although materials 5 and 6 were designed from DMI and a diol, the cross-linking density of these two polymers is very different due to the size of those diols. Polyester 5 was composed of DMI and CHDM, a small and cyclic diol. As such, elastomer 5 is very strong and very brittle; its YM, UTS, and RS values are 380 MPa, 16.5 MPa, and 6 %, respectively (Table 5.3). Since this polymer is linear and hydrophobic, it displays a very similar mechanical profile when it is hydrated. However, polyester 6 is based on a PEG macromonomer, which provides more space between cross-linking sites. The result is a material that is more flexible than the other homopolymers. The YM, UTS, and RS values for elastomer 6 are approximately 7.5 MPa, 2.7 MPa, and 45 %, respectively. This polymer was unique in terms of its hydrated mechanical profile; the YM increased by 85 % (13.85

MPa), the UTS decreased by 64 % (1 MPa), and the RS decreased by 73 % (12 %). Current studies are attempting to understand the difference between the mechanical properties of the dry state and those of the hydrated state.

Materials 5 and 6 are both homopolymers based on DMI. However, the choice of extremely different diols (CHDM versus PEG) allowed for the synthesis of dissimilar polymers. Polyester 5 was expected to be very hydrophobic due to the cyclic hydrocarbon interior of CHDM. This hypothesis was validated by the contact angle (79.5 °) and water swelling results (6.1 %) (Table 5.4, Figure 5.3). Also, because polymer 5 was a homopolymer, the prevalence of itaconate motifs resulted in a highly cross-linked network with a low soluble fraction (6.7 %). Polyester 6 was thought to be very hydrophilic since a large PEG diol (400 g/mol) was employed as a macromonomer. The degree of swelling in water – 60 % – supported this expectation; material 6 swelled at least 4-times as much as any of the other polyesters in this study. However, the contact angle implied that this polymer was surprisingly hydrophobic (87.4 °). The interactions between material 6 and water potentially required a large amount of time; contact angle measurements occur on the order of minutes while water swelling takes place over a 24 h period. Additionally, due to the fact that material 6 is a homopolymer, the soluble fraction was very low (3.6 %).

5.3.5 Poly(3-Methyl-1,5-Pentanediol Itaconate -*co*- 3-Methyl-1,5-Pentanediol Adipate)

When PP5 and PP6 were cured, the resulting polymers were brittle due to the high-cross-linking density which is due to each repeat unit containing a site for radical cross-linking. We hope to further increase the flexibility of itaconate-based polyesters by producing a copolymer in an attempt to dilute the cross-linking sites. In order to accomplish this goal, AA was included in the monomer feed; DMI:AA:MPD = 1:3:4. The synthesis was

identical to the procedure used for PP5 and PP6. The inclusion of AA caused a large increase in the molecular weight of the pre-polymer, which obtained ‹M_n› = 11900 g/mol (Table 5.2). The T_g of PP7 – -57.6 °C – was again low due to the choice of the diol. The branched structure of MPD prevented efficient packing, which resulted in a low T_g.[38]

In addition to basic structural characterization, the ^{1}H NMR spectra of PP7 allowed for the determination of the ratio of DMI:AA in the purified pre-polymer (Figure E5). The monomer feed contained DMI:AA in a 1:3 molar ratio. By integrating peaks ‘b’ and ‘g’, the ratio of DMI:AA in the final pre-polymer was 1:3.07. In terms of the structural components of PP7, peaks ‘a’ and ‘b’ are common to PP5 and PP6 as all three are based on DMI. Again, their presence is critical because the pendant alkene is preserved through the enzymatic polymerization. Peaks ‘g’ and ‘h’ are the methylene groups from the adipate unit in the co-polymer. Peaks ‘c’ – ‘f’ are associated with the hydrophobic core of the diol, MPD.

Curing PP7 led to the design of a tough and flexible polyester, which was intended. Adipic acid was included so as to decrease the relative concentration of cross-linking sites in the resulting thermoset. Polymer 4 displayed a YM, UTS, and RS of approximately 2 MPa, 2 MPa, and 100 %, respectively (Table 5.3). The hydrated state of this polyester produces similar mechanical characteristics; the new values are 2.4 MPa (YM), 1.9 MPa (UTS), and 100 % (RS).

Polyester 7 is the most hydrophobic material that was designed for this study. Three factors led to this result: (i) PP7 was linear; (ii) the diol used in the polymerization, MPD, was hydrophobic; (iii) a significant portion of AA was employed as a co-monomer. As stated previously, AA contains a longer hydrocarbon segment than IA. Because of this hydrophobic nature, the water swelling value was low (1.6 %) while the contact angle

measurement was high (96.0 °) (Figure 5.3, Table 5.4). Finally, the soluble fraction of this thermosets was similar to that of the 3 homopolymers studied here (5.6 %).

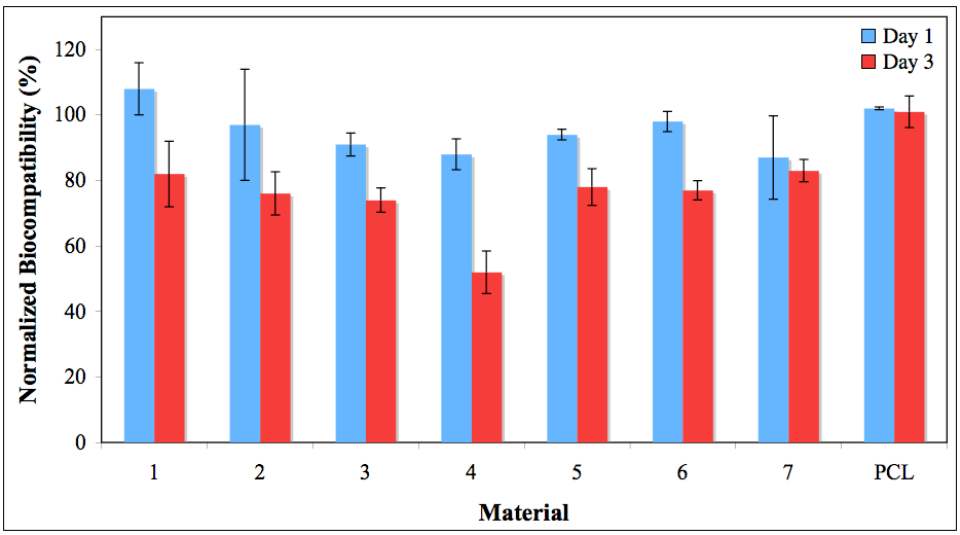

Figure 5.6. *In vitro* cytotoxicity based on an ATP-luminescence assay. SAFs were cultured on tissue culture plastic in the presence of itaconate-based polyesters. As a positive material control, cells were cultured in the presence of PCL. The viability of the cells exposed to polymer samples was expressed as a percentage of the viability of cells grown in the absence of polymers.

5.3.6 *In Vitro* Cytotoxicity

These polyesters were designed for drug delivery, tissue engineering, and other biomedical applications. As such, the cytotoxicity of these elastomers was studied by monitoring the intracellular concentration of ATP. Polyester thermosets were sterilized in ethanol and then soaked in PBS under a germicidal lamp in order to remove any remaining ethanol. SAFs were cultured in a 24-well plate containing transparent and permeable inserts. Because preliminary data suggested that viability could be limited by polymer samples resting directly on cells, thermoset samples were placed in the inserts to prevent direct contact between polyesters and cells. During culture, the cells were exposed to the soluble fraction of the polyesters and any degradation products, both of which were able to diffuse

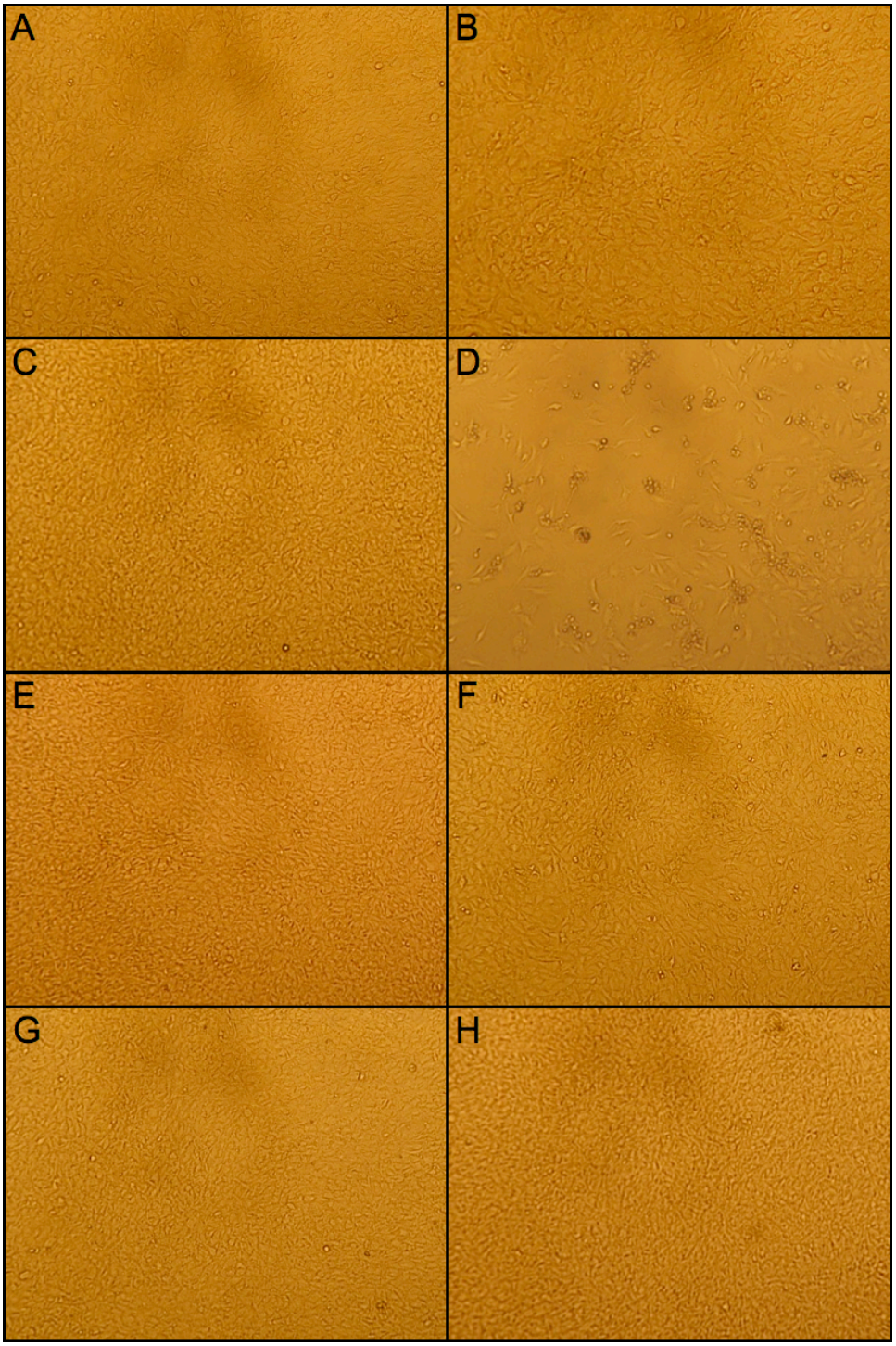

Figure 5.7. Optical micrographs from *in vitro* cytotoxicity assay. SAFs were imaged after 72 h of culture with materials 1 (A), 2 (B), 3 (C), 4 (D), 5 (E), 6 (F), and 7 (G). As a control, cells were cultured with samples of PCL (H). Only material 4 displayed significant toxicity towards SAFs.

through the permeable inserts. Two positive controls were employed during these studies: cells were exposed to no polyester extracts and to PCL as a material control. The cytotoxicity was evaluated after 24 h and 72 h. As seen in Figure 5.6, cultured SAFs showed no negative response to any of the polyesters after the first day. After 3 d, all of the materials showed good toxicity profiles except for material 4, which displayed moderate toxicity (Figure 5.7). During the study, the culture medium that was exposed to material 4 turned from red to yellow; this change in color indicated a drop in pH. This observation is consistent with the fact that material 4 has the highest soluble fraction and is the most hydrophilic (contact angle of 29.4 °), allowing water to interact with the free carboxylic acid. The other materials allowed ≥85 % and ≥75 % of the viability associated with cells that were not exposed to polymer extracts after 24 h and 72 h, respectively. This preliminary biological data indicate that photocured itaconate-based polyesters warrant further exploration as novel biomaterials.

5.3.7 Polymer Molding

Biodegradable materials often need to be molded into complex 3-dimensional structures for specific applications in tissue engineering or drug delivery.[7,35,39] Therefore, itaconate-based materials were engineered and molded with a variety of strategies (Figure 5.8). Utilizing Particle Replication In Non-wetting Templates (PRINT), 2 μm x 2 μm x 1 μm particles of polymer 5 were fabricated in the shape of rectangular prisms (Figure 5.8A). Additionally, an embossed film of material 1 was designed on a glass slide with 2 μm x 2 μm x 6 μm features by employing a similar perfluoropolyether template (Figure 5.8B). Also, porous scaffolds were fabricated due to their importance in tissue engineering.[11,12] Pre-polymer 3 was dissolved in PEGMEM or MEA so that it could act as a poly-functional cross-

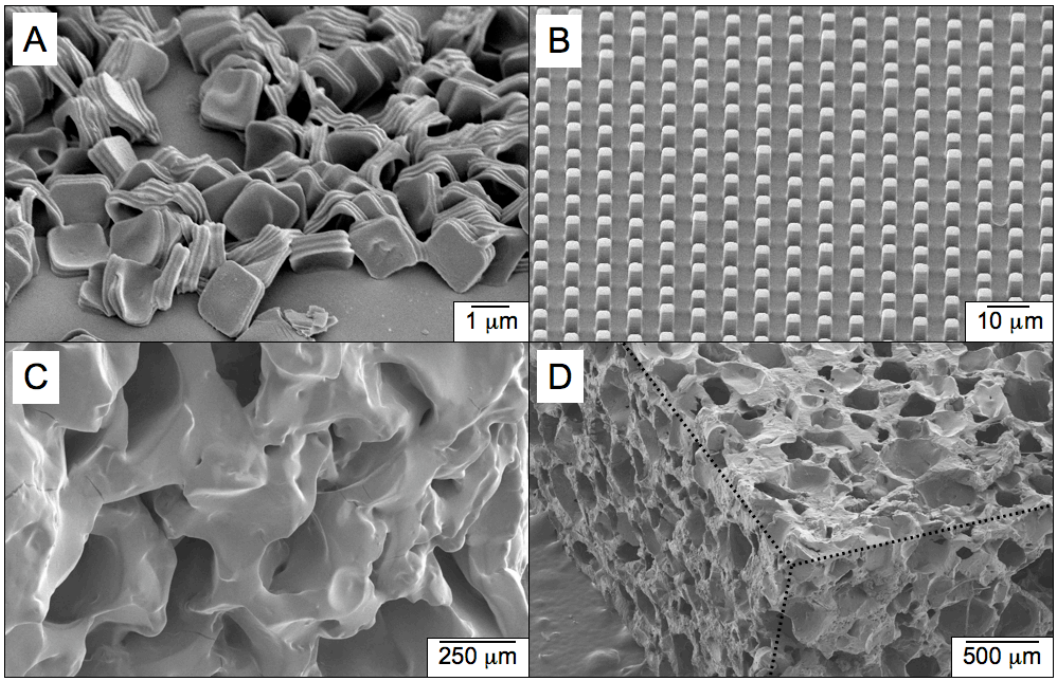

Figure 5.8. Scanning electron microscopy images of 3-dimensional itaconate-based thermosets. (A) Curing pre-polymer 5 in the presence of a patterned perfluoropolyether film enabled the design of micron-scale particles (2 μm x 2 μm x 1 μm). (B) On a glass slide, an embossed film of material 1 was designed with features of 2 μm x 2 μm x 6 μm by utilizing a similar perfluoropolyether mold. (C) Pre-polymer 3 was used as a cross-linking agent for PEG methyl ether methacrylate. Sieved salt was employed as a porogen, which, after leaching in water, enabled the fabrication of porous scaffolds. (D) Pre-polymer 3 was also employed as the cross-linking agent in a porous film of 2-(methacryloyloxy)ethyl acetoacetate. The dotted lines help to display three faces of the scaffold converging at a corner. Sieved salt was again utilized as the porogen.

linker; no solvent was added. The solution was combined with DEAP and sieved NaCl, cured, and swelled in water for 4 d. As the water dissolved the salt, the films became porous (Figure 5.8C, 5.8D). Importantly, materials 1 – 3 can act as cross-linking agents for other acrylate- and methacrylate-based monomers, increasing their versatility in the design of biodegradable materials.

As described above, these itaconate-based polyesters were compatible with PRINT, a fabrication technique that allowed for the design of particles. If one of the hyperbranched materials (materials 1 – 4) were molded, the resulting particles would contain free acids and

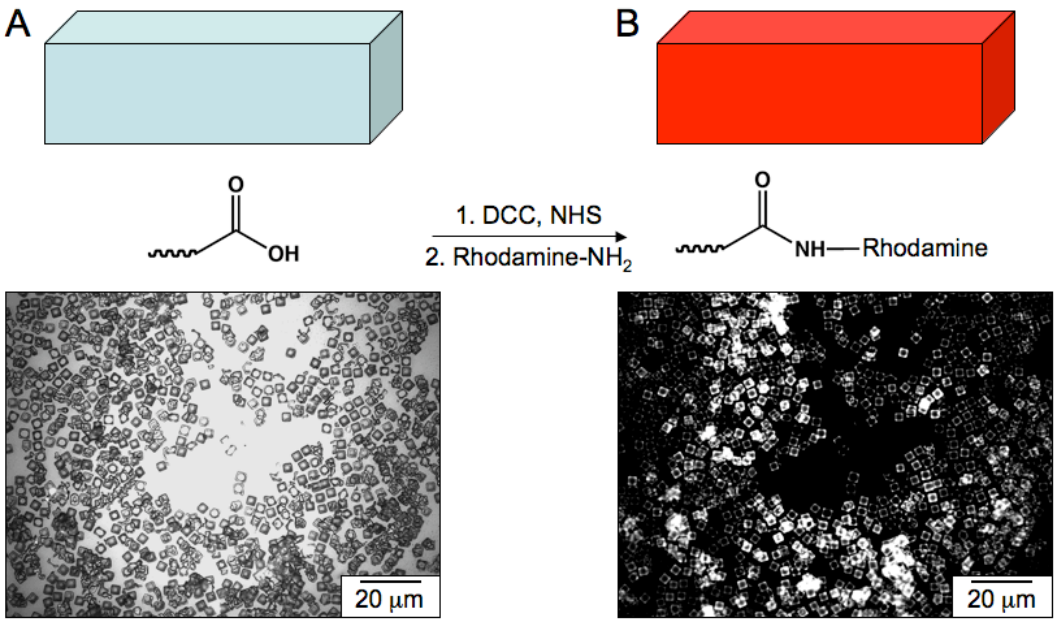

Figure 5.9. Amidation-based functionalization of acid-containing particles. (A) Material 2, a hyper-branched polyester, was cured into particles (3 μm x 3 μm x 1 μm) through PRINT. As Material 2 was cross-linked radically, the particles contain free acids that are capable of functionalization. The particles were visualized by optical microscopy. (B) An amine-functionalized rhodamine dye was coupled to the particles through standard DCC/NHS chemistry. As seen by fluorescent microscopy, the resulting particles were fluorescent due to the immobilized dye.

alcohols, as cross-linking through the alkenes does not involve esterification. This fact implies that functionalization could occur through the unreacted functional groups. In order to demonstrate this, material 2 was cured into particles (3 μm x 3 μm x 1 μm) through the PRINT methodology (Figure 5.9A). After harvesting the particles, they were re-suspended in DMF with excess NHS and DCC for 30 min. An amine-modified rhodamine dye was then added to the reaction, followed by 5 h of agitation. The reaction was halted by centrifuging the particles and discarding the supernatant. Purified fluorescent particles were obtained after repeated rounds of re-suspension in acetone, centrifuging, and decanting the solution; the purification process was ended when the acetone solution containing suspended particles was colorless. The resulting particles were imaged on a fluorescent microscope due to the

conjugation of the rhodamine dye (Figure 5.9B). This amidation strategy is extremely versatile, resulting in the immobilization of hydrolytically stable ligands; labile bonds could also be introduced through esterification. While material 2 was chosen as an example, this functionalization strategy should be compatible with particles composed of any polymer that includes free carboxylic acids.

5.4 Conclusions

We have designed several novel photocurable polyester elastomers based on IA, a natural and renewable monomer. Established polyester synthesis strategies are compatible with IA and DMI, allowing for the development of photocurable polyesters in one step without secondary steps or end-capping. Altering the polyol and the cross-linking density of the itaconate-containing family of materials provides control of the mechanical profiles, hydrophobicity, and other macromolecular properties. The mechanical properties of many biological materials fall within the values displayed by these hyperbranched itaconate-based polyesters.[1-3] Furthermore, numerous mechanical profiles can be achieved by the design of new materials from unique monomer feeds. The pre-polymers are also compatible with imprint lithography and other fabrication techniques; particles and complex scaffolds can be easily designed for potential biomedical applications. To the best of our knowledge, this is the first use of IA in thermally synthesized hyperbranched polyesters, the first use of CALB to enzymatically synthesize itaconate-based polymers, and the first use of itaconate-based materials in combination with the photoinitiator DEAP. Additionally, water-soluble polymers, such as poly(itaconate sorbitol -*co*- succinate sorbitol), offer versatility because they can also be used to design hydrogels. Future work will focus on new polymer formulations and *in vivo* characterization of this class of polyester thermosets in regards to

tissue engineering and drug delivery. Based on our preliminary results, we believe that the poly(polyol itaconate) series of polyester elastomers should find wide use in the biomedical and biotechnological fields.

5.5 Acknowledgement

The authors thank the Ashby and DeSimone research groups, Dr. Andrew Brown, and Sarah White for insightful discussions. This work was supported by the National Cancer Institute (MNY), the National Science Foundation (MNY), and the Charles Lee Raper Dissertation Fellowship (DGB).

5.6 References

(1) Amsden, B. *Soft Matter* **2007**, *3*, 1335-1348.

(2) Webb, A. R.; Yang, J.; Ameer, G. A. *Expert Opin. Biol. Ther.* **2004**, *4*, 801-812.

(3) Barrett, D. G.; Yousaf, M. N. *Molecules* **2009**, *14*, 4022-4050.

(4) Albertsson, A.; Varma, I. K. *Biomacromolecules* **2003**, *4*, 1466-1486.

(5) Shi, R.; Chen, D.; Liu, Q.; Wu, Y.; Xu, X.; Zhang, L.; Tian, W. *Int. J. Mol. Sci.* **2009**, *10*, 4223-4256.

(6) Wang, Y.; Kim, Y. M.; Langer, R. *J. Biomed. Mater. Res. A.* **2003**, *66*, 192-197.

(7) Gratton, S. E. A.; Williams, S. S.; Napier, M. E.; Pohlhaus, P. D.; Zhou, Z.; Wiles, K. B.; Maynor, B. W.; Shen, C.; Olafsen, T.; Samulski, E. T.; DeSimone, J. M. *Acc. Chem. Res.* **2008**, *41*, 1685-1695.

(8) Htay, T.; Liu, M. W. *Vasc Health Risk Manag* **2005**, *1*, 263-276.

(9) Tsao, G. T.; Cao, N. J.; Du, J.; Gong, C. S. *Adv. Biochem. Eng. /Biotech.* **1999**, *65*, 243-280.

(10) Wang, Y.; Ameer, G. A.; Sheppard, B. J.; Langer, R. *Nat. Biotechnol.* **2002**, *20*, 602-606.

(11) Yang, J.; Webb, A. R.; Ameer, G. A. *Adv. Mater. (Weinheim, Ger.)* **2004**, *16*, 511-516.

(12) Yang, J.; Webb, A. R.; Pickerill, S. J.; Hageman, G.; Ameer, G. A. *Biomaterials* **2006**, *27*, 1889-1898.

(13) Barrett, D. G.; Yousaf, M. N. *Biomacromolecules* **2008**, *9*, 2029-2035.

(14) Rolland, J. P.; Hagberg, E. C.; Denison, G. M.; Carter, K. R.; DeSimone, J. M. *Angew. Chem. Int. Ed.* **2004**, *43*, 5796-7599.

(15) Rolland, J. P.; Van Dam, R. M.; Schorzman, D. A.; Quake, S. R.; DeSimone, J. M. *J. Am. Chem. Soc.* **2004**, *126*, 2322-2323.

(16) Rolland, J. P.; Maynor, B. W.; Euliss, L. E.; Exner, A. E.; Denison, G. M.; DeSimone, J. M. *J. Am. Chem. Soc.* **2005**, *127*, 10096-10100.

(17) Zhang, X. Q.; Tang, H.; Hoshi, R.; De Laporte, L.; Qiu, H.; Xu, X.; Shea, L. D.; Ameer, G. A. *Biomaterials* **2009**, *30*, 2632-2641.

(18) Chan, E. W. L.; Yousaf, M. N. *J. Am. Chem. Soc.* **2006**, *128*, 15542-15546.

(19) Pulsipher, A.; Westcott, N. P.; Luo, W.; Yousaf, M. N. *J. Am. Chem. Soc.* **2009**, *131*, 7626-7632.

(20) Sen, M.; Guven, O. *Euro. Polym. J.* **2002**, *38*, 751-757.

(21) Gebelein, C. G.; Dunn, R. L., Eds.; In *Progress in Biomedical Polymers;* Plenum Press: New York, NY, 1990; .

(22) Carnahan, M. A.; Grinstaff, M. W. *Macromolecules* **2006**, *39*, 609-616.

(23) Kulshrestha, A. S.; Gao, W.; Fu, H.; Gross, R. A. *Biomacromolecules* **2007**, *8*, 1794-1801.

(24) Bruggeman, J. P.; de Bruin, B. J.; Bettinger, C. J.; Langer, R. *Biomaterials* **2008**, *29*, 4726-4735.

(25) Won, C. -.; Chu, C. -.; Yu, T. -. *Macromol. Rapid Commun.* **1996**, *17*, 653-659.

(26) Sontjens, S. H. M.; Nettles, D. L.; Carnahan, M. A.; Setton, L. A.; Grinstaff, M. W. *Biomacromolecules* **2006**, *7*, 310-316.

(27) Heller, J. *Biomaterials* **1990**, *11*, 659-665.

(28) Kirimura, K.; Sato, T.; Nakanishi, N.; Terada, M.; Usami, S. *Appl. Microbiol. Biotechnol.* **1997**, *47*, 127-131.

(29) Willke, T.; Vorlop, K. -. *Appl. Microbiol. Biotechnol.* **2001**, *56*, 289-295.

(30) Willke, T.; Vorlop, K. -. *Appl. Microbiol. Biotechnol.* **2004**, *66*, 131-142.

(31) Nagaraja, U. P.; Kishore, G. *Trends Biomater. Artif. Organs* **2005**, *18*, 158-165.

(32) Kovarik, R. E.; Haubenreich, J. E.; Gore, D. *J. Long-Term Eff. Med.* **2005**, *15*, 655-671.

(33) Singh, M.; Rathi, R.; Singh, A.; Heller, J.; Talwar, G. P.; Kopecek, J. *Int. J. Pharm.* **1991**, *76*, R5-R8.

(34) Nijst, C. L.; Bruggeman, J. P.; Karp, J. M.; Ferreira, L.; Zumbuehl, A.; Bettinger, C. J.; Langer, R. *Biomacromolecules* **2007**, *8*, 3067-3073.

(35) Barrett, D. G.; Luo, W.; Yousaf, M. N. *Polym. Chem.* **2010**, , 296-302.

(36) Gotor-Fernandez, V.; Busto, E.; Gotor, V. *Adv. Synth. Catal.* **2006**, *348*, 797-812.

(37) Olson, D. A.; Sheares, V. V. *Macromolecules* **2006**, *39*, 2808-2814.

(38) Takasu, A.; Makino, T.; Yamada, S. *Macromolecules* **2010**, *43*, 144-149.

(39) Barrett, D. G.; Yousaf, M. N. *Macromolecules* **2008**, *41*, 6347-6352.

Chapter VI

GENERAL CONCLUSIONS AND FUTURE DIRECTIONS

6.1 General Conclusions

This dissertation focused on the synthesis and fabrication of novel polyester thermosets for use in the biomedical field. Chapter II discussed the synthesis of amorphous and semi-crystalline polyesters based on erythritol, a FDA-approved sugar alcohol. These materials degraded significantly over the course of a 6-week study in physiological conditions. All of the materials showed good biocompatibility. These materials are promising as degradable and elastomeric scaffolds.

Chapter III described the design of polyketoester thermosets based on α-ketoglutaric acid. Three pre-polymers led to the design of many polyester solids. These pre-polymers were thermally cured, resulting in non-toxic elastomers with very diverse mechanical profiles. These materials were biologically inert as they prevented the non-specific adhesion of cells. However, upon immobilization of a cell-adhesive peptide, fibroblasts were able to attach, spread, and proliferate on these polyesters. Accelerated degradation was observed as a result of the adjacent location of the ketone relative to the acid/ester.

Chapter IV introduced the poly(diol 4-ketopimelate -co- diol citrate) family of polyketoesters. Due to the increase in spacing between the acids/esters and the ketone, these thermosets degraded substantially slower than the materials described in Chapter II – weeks versus days. The mechanical and physical properties of these polyketoesters were characterized. After *in vitro* testing implied that these polymers were non-toxic, *in vivo* studies were also conducted. Both histological data and blood analyses offered evidence that the poly(diol 4-ketopimelate -co- diol citrate) series deserves future studies as *in vivo* biomaterials.

Chapter V focused on the design and synthesis of photocurable polyesters based on itaconic acid, a natural and renewable monomer. The pre-polymers were obtained in a single synthetic step. No post-polymerization modifications were needed as itaconic acid contains a methacrylate-like motif. Pre-polymers were synthesized from thermal polyesterification and from enzymatic polymerization. The mechanical and physical attributes of these materials were studied. *In vitro* cytotoxicity reports indicated that these polyesters were non-toxic and warrant further studies regarding their effect on living systems.

6.2 Future Directions

As discussed in this dissertation, polyester elastomers have been the focus of a great deal of recent publications. All of the materials described here should be studied further *in vivo* to gain a more complete understanding of their interactions with living systems. Also, continued characterization of these polymers can allow for the most appropriate applications to be determined. The poly(erythritol dicarboxylate) series from Chapter II provides a basic and versatile scaffolding material for future tissue engineering studies. Specific applications could range from vasculature engineering to stent design. In Chapter III, the poly(triol α-ketoglutarate) family was described as hydrolyzing exceptionally rapidly. As such, these or similar polymers may be ideal for the burst release of therapeutic agents. In Chapter IV, an exciting new class of polyketoester thermosets was discussed. These materials degrade at a physiologically relevant rate. Due to the presence of a ketone in the repeat unit, post-polymerization modifications are possible through the formation of oximes. Oxyamines are easily incorporated into a wide variety of biologically relevant molecules including carbohydrates, peptides, nucleic acids, and drugs. The conjugation of biomolecules could induce a desired response from a biological system. Finally, the itaconate-based polyesters

described in Chapter V have tremendous potential in tissue engineering and drug delivery. Because they are photocurable, encapsulation of small molecules in these polyesters is straightforward. Therefore, drug-eluting particles, scaffolds, or stents could be designed. As itaconic acid is a natural and fully renewable resource, this class of polymers provides a route to green chemistry in addition to useful biomaterials.

Appendix A

Etching and Oxime-Based Functionalization of Poly(Triol α-Ketoglutarate) with Microfluidics

Reproduced in part with permission from:
Barrett, D. G.; Lamb, B. M.; Yousaf, M. N. *Langmuir* **2008**, *24*, 9861-9867.

A.1 Introduction

A significant amount of research has recently been focused on the design of new biodegradable materials for environmentally responsible applications and for biomedical applications.[1-4] However, the design of new techniques to process, pattern, and tailor these materials is equally critical to the continued progression of new polymers in these emerging research fields.[5-8] Microfabrication is a commonly used method to generate features in materials at the micron scale length compatible with single cell studies.[9-12] However, the direct microfabrication of features in biodegradable materials has proven far more difficult.[13-15] One strategy relies on the patterning of biodegradable materials directly on microfabricated polydimethylsiloxane (PDMS).[14] After creating PDMS templates, polyesters are applied, cured, and molded, allowing the inverse features to be transferred from the PDMS. However, some examples involve complex processes that combine thermal curing and the application of external pressure to ensure that the patterns transfer with high fidelity. Other examples involve the use of sacrificial layers of sucrose on silicon templates, which causes significant loss of feature resolution.[15] Also, the more processing steps between the initial microfabrication and the final patterning of the material reduces the overall resolution of the process. A technology that is amenable to a large range of polyesters, including brittle and semi-crystalline materials, and that could simplify the number of steps and conditions required to create micron-scale polymer features would allow for a range of complex biomaterials to be generated for a variety of applications.

In addition to the ability to generate micron-scale features in biomaterials, the inclusion of a chemoselective immobilization patterning strategy is essential to maximize the full potential of a biodegradable system. Recently, significant progress has been made to include chemoselective ligand immobilization strategies in polyesters.[16-20] The ability to

modify a biodegradable polymer quickly and easily would greatly enhance its versatility by allowing an application to be defined by the immobilized ligand as well as the inherent characteristics of the polymer itself. The same material could potentially be used for completely different purposes by utilizing ligands that lend themselves to opposing applications. Outside of the need for a ligand immobilization strategy, no system is currently available to selectively functionalize newly generated micro-features. If a functionalization strategy could be combined with a microfabrication system that allowed for feature-specific functionalization, the results would have an immediate impact on a wide range of research fields. The potential applications could range from, but are not limited to, functionalizable microfluidic chips to extremely complex patterned cell scaffolds for tissue engineering.

This appendix describes the microfluidic etching of poly(1,2,6-hexanetriol α-ketoglutarate) (PHa). By flowing NaOH solutions through a microfluidic cassette, micron-scale features can easily be etched into polyester elastomer films. Due to the presence of a ketone in the polyester repeat unit, chemoselective modifications can be subsequently performed in the same etched polyester channels, enabling application-specific functionalization and therefore chemical tailoring of the microchannel features through oxime chemistry. These etched films can also be fused to flat pieces of PHa, creating enclosed micro-channels that can be used as microfluidic devices. As a control, poly(1,2,6-hexanetriol β-ketoglutarate) (PHb) was synthesized. Demonstrating the chemistry-specific dependence of the etching process, PHb, which differs from PHa only in the location of the ketone, is unable to be etched by basic solutions. These observations support the conclusion that the success of NaOH as a polyester etchant is directly related to the chemistry of the repeat unit of the polyester.

A.2 Experimental Section

A.2.1 Materials

All chemicals were purchased from Sigma-Aldrich (Milwaukee, WI) or Fisher Scientific (Philadelphia, PA), and used without further purification unless otherwise noted. α-ketoglutaric acid (αKG) was recrystallized from ethyl acetate while diethyl β-ketoglutarate (βKG) was distilled prior to use.

A.2.2 Elastomer Synthesis

To synthesize PHa, equimolar amounts of αKG and 1,2,6-hexanetriol were combined in a round bottom flask and stirred in an inert environment of N_2 at 125 °C. After a homogenous melt formed, the mixture was stirred for an additional hour. PHa pre-polymers were then precipitated in −78 °C methanol (MeOH), concentrated by rotary evaporation, and dried under vacuum at room temperature. To cross-link PHa to form elastomeric films, pre-polymers were cured at 120 °C for 1 d. To synthesize PHb, equimolar amounts of βKG and 1,2,6-hexanetriol were combined in a round bottom flask and stirred in an inert environment of N_2 at 135 °C. The mixture was stirred for 5 h, precipitated in −78 °C MeOH, concentrated by rotary evaporation, and dried under vacuum at room temperature. To cross-link PHb to form elastomeric films, pre-polymers were cured at 120 °C for 4 d.

A.2.3 Polymer Characterization

Thermal properties were recorded by differential scanning calorimetry (DSC) and thermogravimetric analysis (TGA). Using a Seiko 220C DSC, pre-polymer glass transition temperatures were measured during the second heating cycle (10 °C/min). Thermal degradation data was collected with a Perkin-Elmer TGA with a heating rate of 10 °C/min in an atmosphere of N_2.

Tensile tests were conducted on an Instron 5566 at a crosshead speed of 10 mm/min at 25 °C. Samples were cured in a dog-bone-shaped mold with approximate dimensions of 10 mm x 3 mm x 1.5 mm. The Young's modulus (YM) was calculated according to the linear segment of the stress/strain curve. Three trials were performed and the average was reported. Using

$$n = \mathrm{YM}(3\mathrm{RT})^{-1} \quad (1)$$

where R is the universal gas constant and T is the temperature in K, the cross-linking density (n) was calculated.

Sol-gel analysis was conducted by soaking films in THF for 24 h at room temperature. After solvent removal, the films were dried, and the percent soluble fraction (Q_s) was calculated by

$$Q_s = \frac{m_i - m_f}{m_i} \times 100 \quad (2)$$

where m_i and m_f represent the initial and final mass of the elastomer films, respectively. Three trials were performed and the average was reported.

To obtain standard degradation rates, approximately 75 mg segments of each elastomer were placed in scintillation vials. Vials were filled with phosphate buffered saline (PBS) and samples were then stored in an incubator (37 °C). At predetermined intervals, samples were removed from the incubator, rinsed thoroughly, dried, and weighed again. To prevent saturation, PBS was replaced every 7 days. Each data point was repeated in triplicate and results were reported as the average percent of the original mass lost.

A.2.4 Surface Functionalization

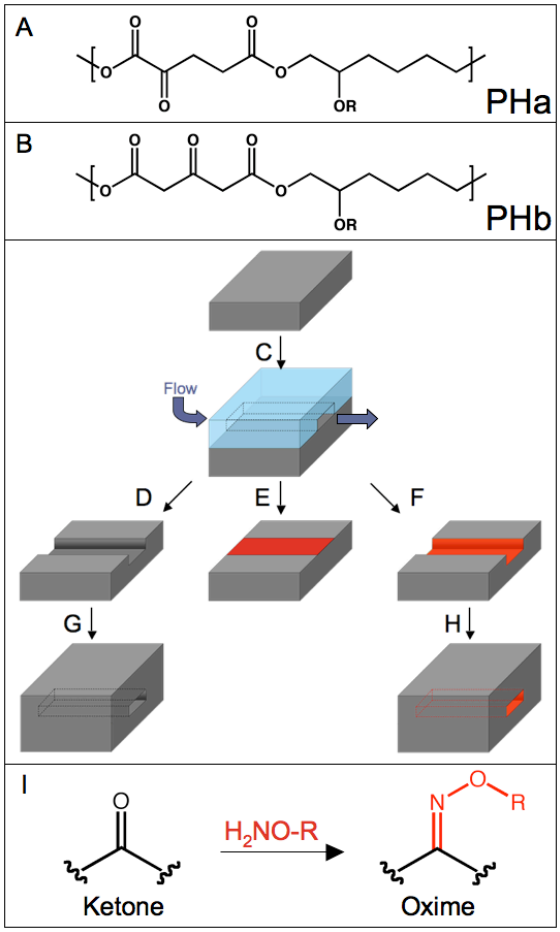

Figure A1. Schematic of microfluidic etching and functionalization of polyketoesters. (A) The repeat unit of PHa contains a ketone in the alpha position to an ester. (B) PHb differs from PHa only in the location of the ketone, which is in the beta position to both esters. (C) By placing a microfluidic cassette in direct contact with a polyketoester film, three modifications are possible. (D) By flowing a NaOH solution through the microfluidic chip, accelerated hydrolytic degradation causes the formation of etched micro-channels. (E) By reacting the surface with oxyamine-tethered ligands (R-ONH_2), controlled formation of oximes results in patterned covalent immobilization of molecules. (F) By etching, as in (D), and then conjugating oxyamine-containing molecules, as in (E), functionalized micro-channels are formed. (G, H) By placing the etched film in contact with a flat piece of PHa and thermally curing, enclosed micro-channels are formed. (I) Representation of a ketone and an oxyamine reacting to form an oxime.

Microfluidic cassettes were designed as previously described.[21, 22] A PDMS microfluidic cassette was reversibly sealed to a PHa film. With the aid of negative pressure at the exit port, a 5 mM solution of an oxyamine-modified rhodamine dye (Rhod-ONH_2) in MeOH was flowed through the channels. The patterns were then rinsed with 100 μL MeOH

and dried with N_2. Fluorescent images were taken using a Nikon Eclipse TE2000-E inverted microscope.

A.2.5 Microfluidic Etching

To etch PHa, a PDMS microfluidic cassette was placed in direct contact with the polyketoester film, creating a seal. Aided by negative pressure at the exit port, a 2.5 % NaOH solution in 1:1 H_2O:2-propanol (iPrOH) was then flowed through the microfluidic channels, followed by a chase rinse with ~ 50 μL of ethanol (EtOH). To etch PHb, the same procedure was followed with an acidic etching solution (equal parts H_2O, EtOH, and concentrated H_2SO_4). To image the patterns, the etched elastomeric films were then coated in ~ 2 nm of a Pd/Au alloy (Cressington 108 auto sputter coater, Cressington Scientific Instruments Ltd.) and imaged using a Hitachi model 2-4700 scanning electron microscope (SEM).

A.2.6 Functionalization of Micro-Channels

PHa was etched as described above. Without removing the PDMS microfluidic cassette, a 5 mM solution of an oxyamine-modified Rhod-ONH_2 in MeOH was flowed through the channels. The patterns were then rinsed with 100 μL MeOH and dried with N_2. Fluorescent images were taken using a Nikon Eclipse TE2000-E inverted microscope.

A.2.7 Synthesis of *O*-Dodecylhydroxylamine

N-hydroxyphthalimide (2.06 g, 12.7 mmol) and $NaHCO_3$ (1.06 g, 12.7 mmol) were dissolved in 65 mL of DMF and heated to 90 °C. After stirring for 20 min, 1-bromododecane (1.22 mL, 5.1 mmol) was added and the reaction continued for 15 h. The solution was added to a separatory funnel containing water and DCM. The aqueous layer was discarded and extractions were continued with DCM and water until the aqueous layer was colorless. The DCM layer was dried with $MgSO_4$, filtered, and concentrated by rotary evaporation. The

product, 2-(dodecyloxy)isoindoline-1,3-dione (1.61 g, 4.8 mmol), was then dissolved in DCM and stirred in an inert environment of argon. Hydrazine (0.62 mL, 12.7 mmol) was then added, and the reaction continued for 15 h. The solution was filtered, washed (twice with water, once with a saturated NaCl solution), dried with $MgSO_4$, filtered, and concentrated by rotary evaporation. Yield: 56.2 %.

A.2.8 Contact Angle Measurements

PHa films were prepared by flattening pre-polymers with a piece of PDMS. To simulate the etching process, films were rinsed for 45 s with the same NaOH solution used for etching. To functionalize the surface, films were immersed in a 10 mM solution of *O*-dodecylhydroxylamine in EtOH for 2 h. Contact angle measurements were performed on a KSV CAM200 contact angle meter with water as the wetting liquid.

A.2.9 Polymer Sealing

To seal polyketoester devices, the surface of a flat PHa film was exposed to a 2.5 % NaOH solution in 1:1 H_2O:iPrOH for several seconds. After rinsing thoroughly with water, the elastomeric film was dried with N_2. The base-washed face of the polyketoester film was then placed in contact with the surface (flat or etched) of another PHa film and allowed to seal for 3 h in a vacuum oven (50 torr) at 60 °C. To image the enclosed micro-channels, a cross-section of a sealed device was coated in ~ 2 nm of a Pd/Au alloy and imaged on an SEM.

A.2.10 Biodegradable Microfluidics

Figure A2. PHa patterned with a fluorescent dye. Using microfluidics, a solution of an oxyamine-modified rhodamine in MeOH was reacted and patterned on a flat PHa surface. After rinsing the surface, the fluorescent pattern is clearly visible against the non-modified background.

After creating enclosed channels by sealing an etched PHa film to a flat PHa film (as described above), the top layer was pierced with a 22-gauge needle in order to create access ports to the channels. As a staining solution, black ink from a pen was diluted with 2 mL of EtOH in order to reduce the viscosity. With the aid of negative pressure at the exit port, the ink solution was flowed through the channels. Images were recorded using a digital camera.

A.3 Results and Discussion

A.3.1 Microfluidic Delivery of Ligands

We recently reported the synthesis and characterization of poly(triol α-ketoglutarate).[23] By combining α-ketoglutaric acid and a triol (glycerol, 1,2,4-butanetriol, 1,2,6-hexanetriol), a series of elastomers were designed that ranged from strong and rigid to weak and flexible. This appendix focuses on poly(1,2,6-hexanetriol α-ketoglutarate) (PHa), although multiple triols can be used with similar results. The etching reactivity and oxime conjugation of this polyketoester is mainly due to the presence of the α-ketoglutaric acid – the triol monomer is used as a facile method to tailor the polymer properties such as hydrophobicity and to control the rate of degradation.

One key feature of PHa is the presence of a ketone group in each repeat unit, which allows for the immobilization of oxyamine-containing molecules.[16, 19, 24-27] Importantly, after

Table A1. Etching Conditions for Polyketoesters Films

Etch	Polymer	Etchant	Time (s)	Channel Depth (μm)
1	PHa	NaOH	10	8
2	PHa	NaOH	20	15
3	PHa	NaOH	60	65
4	PHa	H_2SO_4	120	0
5	PHb	NaOH	120	0
6	PHb	H_2SO_4	60	2

cross-linking, the ketones retain their reactivity towards oxyamine-tethered ligands, creating tailored chemoselective polyester films (Figure A1). By placing a microfluidic cassette in direct contact with a PHa film, a seal is created that allows for solutions to be delivered with spatial control to the surface of the polyketoester. Complex patterns of immobilized molecules can be easily designed due to the rapid nature of the oxime-forming reaction. To demonstrate microfluidic delivery and reactivity to the polyketoester film, a solution of an oxyamine-modified rhodamine dye in MeOH was flowed through the microfluidic chip. Figure A2 shows fluorescent patterns of rhodamine conjugated to the polyketoester.[28] As a control, the same experiment was conducted with a fluorescent dye that was not labeled with an oxyamine. No fluorescent patterns were observed.

A.3.2 Etching of Poly(α-Ketoester) By Alkaline Solutions

Our initial goal was to develop a straightforward, inexpensive and rapid strategy to create tailored and biodegradable microfluidic devices. However, because PHa has a ketone located adjacent to an ester linkage, the rate of hydrolysis is increased due to the enhanced electrophilicity of the nearby ester carbon (Figure A1).[20, 23] Using this knowledge, we developed a basic solution etch combined with microfluidics to generate micron-sized features in PHa. By flowing a solution of NaOH through a PDMS microfluidic cassette in

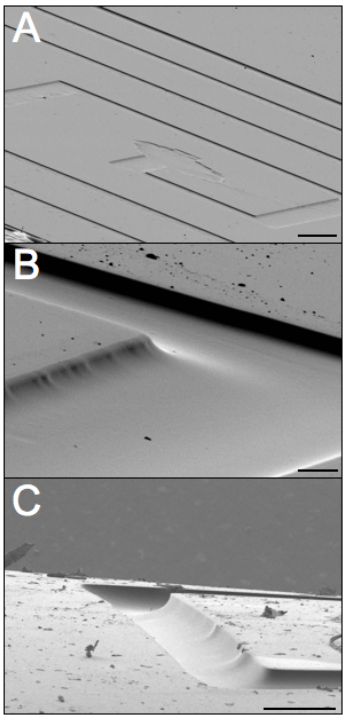

Figure A3. Scanning electron micrographs of base-etched PHa. A) The seal between PHa and the microfluidic chip is liquid-tight, as demonstrated by the high fidelity of the etching (scale bar represents 250 μm). The depth of the etched features could be varied, as shown by (B) 15 μm micro-channels (scale bar represents 25 μm) and (C) 65 μm micro-channels (scale bar represents 250 μm).

contact with a PHa film, various features can be etched into the polyketoester film via selective hydrolysis. By changing the etching duration, the feature depth can be precisely controlled (Table 1). As seen in Figure A3, the etched patterns correspond with the microfluidic channels with a high level of fidelity. The aforementioned imprint lithography techniques use external pressure to mold the polyesters, eventually resulting in the destruction of the PDMS template. This etching technique is fast and low impact, allowing the microfluidic cassette to be used repeatedly.[14] The NaOH-based etching methodology is compatible with other polyesters containing α-ketoglutaric acid as the diacid, allowing for modulation of polymer properties by varying the triol. Figures A-S1 and A-S2 (Supplemental

Materials) show etched patterns in poly(1,2,4-butanetriol β-ketoglutarate) (PBa) and poly(glycerol α-ketoglutarate) (PGa), respectively.

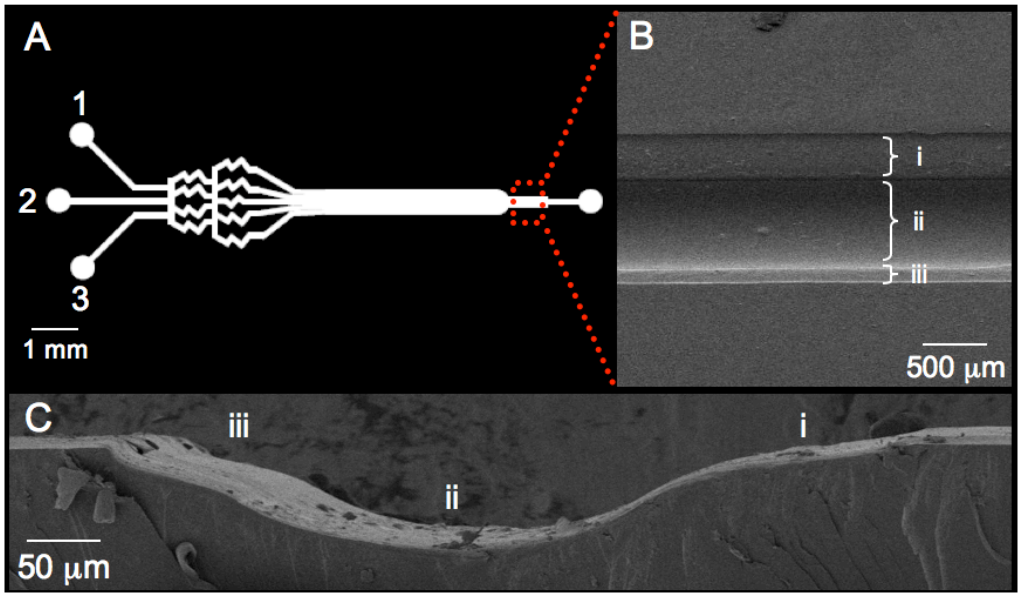

Figure A4. Multi-depth etching based on diffusive mixing of parallel solutions. A) The photomask used to create the microfluidic chip for multi-depth etching has three delivery ports. Ports 1 and 3 were used to deliver solvent, while port 2 was used to deliver NaOH. B) SEM of area represented by the red, dashed box in (A). Note the appearance of multiple etched areas within the channel (i, ii, iii), caused by differential etching based on the local NaOH concentration. C) A cross-section of the channel in (B), showing the different etching depths. Regions i, ii, and iii are labeled as in (B).

In addition to its ability to create micro-patterned features of consistent depth, the microfluidic etching methodology also enables the design of multidimensional features by utilizing parallel flow in a single microfluidic cassette.[29, 30] This method can be routinely used to create complex and intricate multi-depth features that otherwise might not be possible with conventional microfabrication techniques. For example, a microfluidic cassette utilizing parallel flow was designed to simultaneously etch multiple depths based on the concentration of NaOH. Multiple intake ports and diffusive mixing points were designed to generate patterns that allowed for several solutions to converge and combine into a single channel

(Figure A4B). Ports 1 and 3 were loaded with an H_2O-EtOH (1:1) solution while port 2 was loaded with the same solution containing 2.5 % NaOH. With the aid of negative pressure at the outlet, a single channel was etched with multiple depths, based on the varying concentrations of the etchant, immediately adjacent to each other (Figure A4B).

Table A2. Contact Angle of PHa with and without NaOH etch and DDHA

Material	Contact Angle (°)
PHa	57.7 ± 5.7
PHa + C_{12}-ONH_2	82.5 ± 5.2
PHa + Etch	41.7 ± 2.6
PHa + Etch + C_{12}-ONH_2	54.3 ± 2.0

A.3.3 Functionalization of Etched Polyesters

A major advantage of this micro-patterning tool is its compatibility with an existing immobilization strategy in PHa. Due to the presence of a ketone in αKG-based polymers, oxyamine-tethered ligands can be directly conjugated to the polymer surface. To determine whether the ketones were still reactive to ligand conjugation after the etching process, two experiments were performed. Contact angle measurements of non-etched and etched polymer surfaces were obtained, with and without conjugation to *O*-dodecylhydroxylamine (DDHA), a ligand that greatly increases the hydrophobic nature of surfaces (Table 2). To functionalize surfaces, films were immersed in DDHA solutions for several hours. To mimic etching, films were rinsed with NaOH solutions for approximately 45 s. Based on contact angle data, the ketones are still reactive after exposure to the basic etching solution. In order of most hydrophobic to most hydrophilic surface character, the films ranked: DDHA-conjugated, non-etched PHa (82.5 °); non-etched PHa (57.7 °); DDHA-conjugated, etched

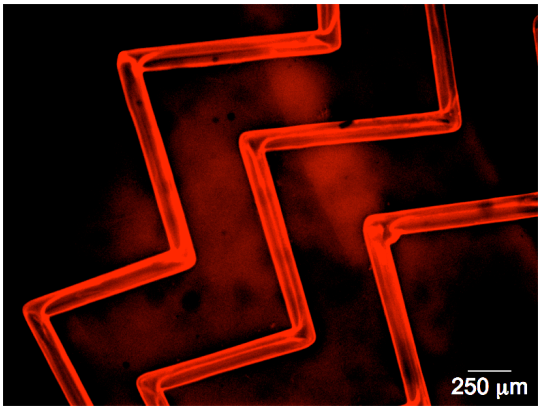

Figure A5. Oxime functionalization of etched microchannels. After PHa was etched with NaOH, an oxyamine-modified rhodamine fluorescent dye was delivered to the channels. The fluorescence of the channels demonstrates that the ketones are still reactive to oxyamine-tethered molecules after the etching process.

PHa (54.3 °); non-functionalized, etched PHa (41.7 °). The results indicate that the ketones are still able to chemoselectively react with oxyamines after exposure to NaOH solutions.

A second experiment to demonstrate the reactivity of ketones after etching involved the delivery of an oxyamine-modified rhodamine fluorescent dye.[28] After microfluidic etching, and without removing the microfluidic cassette, the dye was delivered to the etched PHa surface (Figure A5). The etched and functionalized channels are clearly visible using fluorescence microscopy after the immobilization of the rhodamine analogue.

A.3.4 Fully Biodegradable Microfluidic Devices

All of the previously described experiments involved a hybrid microfluidic system composed of PHa and PDMS. However, in an attempt to design a functionalizable and fully biodegradable microfluidic system, we tested the ability of an etched PHa surface to bond to another, generating enclosed polyketoester channels. A flat film was briefly rinsed with a solution of NaOH, hydrolyzing a minimal amount of surface esters into acids and alcohols. The process was repeated with a second film that was previously etched using the above microfluidic strategy to generate microchannel features. The result was two pieces of

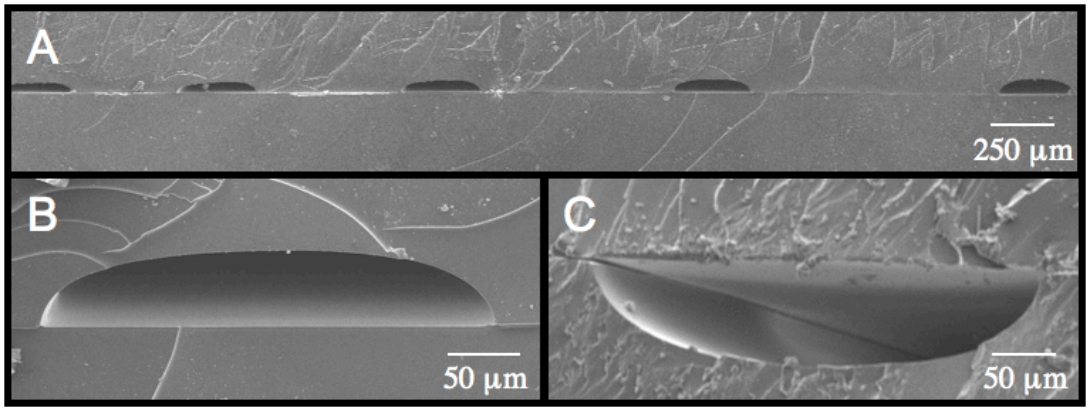

Figure A6. Cross-section of sealed channels. Creating different feature widths and depths is straightforward by varying the microfluidic cassette design and the etching conditions, respectively. (A) The cross-section of a sealed spiral pattern shows that the etching is precise, leading to features that are approximately 250 µm wide and 50 µm deep. B) A channel that is approximately 300 µm wide and 50 µm. C) A channel that is approximately 350 µm wide and 85 µm deep.

PHa with exposed acids and alcohols, one of the two films being etched. After the two segments of polyketoester film were placed in contact with each other, with the NaOH-washed faces together, the device was placed in an oven for 12 h at 60 °C. The thermal curing period allowed surface acids and alcohols from both pieces to cross-link with each other, forming new ester bonds. To examine and view the fully enclosed micro-channels, a device was cut in half, exposing the cross-section (Figure A6). In order to determine whether

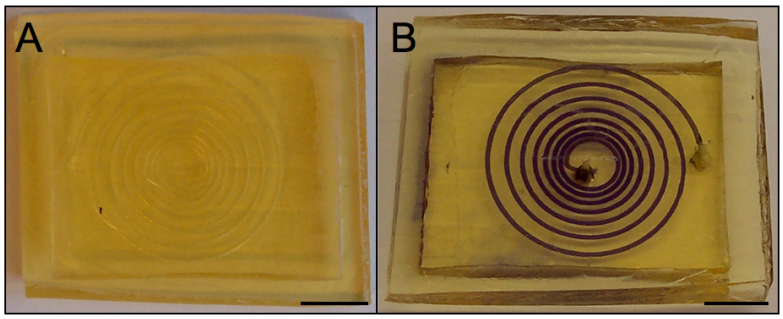

Figure A7. Biodegradable microfluidic device. A) By sealing an etched piece of PHa to a flat piece, enclosed micro-channels were produced. B) After producing access inlet and outlet ports to the channels, an ethanolic solution of black ink was delivered in order to visualize the patterns. Scale bars represent 1 cm.

the resulting seal was liquid-tight, the PHa device was tested as a microfluidic network. After the sealing process, the micro-channels were fairly transparent but still visible (Figure A7A). The fluid used to test the utility of PHa in microfluidics was an ethanolic dilution of pen ink. As can be seen in Figure A7B, the polyketoester device was sealed in a way that liquid does not escape the micro-channels. The fabrication of a chemoselective and biodegradable microfluidic chip allows for future applications to focus on a range of applications, including artificial vasculature, once the system has been optimized for cell culture conditions.

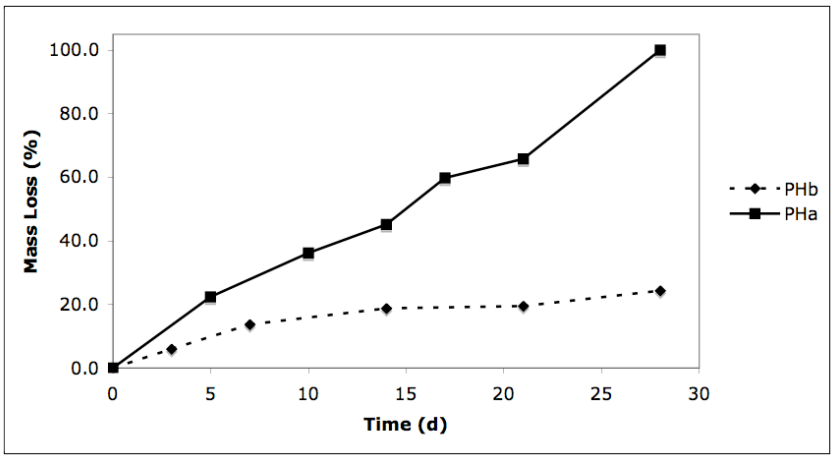

Figure A8. Comparison of the degradation rates for PHa and PHb. The difference in degradation rates is controlled by the location of the ketone. When adjacent to an ester (PHa; solid line), the ketone causes rapid degradation. However, when the ketone is beta to both esters (PHb; dashed line), the rate of degradation is significantly slower.

A.3.5 Etching of Poly(1,2,6-hexanetriol β-ketoglutarate)

To ensure that the base etching was chemistry dependent, a control material, poly(1,2,6-hexanetriol β-ketoglutarate) (PHb) was also synthesized. The only difference between PHa and PHb is the location of the ketone (Figure A1). In PHb, one methylene group separates all the esters from the ketone. This spacing minimizes the electron-withdrawing ability of the ketone and decreases the electrophilicity of the ester carbons. As a

result, the degradation rate of PHb is significantly slower than that of PHa (Figure A8). This trend is also evident in that PHb cannot be etched under the same conditions as PHa (Table 1). Aqueous basic solutions are not able to create features in PHb. We believe that NaOH solutions are also unable to etch PHb due to the fact that the repeat unit has several acidic protons (Supplemental Materials). The presence of multiple β-dicarbonyl species may result in deprotonation by NaOH instead of ester hydrolysis. After attempting base as an etchant, acid was also attempted to catalyze ester hydrolysis. Using extremely strong H_2SO_4 solutions, only shallow channels (~ 2 μm deep) were formed (Figure A9). Again, as a control, the acidic solution was used to etch features in PHa. However, these etching conditions were unsuccessful.

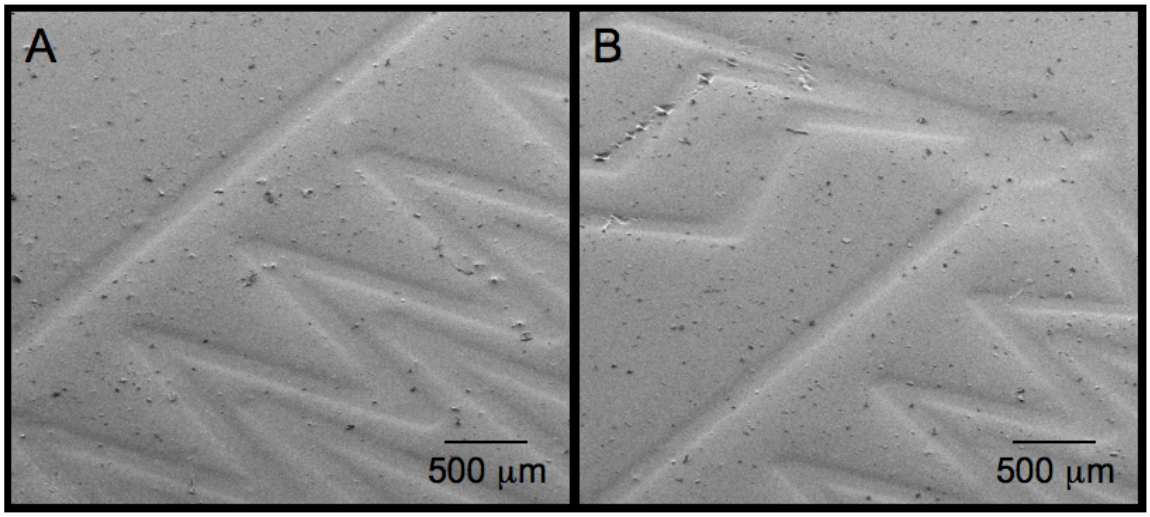

Figure A9. Scanning electron micrographs of acid-etched PHb. Repeated trials only yielded shallow channels (~ 2 μm) when PHb was etched using H_2SO_4 solutions. However, the pattern was still etched with a high level of fidelity, as seen in (A) and (B).

A.3.6 Microfluidic Etching by Dissolution

To determine how flexible the microfluidic etching strategy is for polyesters, we used this approach on a common commercially available material, poly(ε-caprolactone) (PCL).

PCL was melted and poured into a mold, creating a flat surface upon cooling. After placing a microfluidic cassette directly in contact with the PCL film, etching was attempted with basic solutions. Neither a 2.5 % nor a 5.0 % solution of NaOH was able to facilitate hydrolysis in a manner that led to the formation of micro-channels. This result was likely due to the hydrophobic and semi-crystalline characteristics of PCL. However, as PCL is not a cross-linked material, another option for the etchant was the use of a dissolving solvent. Instead of local hydrolytic degradation, local dissolution of the polyester film resulted from the use of acetone as the etchant (Supplemental Materials). Etching can also be combined with ligand immobilization in many materials based on ring-opening polymerizations due to the numerous examples of chemoselective functionalization strategies that have recently been described. [16-19] We believe that the microfluidic etching strategy has the potential to allow for direct etching and subsequent patterning of a broad range of biodegradable materials.

A.4 Conclusions

We have described a straightforward, flexible, and inexpensive method to etch polyketoester PHa films. The location of the ketone, alpha to the ester, renders PHa extremely sensitive to aqueous solutions of base, allowing for microfluidic etching with NaOH solutions to generate patterned micron-scale channels. In addition, the presence of a ketone allowed for chemoselective immobilization of oxyamine-modified ligands, enabling the design of functionalized and tailored micro-channels. Furthermore, by sealing an etched film to a second flat surface of PHa, a biodegradable microfluidic device could be designed. The microfluidic strategy can also be used to introduce etched features into commercially available, semi-crystalline polyesters, such as poly(ε-caprolactone). Future work will continue to explore PHa as a biodegradable and alternative material for use in microfluidic

devices and the etching potential of commercially available polyesters. Particular effort will be focused on the design of delivery vehicles and 3 –dimensional cell scaffolds for tissue engineering applications using this technology.

A.5 Acknowledgments

This work was supported by the Carolina Center for Cancer Nanotechnology Excellence and the Burroughs Wellcome Foundation (Interface Career Award).

A.6 References

(1) Lu, Y.; Chen, S. C. *Adv. Drug Delivery Rev.* **2004**, *56*, 1621-1633.

(2) Gomes, M. E.; Reis, R. L. *Int. Mater. Rev.* **2004**, *49*, 261-273.

(3) Gunatillake, P. A.; Adhikari, R. *Eur. Cells Mater.* **2003**, *6*, 1-16.

(4) Ikada, Y.; Tsuji, H. *Macromol. Rapid. Commun.* **2000**, *21*, 117-132.

(5) Rolland, J. P.; Maynor, B. W.; Euliss, L. E.; Exner, A. E.; Denison, G. M.; DeSimone, J. M. *J. Am. Chem. Soc.* **2005**, *127*, 10096-10100.

(6) Lee, K. -.; Kim, D. J.; Lee, Z. -.; Woo, S. I.; Choi, I. S. *Langmuir* **2004**, *20*, 2531-2535.

(7) Glangchai, L. C.; Caldorera-Moore, M.; Shi, L.; Roy, K. *J. Controlled. Release* **2008**, *125*, 262-272.

(8) Teo, W. E.; Ramakrishna, S. *Nanotechnology* **2006**, *17*, R89-R106.

(9) Khademhosseini, A.; Langer, R.; Borenstein, J.; Vacanti, J. P. *Proc. Natl. Acad. Sci. U. S. A.* **2006**, *103*, 2480-2487.

(10) Rogers, J. A.; Nuzzo, R. G. *Mater. Today* **2005**, *5*, 50-56.

(11) Quake, S. R.; Scherer, A. *Science* **2000**, *290*, 1536-1540.

(12) Xia, Y.; Whitesides, G. M. *Annu. Rev. Mater. Sci* **1998**, *28*, 153-184.

(13) Wang, G. -.; Hsueh, C. -.; Hsu, S. -.; Hung, H. -. *J. Micromech. Microeng.* **2007**, *17*, 2000-2005.

(14) King, K. R.; Wang, C. C. J.; Kaazempur-Mofrad, M. R.; Vacanti, J. P.; Borenstein, J. T. *Adv. Mater.* **2004**, *16*, 2007-2012.

(15) Bettinger, C. J.; Weinberg, E. J.; Kulig, K. M.; Vacanti, J. P.; Wang, Y.; Borenstein, J. T.; Langer, R. *Adv. Mater. Deerfield* **2005**, *18*, 165-169.

(16) Taniguchi, I.; Mayes, A. M.; Chan, E. W. L.; Griffith, L. G. *Macromolecules* **2005**, *38*, 216-219.

(17) Riva, R.; Schmeits, S.; Jerome, C.; Jerome, R.; Lecomte, P. *Macromolecules* **2007**, *40*, 796-803.

(18) Li, H.; Riva, R.; Jerome, R.; Lecomte, P. *Macromolecules* **2007**, *40*, 824-831.

(19) Van Horn, B. A.; Iha, R. K.; Wooley, K. L. *Macromolecules* **2008**, *41*, 1618-1626.

(20) Barrett, D. G.; Yousaf, M. N. *Chembiochem* **2008**, *9*, 62-66.

(21) Westcott, N. P.; Pulsipher, A.; Lamb, B. M.; Yousaf, M. N. *Langmuir* **2008**, *24*, 9237-9240.

(22) Westcott, N. P.; Yousaf, M. N. *Langmuir* **2008**, *24*, 2261-2265.

(23) Barrett, D. G.; Yousaf, M. N. *Macromolecules* **2008**, *41*, 6347-6352.

(24) Barrett, D. G.; Yousaf, M. N. *Biomacromolecules* **2008**, *9*, 2029-2035.

(25) Lee, D. -.; Chang, B. -.; Morales, G. M.; Jang, Y. A.; Ng, M. -.; Heller, S. T.; Yu, L. *Macromolecules* **2004**, *41*, 1849-1856.

(26) Lee, D. -.; Chang, B. -.; Yu, L.; Frey, S. L.; Lee, K. Y. C.; Patchipulusu, S.; Hall, C. *Langmuir* **2004**, *20*, 11297-11300.

(27) Park, M. -.; Lee, D. -.; Liang, Y.; Lin, G.; Yu, L. *Langmuir* **2007**, *23*, 4367-4372.

(28) Chan, E. W. L.; Yousaf, M. N. *J. Am. Chem. Soc.* **2006**, *128*, 15542-15546.

(29) Jeon, N. L.; Dertinger, S. K. W.; Chiu, D. T.; Choi, I. S.; Stroock, A. D.; Whitesides, G. M. *Langmuir* **2000**, *16*, 8311-8316.

(30) Kenis, P. J. A.; Ismagilov, R. F.; Whitesides, G. M. *Science* **1999**, *285*, 83-85.

A.7 Supplemental Materials

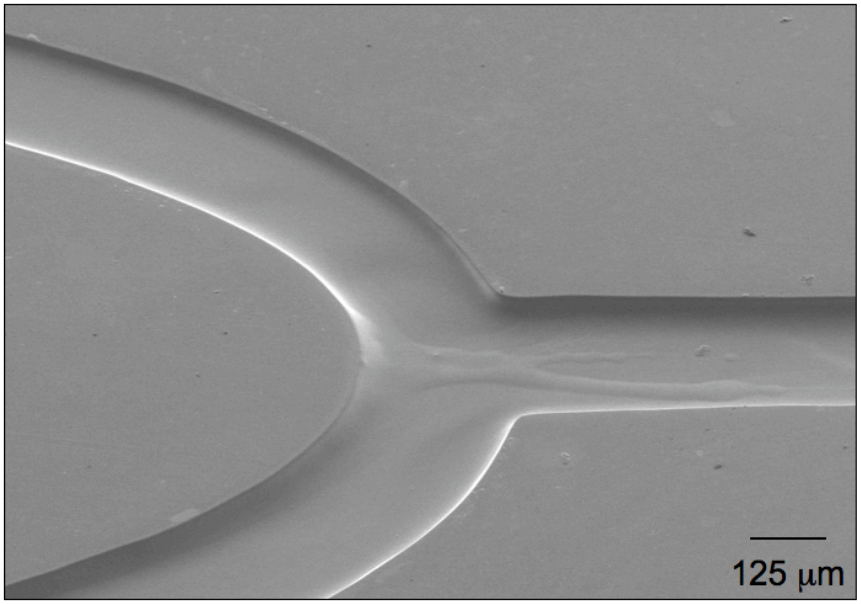

Figure A-S1. Etched patterns in PBa.

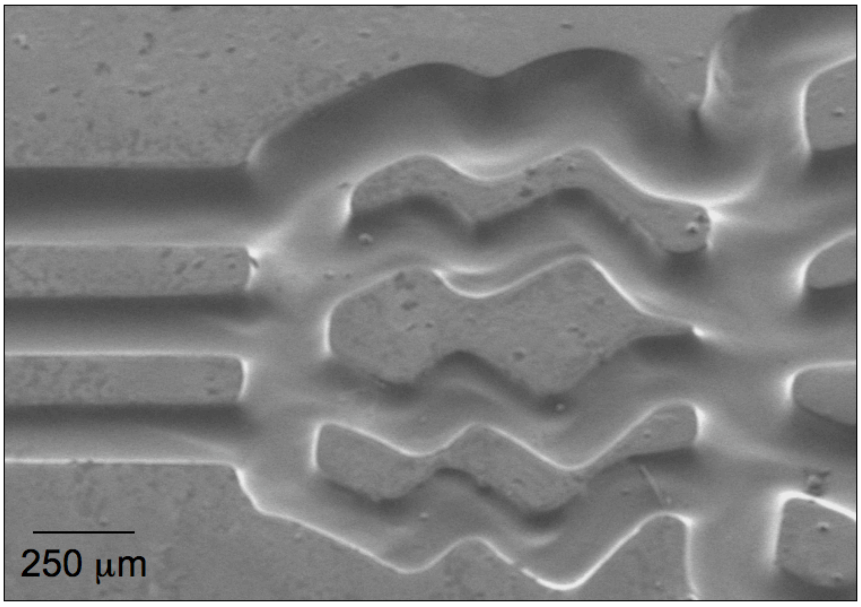

Figure A-S2. Etched patterns in PGa.

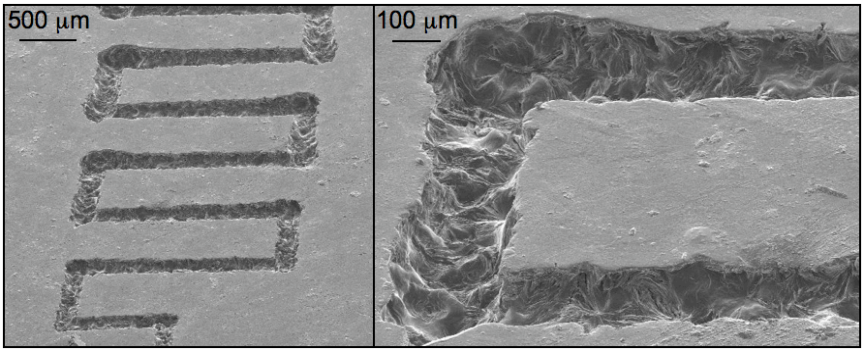

Figure A-S3. Acetone was used to etch poly(ε-caprolactone). Although the pattern transferred with high fidelity (left), the features are extremely rough (right).

Scheme A-S1. Potential Cause for Base Resistance of PHb

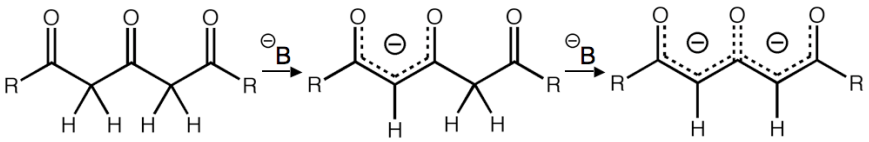

Table A-S1. Mechanical Characteristics of Polyketoester Elastomers

Polyketoester	Weight Loss (°C)[a] 5%	10%	YM [b] (MPa)	UTS [b] (MPa)	RS [b] (%)	n [b] (mmol/L)	Q_s [c] (%)
PHa	306	346	656.2	30.1	21	87900	3.9
PHb	297	330	0.69	0.36	68	92.8	16.5

[a] Determined by TGA. [b] Determined by Instron. [c] Extracted in THF for 24 h at 25 °C.

Appendix B

SUPPLEMENTAL MATERIALS FOR CHAPTER 2

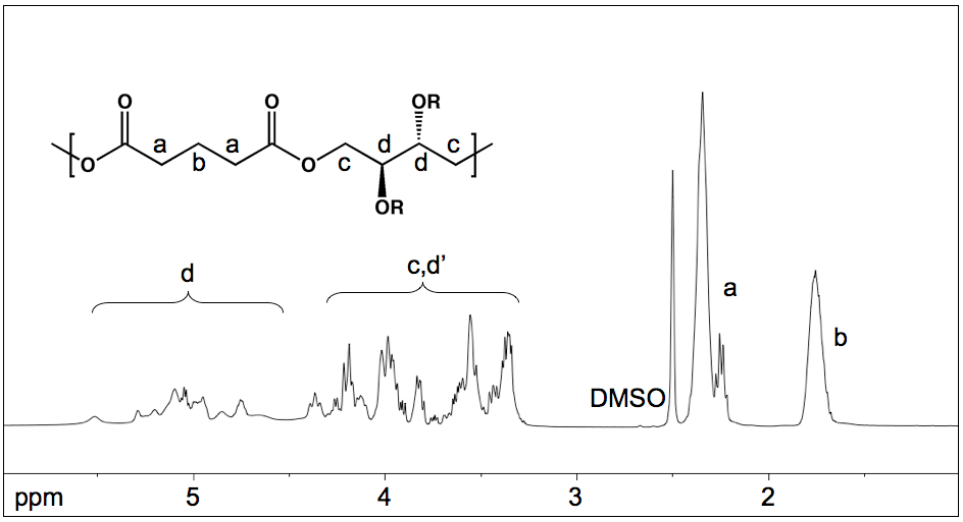

Figure B1. Fully labeled ^{1}H spectrum of OErGl.

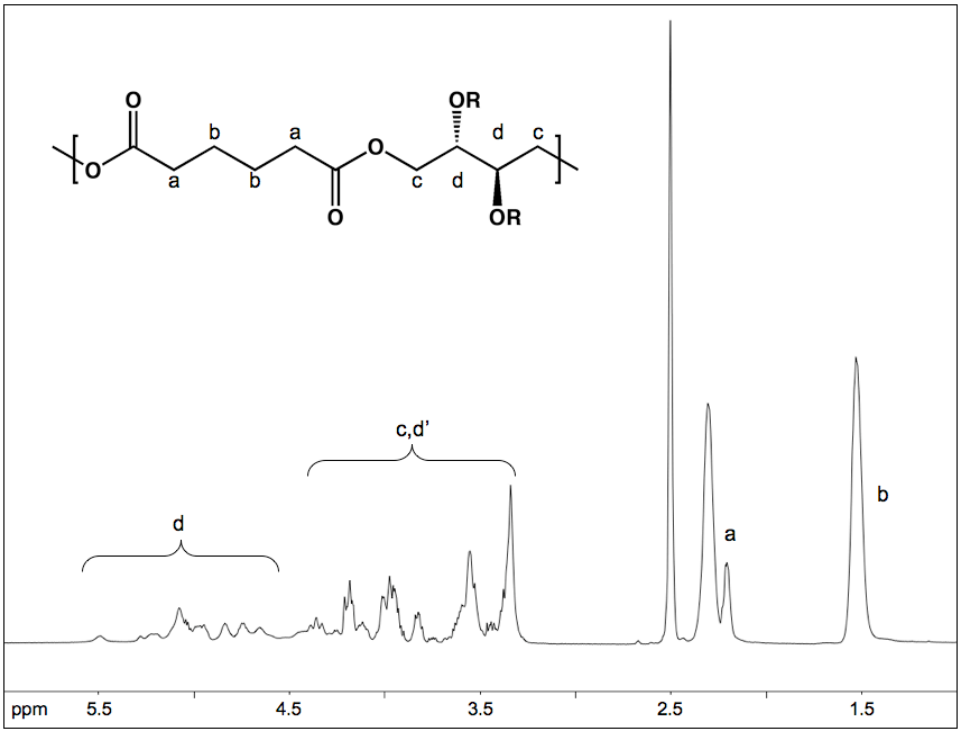

Figure B2. Fully labeled ^{1}H spectrum of OErAd.

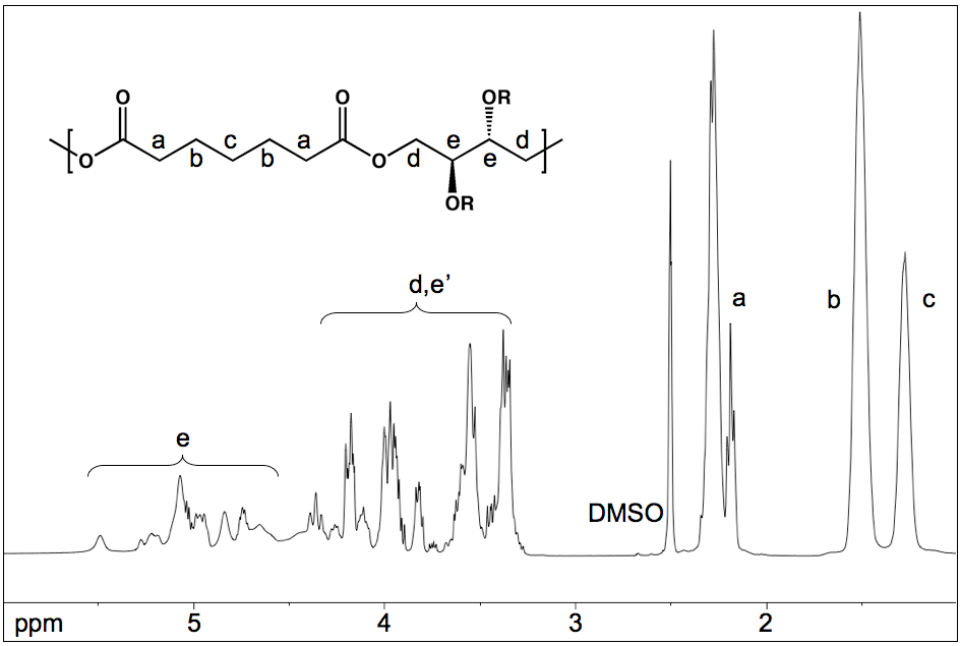

Figure B3. Fully labeled ^{1}H spectrum of OErPi.

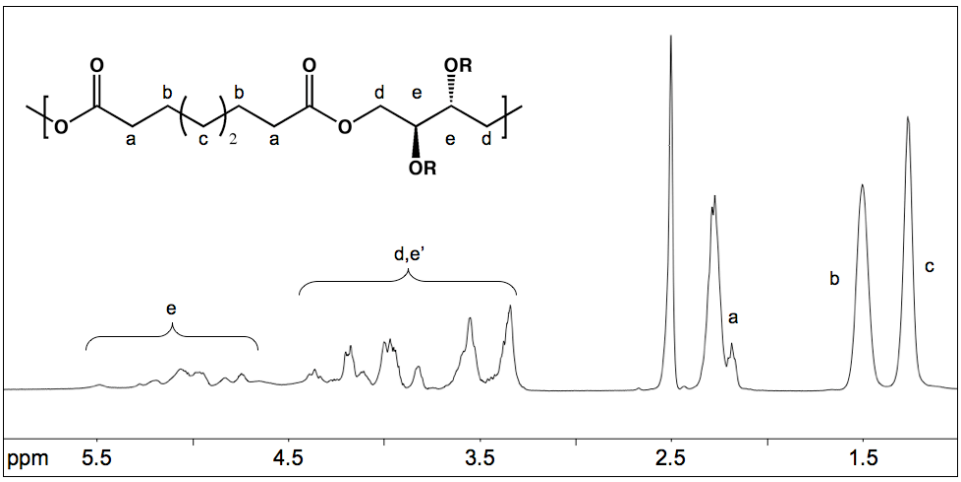

Figure B4. Fully labeled ^{1}H spectrum of OErSu.

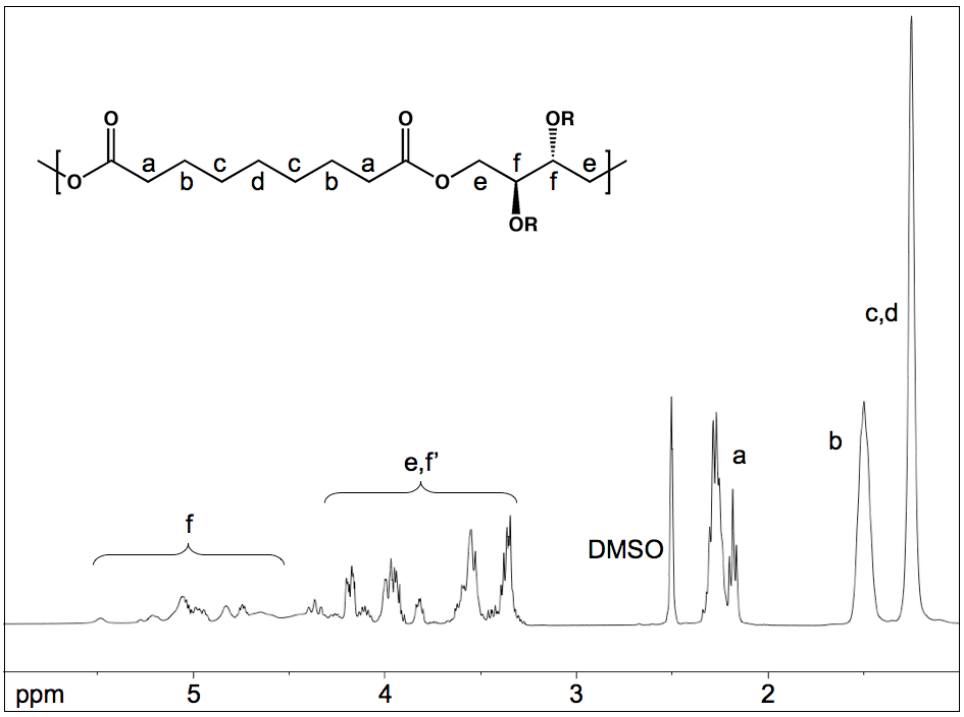

Figure B5. Fully labeled ^{1}H spectrum of OErAz.

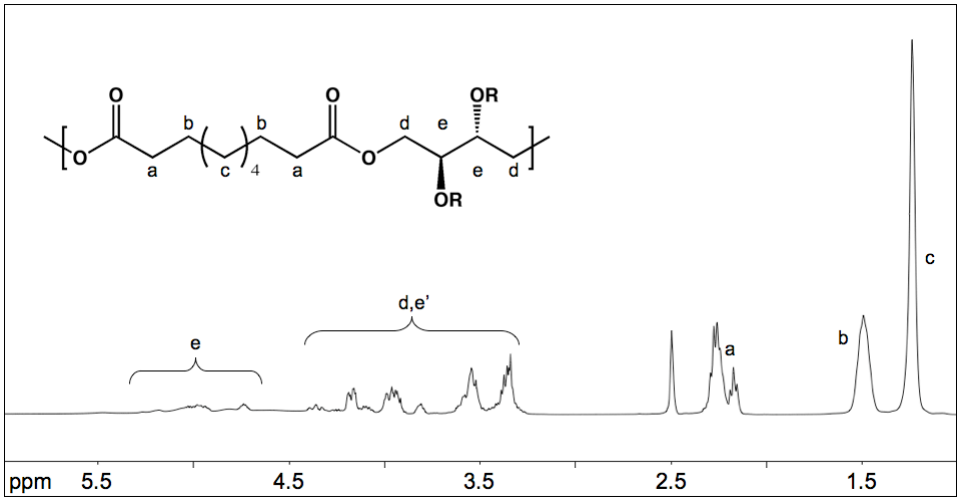

Figure B6. Fully labeled ^{1}H spectrum of OErSe.

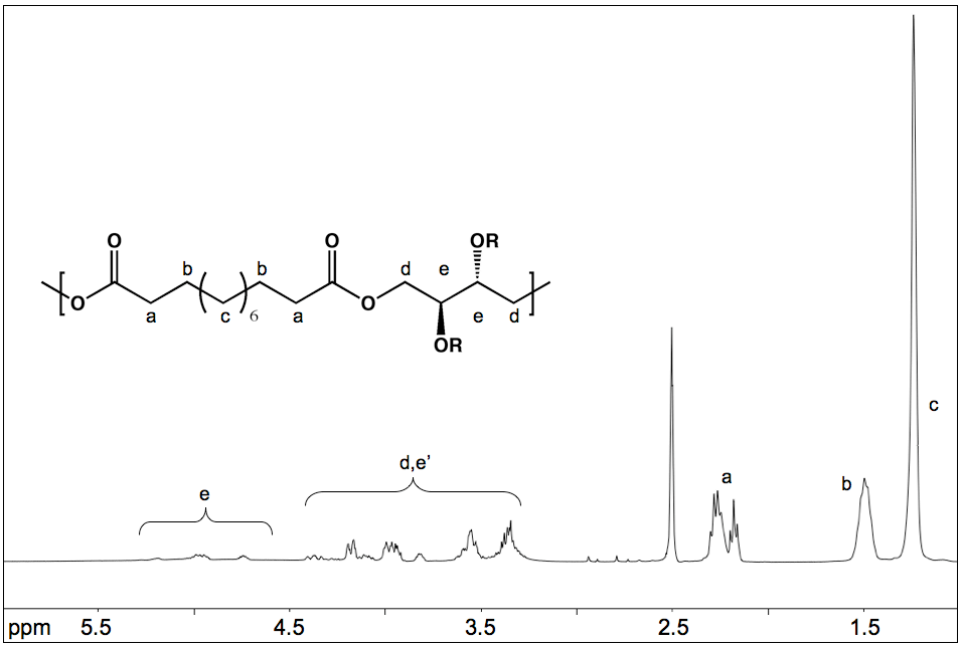

Figure B7. Fully labeled ^{1}H spectrum of OErDo.

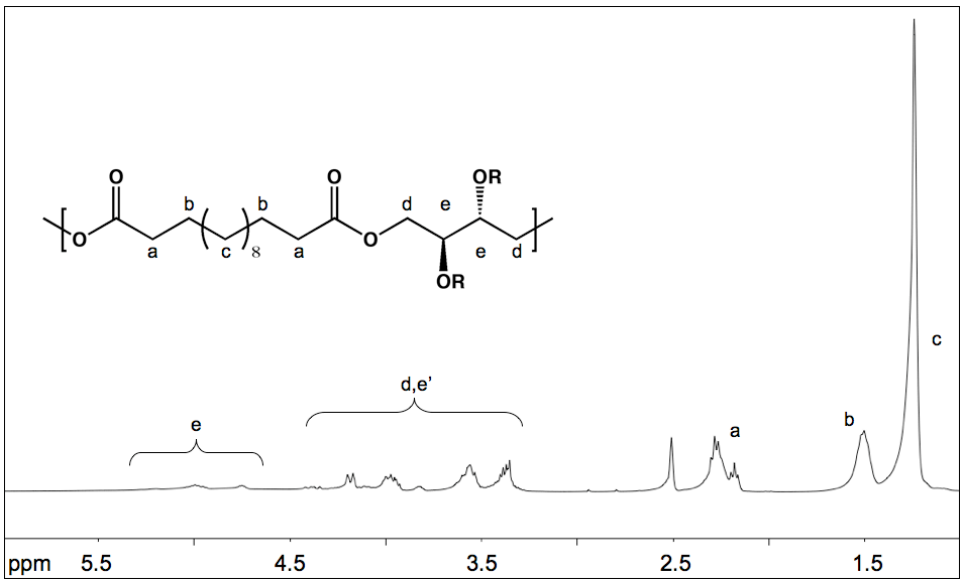

Figure B8. Fully labeled ^{1}H spectrum of OErTe.

Appendix C

SUPPLEMENTAL MATERIALS FOR CHAPTER 3

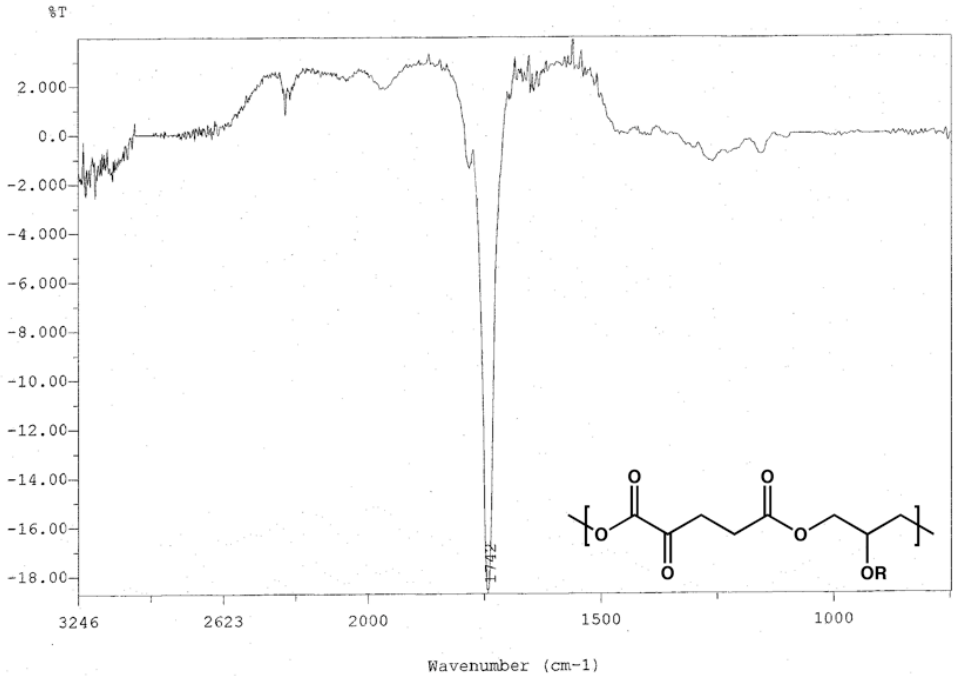

Figure C1. IR spectrum of PGa in THF.

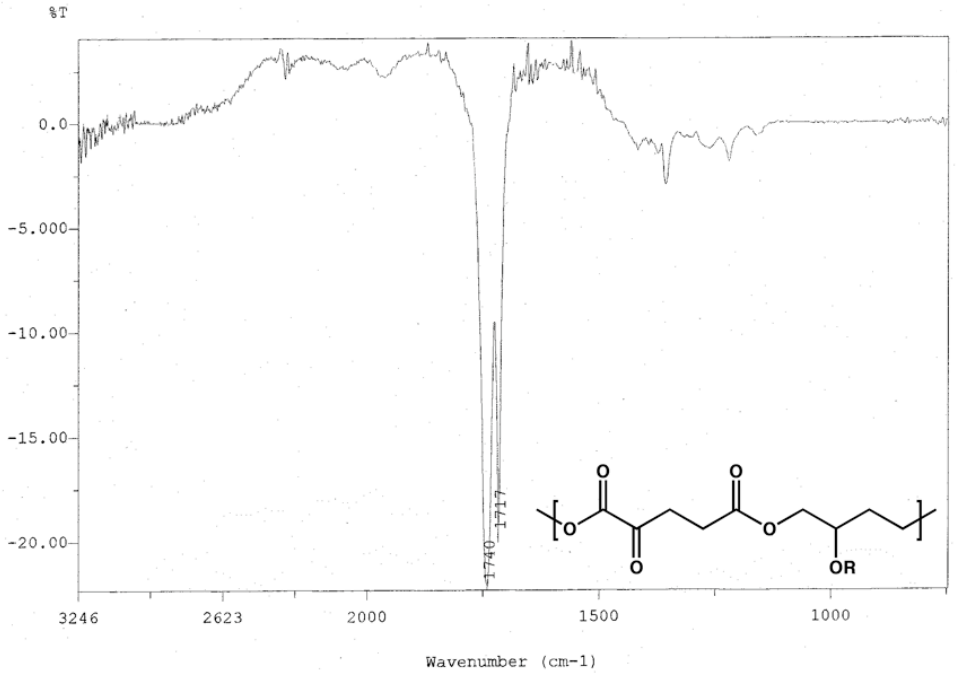

Figure C2. IR spectrum of PBa in THF.

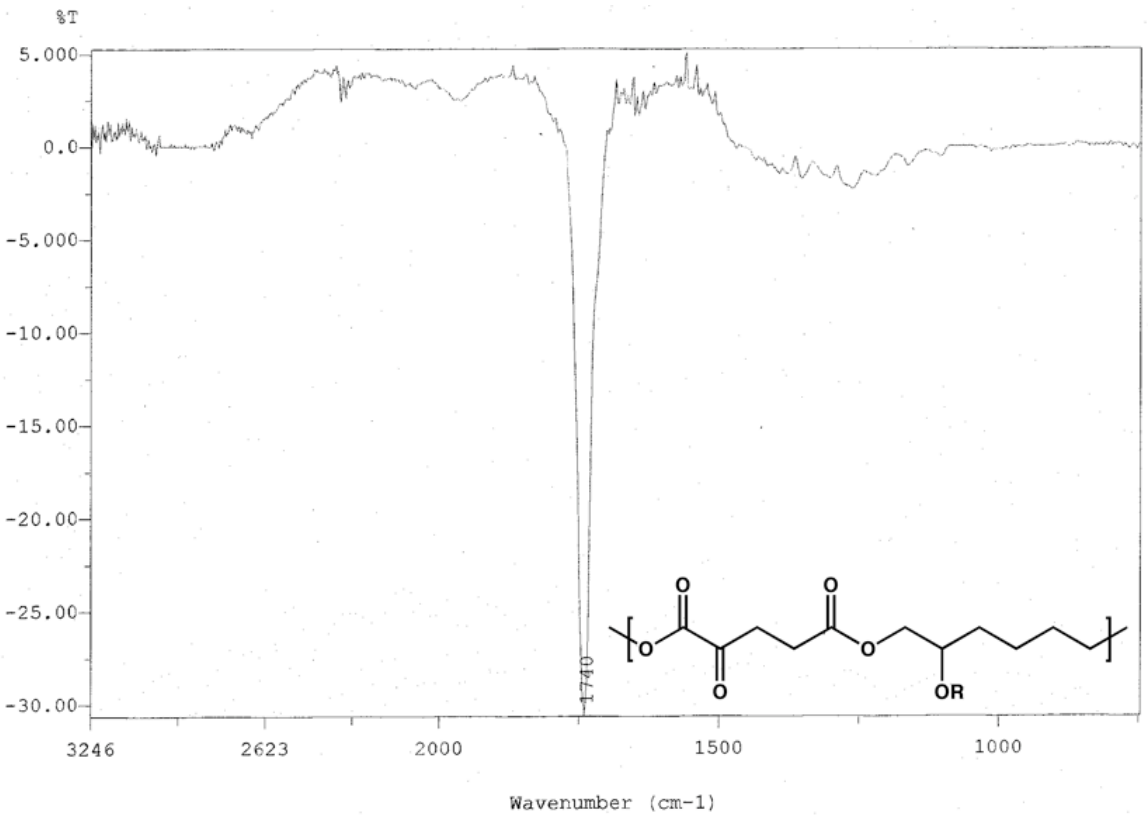

Figure C3. IR spectrum of PHa in THF.

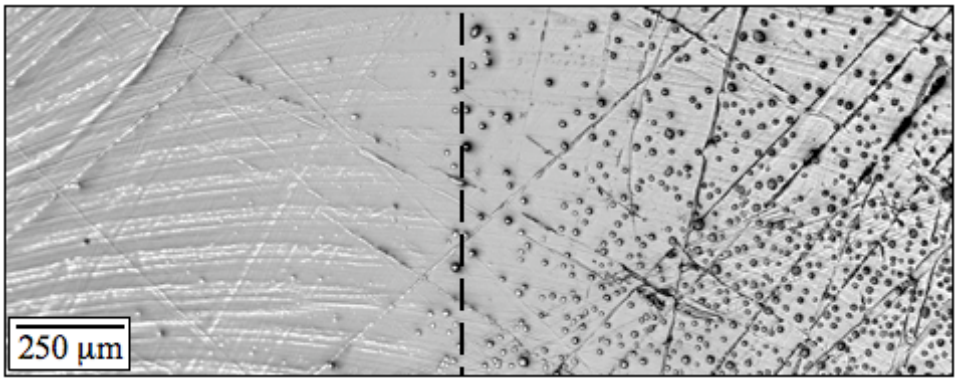

Figure C4. Cells on material 2C, partially functionalized with H_2NO-GRGDS. A small drop of soluble H_2NO-GRGDS was placed on the surface of the film and allowed to react. After rinsing and seeding cells, the border is apparent by viewing where cells did and did not attach.

Appendix D

SUPPLEMENTAL MATERIALS FOR CHAPTER 4

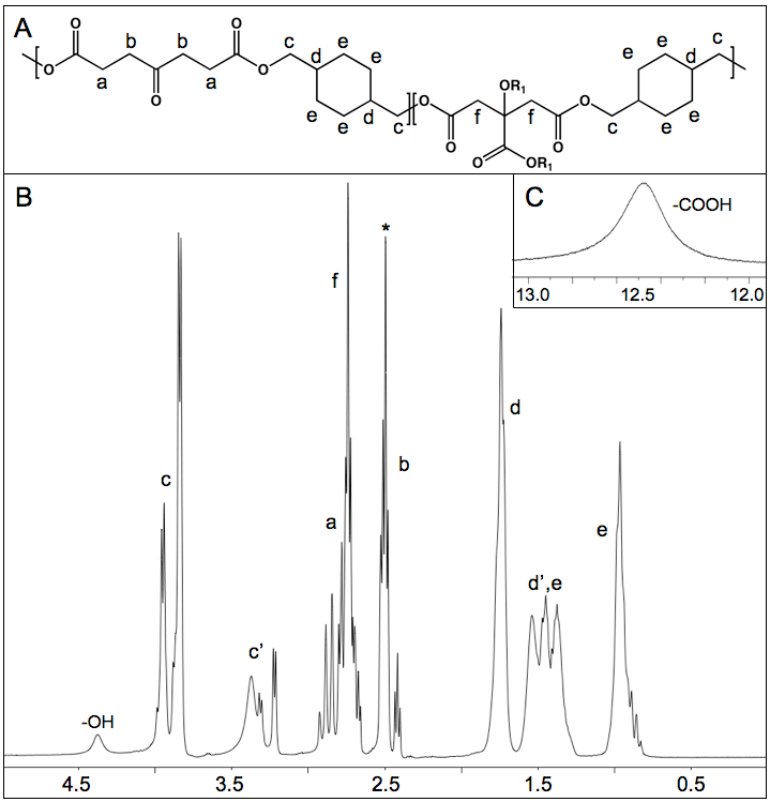

Figure D1. Fully labeled ^{1}H spectrum of PP-CHDM in deuterated DMSO.

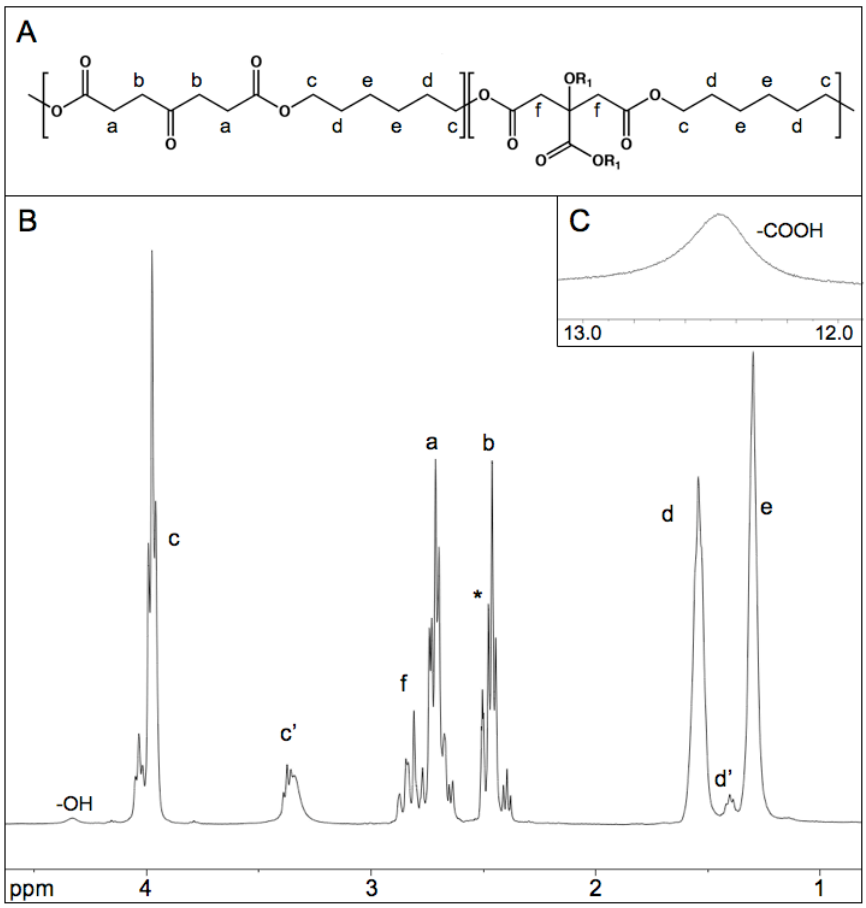

Figure D2. Fully labeled ^{1}H spectrum of PP-HD in deuterated DMSO.

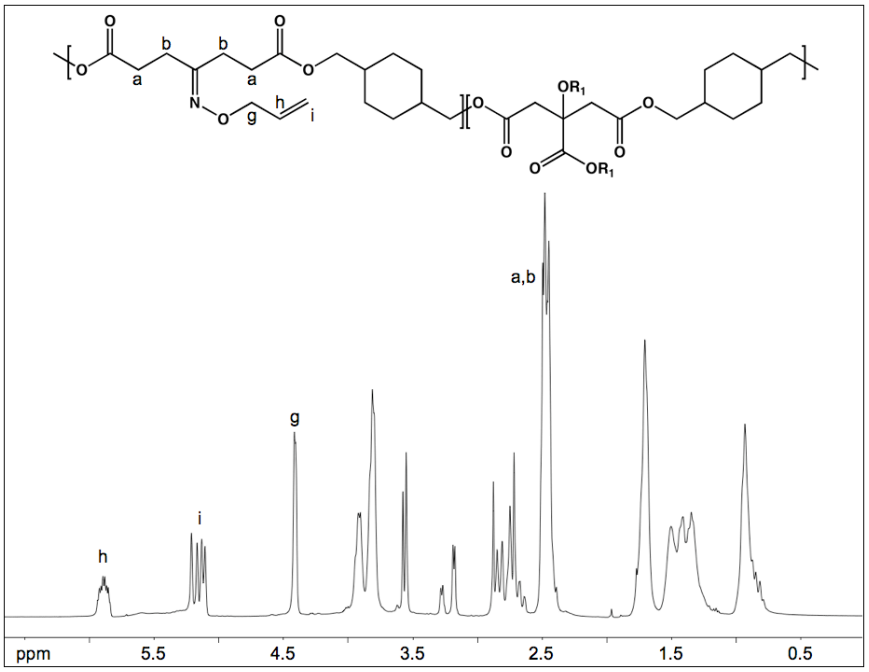

Figure D3. Fully labeled ^{1}H spectrum of PP-CHDM functionalized with *O*-allylhydroxylamine in deuterated DMSO.

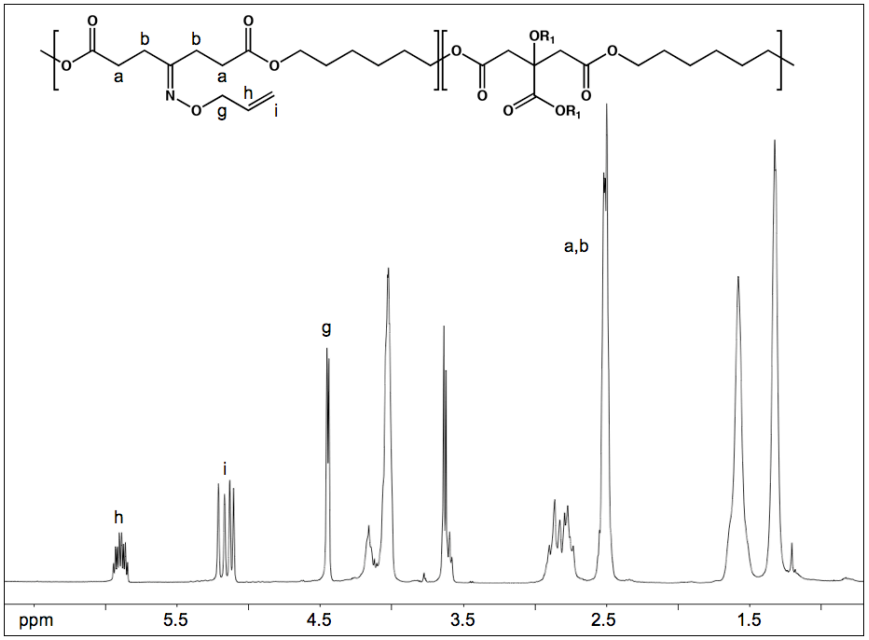

Figure D4. Fully labeled ^{1}H spectrum of PP-HD functionalized with *O*-allylhydroxylamine in deuterated DMSO.

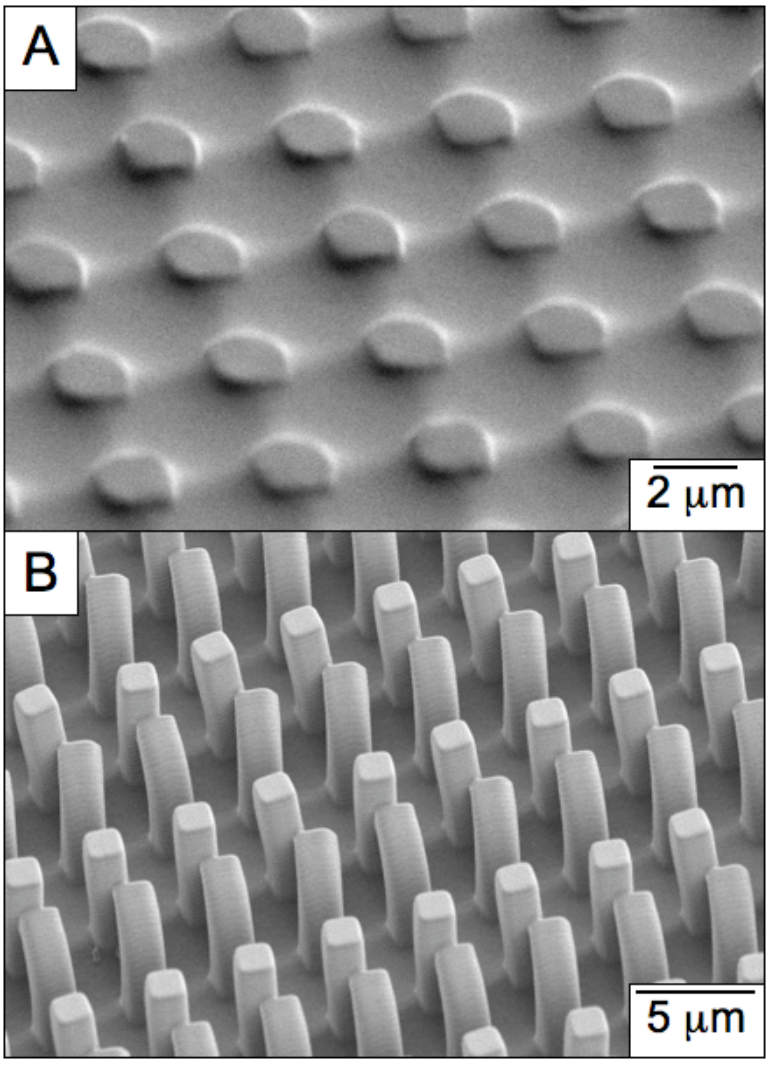

Figure D5. Embossed films of materials 3 (A) and 5 (B) were fabricated by cross-linking in the presence of a PFPE mold.

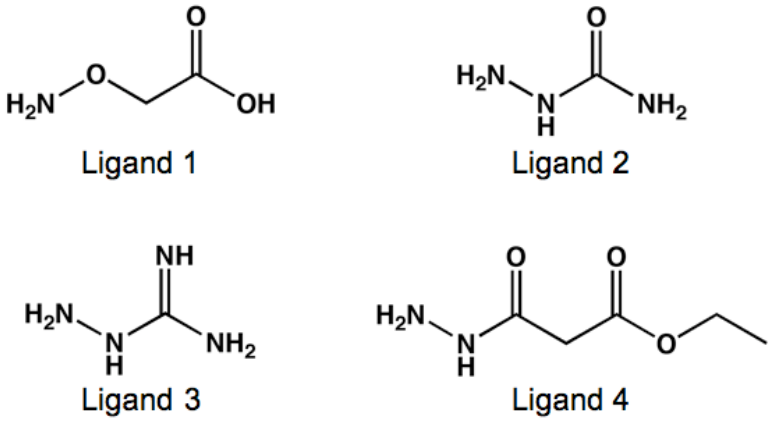

Figure D6. Oxyamine- and hydrazide-containing ligands employed during polymer functionalization studies.

Table D1. Thermogravimetric Analysis of Poly(Diol 4-Ketopimelate -*co*- Diol Citrate) [a]

Elastomer	5 % (°C)	10 % (°C)	50 % (°C)
1	307.0	335.2	438.3
2	310.8	339.8	442.2
3	313.2	343.5	446.8
4	290.7	323.7	428.3
5	296.7	328.9	429.1

[a] determined by TGA in N_2 (10 °C/min).

Table D2. Contact Angle Measurements of Functionalized Polyketoester Films [a]

Ligand	Contact Angle (°)
-	88.10 ± 0.55
1	74.84 ± 0.89
2	77.48 ± 0.62
3	74.80 ± 0.50
4	77.19 ± 0.49

[a] material 5 was used in all functionalization studies.

Appendix E

SUPPLEMENTAL MATERIALS FOR CHAPTER 5

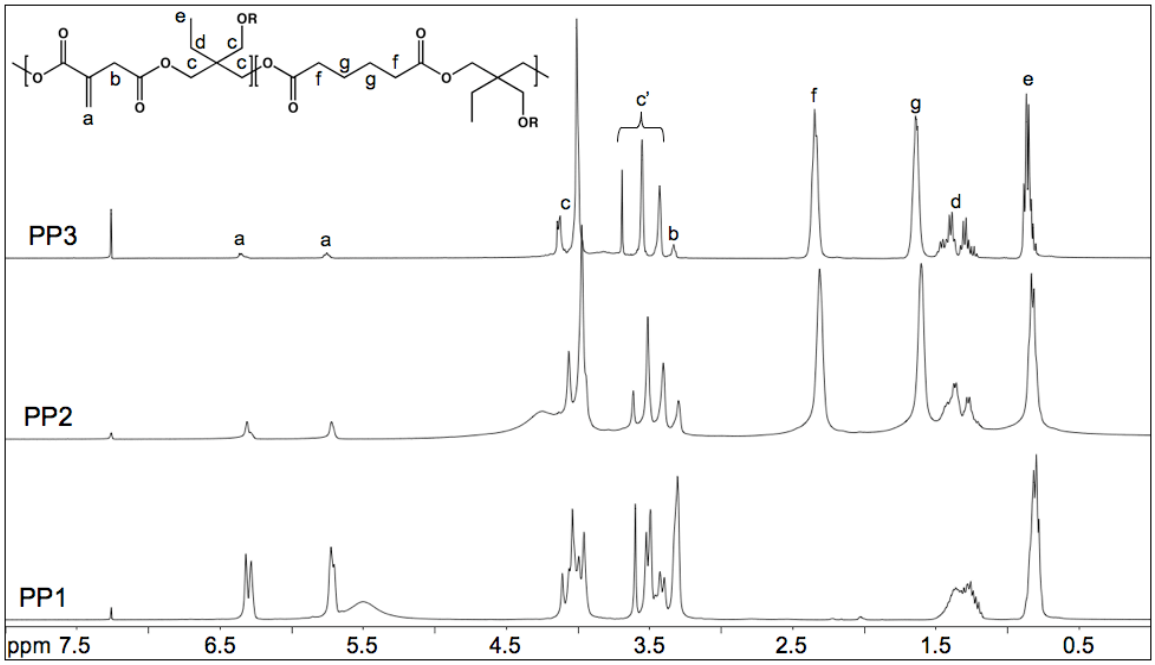

Figure E1. Fully labeled ^{1}H spectrum of PP1, PP2, and PP3 in deuterated chloroform.

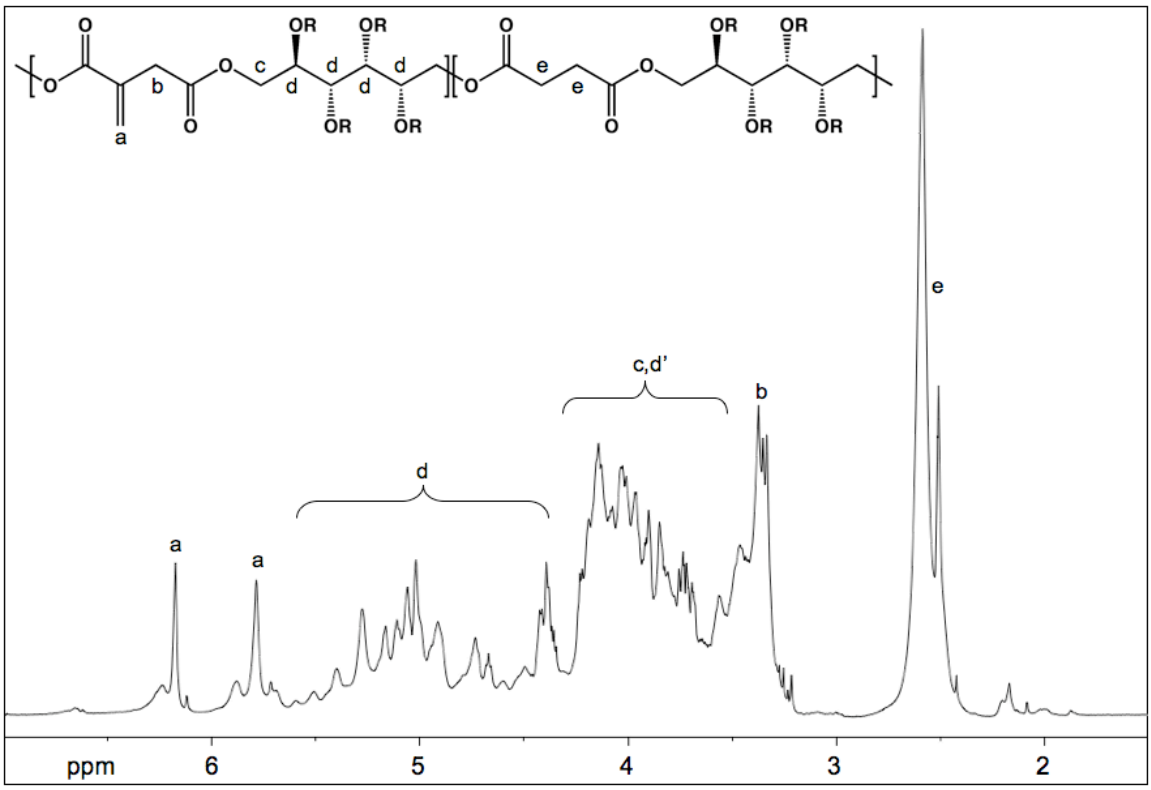

Figure E2. Fully labeled ^{1}H spectrum of PP4 in deuterated dimethyl sulfoxide.

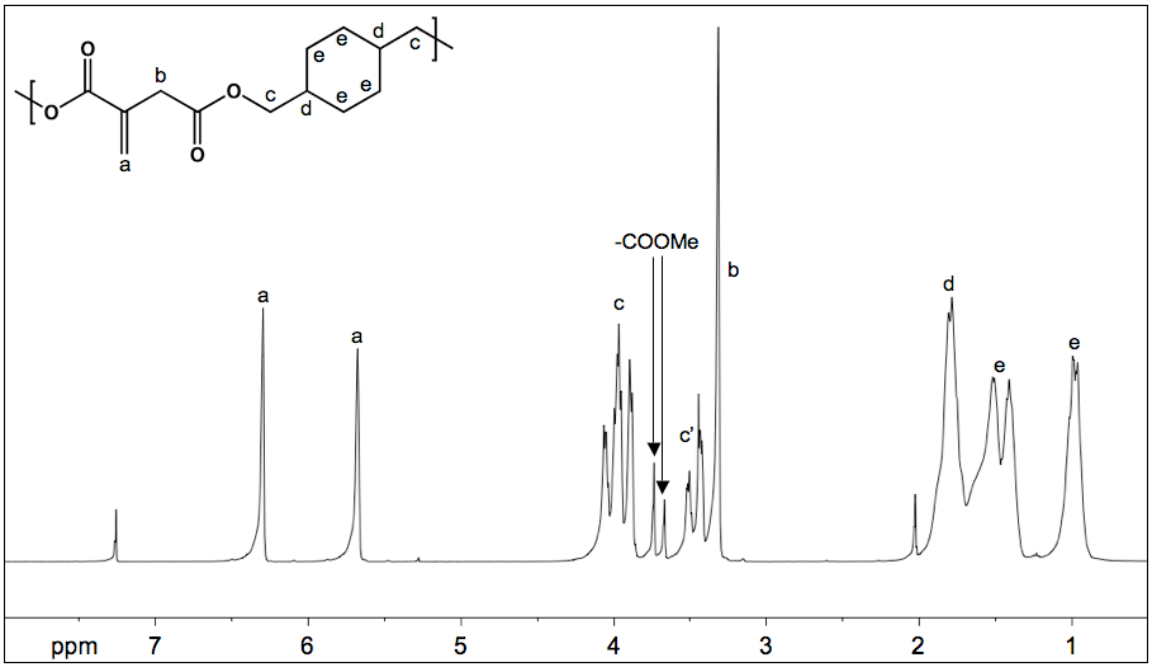

Figure E3. Fully labeled ^{1}H spectrum of PP5 in deuterated chloroform.

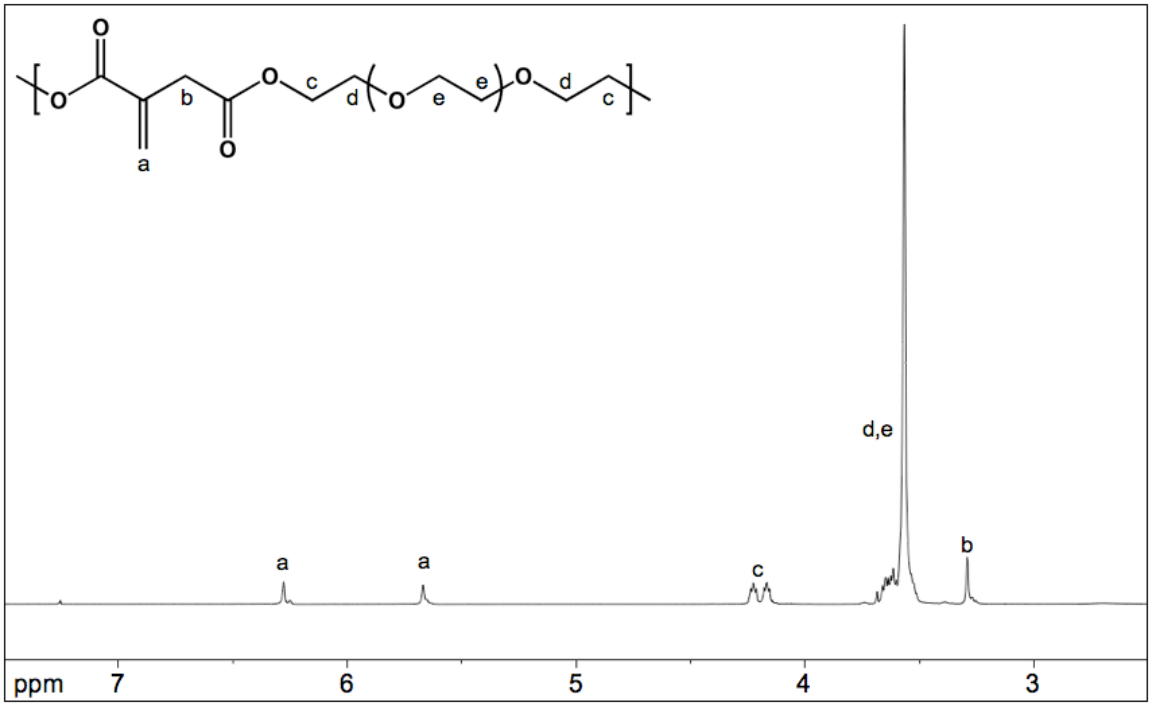

Figure E4. Fully labeled ^{1}H spectrum of PP6 in deuterated chloroform.

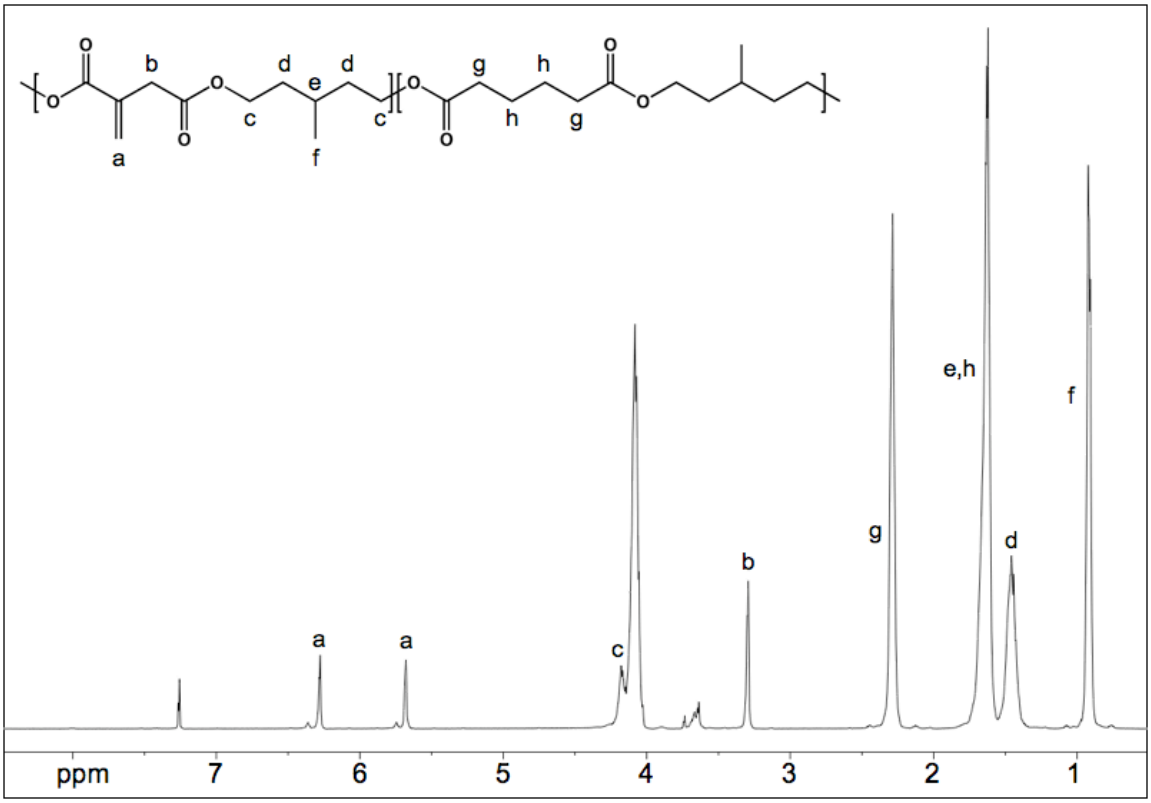

Figure E5. Fully labeled ^{1}H spectrum of PP7 in deuterated chloroform.